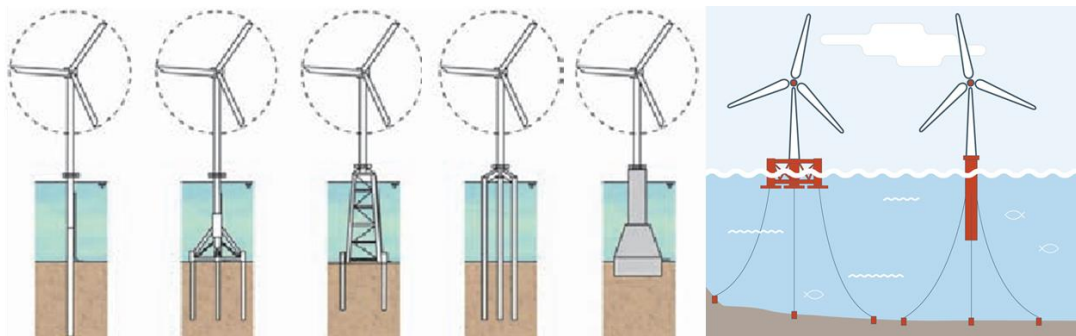




NATIONAL TECHNICAL UNIVERSITY OF  
ATHENS

School of Naval Architecture and Marine Engineering

# **A REVIEW OF THE AVAILABLE TECHNOLOGIES AND STRUCTURAL DESIGN PRACTICES FOR OFFSHORE WIND TURBINES**



Thesis to obtain the Master of Science Degree in  
Naval and Marine Technology and Science

Olympia-Maria Skourti

Supervisor: Prof. Charis Gantes

Co-supervisor: Dr.-Ing. Stefanos Gkatzogiannis

Athens, June 2022

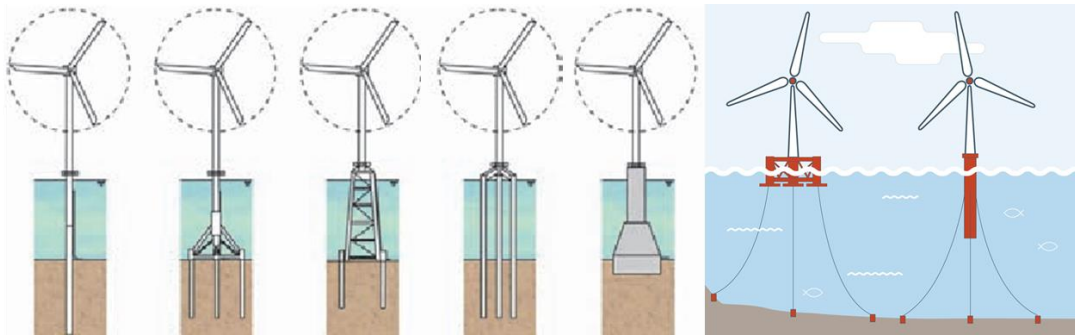




NATIONAL TECHNICAL UNIVERSITY OF  
ATHENS

School of Naval Architecture and Marine Engineering

# A REVIEW OF THE AVAILABLE TECHNOLOGIES AND STRUCTURAL DESIGN PRACTICES FOR OFFSHORE WIND TURBINES



Thesis to obtain the Master of Science Degree in  
Naval and Marine Technology and Science

Olympia-Maria Skourti

Supervisor: Prof. Charis Gantes

Co-supervisor: Dr.-Ing. Stefanos Gkatzogiannis

Athens, June 2022



Copyright © Olympia-Maria Skourti, 2022  
All Rights Reserved

Neither the whole nor any part of this diploma thesis may be copied, stored in a retrieval system, distributed, reproduced, translated, or transmitted for commercial purposes, in any form or by any means now or hereafter known, electronic or mechanical, without the written permission from the author. Reproducing, storing and distributing this thesis for non-profitable, educational or research purposes is allowed, without prejudice to reference to its source and to inclusion of the present text. Any queries in relation to the use of the present thesis for commercial purposes must be addressed to its author.

Approval of this diploma thesis by the School of Naval Architecture and Marine Engineering of the National Technical University of Athens (NTUA) does not constitute in any way an acceptance of the views of the author contained herein by the said academic organisation (L. 5343/1932, art. 202).



Olympia-Maria Skourti (2022)

Master's Thesis

A Review of the Available Technologies and Structural Design Practices for Offshore Wind Turbines  
School of Naval Architecture and Marine Engineering, National Technical University of Athens, Greece





## Acknowledgements

After two years of hard work, by submitting and defending the present thesis I am becoming a Master of Science in Naval and Marine Technology and Science, specialized in Marine Structures and Hydrocarbon Exploitation.

I would like to specially thank Prof. Charis Gantes and Dr.-Ing. Stefanos Gkatzogiannis for their constant guidance, feedback and patience throughout the past academic year that I was working on my dissertation.

I also want to thank Dr. Jason Jonkman for our personal communication during this time and for supporting me with his extensive knowledge on the FAST software.

Last but not least, I appreciate the support of my family and friends, who are always there for me.





NATIONAL TECHNICAL UNIVERSITY OF ATHENS  
SCHOOL OF NAVAL ARCHITECTURE AND MARINE ENGINEERING

MASTER'S THESIS

**A Review of the Available Technologies and Structural Design Practices for  
Offshore Wind Turbines**  
**Olympia-Maria Skourti**

Supervisor: Prof. Charis Gantes  
Co-supervisor: Dr.-Ing. Stefanos Gkatzogiannis  
June 2022

**ABSTRACT**

Nowadays, clean electricity produced by wind turbines makes them stand in the epicenter of green energy transition. The fact that velocities and wind flow are respectively higher and more uniform above sea than onshore renders coastal and offshore grounds more suitable for power production. The growing demand for renewable energy, in conjunction with the continuous development of substructure and foundation technologies to be used in the marine environment, drive wind turbines further and further offshore.

The present work reports on the latest technological advancements in the industry of offshore wind turbines, with emphasis on structural systems and construction practices that are already in use. Both bottom-fixed and floating systems are examined, the selection among which is mainly based on the site depth and seabed soil type. A short overview of the technologies that are currently being developed is also included.

A bottom-fixed offshore wind turbine is analysed on a preliminary level, as a case study. The wind turbine is mounted on a tripod, which in turn is founded on piles. The structure is modeled with two different software, FAST and SAP2000. The operation of the turbine and the dynamic response of the tower and substructure is simulated in FAST, to produce time-series for the loads. Subsequently, snapshots from the time-series, at which critical values of loading are documented, are selected and the corresponding values are assigned to a model of the tower, substructure and foundation built in SAP2000, to enable static analyses for structural optimization purposes.

In order to perform strength checks, estimate exploitation ratios for the members and investigate the extent of the effect of wind loading on the structure, analyses are executed in SAP2000 for three hub-height wind speeds: 7m/s, 11.4m/s (the rated wind speed), and 20m/s, each one for two of the "Power Production" Design Load Cases specified in Part 3-1 of the Wind Energy Generation Systems Standard by the International Electrotechnical Commission (IEC), for the cases of "Extreme Turbulence Model and Normal Sea State" (Case 1.3) and "Normal Turbulence Model And Severe Sea State" (Case 1.6). The exploitation ratios for any wind speed, prove to be in all cases greater, when the wind flow follows the Extreme Turbulence Model rather than the Normal Turbulence Model. Overall, the combination of

Extreme Turbulence Model and Normal Sea State for the rated hub-height wind speed is the most unfavorable loading scenario for the structure.

# TABLE OF CONTENTS

<b>TABLE OF CONTENTS .....</b>	<b>25</b>
<b>LIST OF FIGURES .....</b>	<b>27</b>
<b>LIST OF TABLES .....</b>	<b>31</b>
<b>1 INTRODUCTION .....</b>	<b>1</b>
1.1 OVERVIEW.....	1
1.2 THESIS OUTLINE .....	3
<b>2 STATE OF THE ART OF OFFSHORE WIND TURBINES.....</b>	<b>5</b>
2.1 TECHNOLOGIES WIDELY APPLIED IN PRACTICE.....	5
2.1.1 BOTTOM-FIXED SYSTEMS .....	5
2.1.1.1 MONOPILE .....	5
2.1.1.2 JACKET .....	11
2.1.1.3 TRIPOD.....	17
2.1.1.4 TRIPILE .....	20
2.1.1.5 GRAVITY-BASED FOUNDATION .....	21
2.1.2 FLOATING SYSTEMS .....	24
2.1.2.1 SEMI-SUBMERSIBLE .....	24
2.1.2.2 SPAR.....	26
2.2 LARGEST OFFSHORE WIND FARMS .....	28
2.3 TECHNOLOGY SELECTION CRITERIA.....	29
2.4 CURRENTLY INVESTIGATED TECHNOLOGIES .....	30
<b>3 THEORETICAL BACKGROUND .....</b>	<b>33</b>
3.1 WIND TURBINE CLASSIFICATION .....	33
3.2 LOADS ACTING ON A WIND TURBINE .....	34
3.2.1 WIND.....	34
3.2.2 WAVE.....	36
3.2.3 OTHER LOADS.....	40
3.2.4 LOAD COMBINATIONS .....	41
<b>4 CASE STUDY: CONCEPT DESIGN OF AN OFFSHORE WIND TURBINE WITH A TRIPOD SUBSTRUCTURE .....</b>	<b>43</b>
4.1 OVERVIEW OF METHODOLOGY.....	43
4.2 SITE LOCATION .....	44
4.3 BASIC PROPERTIES OF THE TURBINE .....	46
4.4 SUBSTRUCTURE AND TRANSITION PIECE GEOMETRY .....	46

4.5	TOWER GEOMETRY .....	48
4.6	LOADS .....	50
4.6.1	WIND .....	50
4.6.2	WAVE .....	53
4.7	SOIL PROPERTIES .....	55
4.8	FOUNDATION .....	56
<b>5</b>	<b>RESULTS .....</b>	<b>61</b>
5.1	SUMMARY OF THE ANALYSES PERFORMED .....	61
5.2	WIND FLOW DATA.....	62
5.3	LOADS EXERTED BY THE TURBINE ON THE TOWER TOP.....	63
5.4	DEMAND / CAPACITY RATIOS FOR THE TOWER.....	65
5.5	DEMAND / CAPACITY RATIOS FOR THE SUBSTRUCTURE AND FOUNDATION .....	67
<b>6</b>	<b>CONCLUSIONS AND SUGGESTED FURTHER WORK.....</b>	<b>71</b>
	<b>REFERENCES.....</b>	<b>73</b>
	<b>ANNEX A - SHORT DESCRIPTION OF FAST .....</b>	<b>77</b>
	<b>ANNEX B- FAST INPUT FILES .....</b>	<b>81</b>
	MAIN INPUT FILE .....	83
	TURBSIM INPUT FILE .....	84
	INFLOW WIND INPUT FILE .....	86
	BMODES INPUT FILE .....	88
	BMODES TOWER PROPERTIES FILE .....	91
	ELASTODYN INPUT FILE .....	93
	ELASTODYN TOWER INPUT FILE.....	96
	AERODYN INPUT FILE .....	98
	SERVODYN INPUT FILE .....	101
	HYDRODYN INPUT FILE.....	105
	SUBDYN INPUT FILE.....	113

# LIST OF FIGURES

Figure 1-1 Main parts of a horizontal axis wind turbine ( <a href="http://www.energy.gov">www.energy.gov</a> )	2
Figure 1-2 Typical wind turbine power curve (Source: <a href="http://www.researchgate.net">www.researchgate.net</a> )	2
Figure 1-3 Global average offshore wind turbine capacity, hub heights, and rotor diameters (Musial, et al., 2021)	3
Figure 2-1 Grouted connection between monopile and transition piece (a) cylindrical with shear keys (b) conical without shear keys (DNV-GL, 2016)	6
Figure 2-2 Model of a wind turbine at the Luchterduinen Offshore Wind Farm ( <a href="http://www.dubbelman-ridderkerk.nl">www.dubbelman-ridderkerk.nl</a> )	6
Figure 2-3 Monopile transportation by tug at the Anholt Offshore Wind Farm ( <a href="http://windpoweroffshore.com">windpoweroffshore.com</a> )	7
Figure 2-4 Monopile transportation (a) on a barge at the Borkum Riffgrund II Offshore Wind Farm ( <a href="http://www.wagenborg.com">www.wagenborg.com</a> ) (b) on the deck of the installation vessel at the Dudgeon Offshore Wind Farm ( <a href="http://www.offshorewind.biz">www.offshorewind.biz</a> )	7
Figure 2-5 Monopile upending (a) upending frame at the Kriegers Flak Offshore Wind Farm ( <a href="http://ocean-energyresources.com">ocean-energyresources.com</a> ) (b) crane of an installation vessel uplifting a monopile at the Triton Knoll Offshore Wind Farm ( <a href="http://www.seaway7.com">www.seaway7.com</a> )	8
Figure 2-6 Monopile installation (a) jack-up vessel at the Gode Offshore Wind Farm 1+2 ( <a href="http://www.demegroup.com">www.demegroup.com</a> ) (b) heavy lift crane vessel at the Dudgeon Offshore Wind Farm ( <a href="http://www.offshorewind.biz">www.offshorewind.biz</a> )	8
Figure 2-7 Pile installation (a) hydraulic impact hammer at the Gemini Offshore Wind Farm ( <a href="http://www.gemini.com">www.gemini.com</a> ) (b) vibratory hammer at the Riffgat Offshore Wind Farm ( <a href="http://www.cape-holland.com">www.cape-holland.com</a> )	8
Figure 2-8 Monopile gripper ( <a href="http://www.schuttevaer.nl">www.schuttevaer.nl</a> )	9
Figure 2-9 Seabed drilling rig ( <a href="http://www.bauer.de">www.bauer.de</a> )	9
Figure 2-10 Transition piece being lowered into position at the Gemini Offshore Wind Farm ( <a href="http://www.gemini.com">www.gemini.com</a> )	10
Figure 2-11 Blade installation at the Borkum Riffgrund II Offshore Wind Farm ( <a href="http://www.jandenul.com">www.jandenul.com</a> )	10
Figure 2-12 Pre-assembly of nacelle and blades for the Thornton Bank Offshore Wind Farm ( <a href="http://www.repower.com">www.repower.com</a> )	10
Figure 2-13 Jacket manufacture (a) in two pieces for the Block Island Offshore Wind Farm ( <a href="http://www.blockislandtimes.com">www.blockislandtimes.com</a> ) (b) in one piece for the Borkum Riffgrund 1 Offshore Wind Farm ( <a href="http://www.offshorewindindustry.com">www.offshorewindindustry.com</a> )	11
Figure 2-14 Pre-piling principle (Baert, 2014)	12
Figure 2-15 Pre-piling template being installed for the Beatrice Offshore Wind Farm ( <a href="http://renews.biz">renews.biz</a> )	12
Figure 2-16 Piles being installed for the Beatrice Offshore Wind Farm ( <a href="http://www.beatricewind.com">www.beatricewind.com</a> )	12
Figure 2-17 Jackets being installed on piles for the East Anglia One Offshore Wind Farm ( <a href="http://www.heavyliftnews.com">www.heavyliftnews.com</a> )	13
Figure 2-18 East Anglia One Offshore Wind Farm jacket with stab-ins to be mated with pre-installed piles ( <a href="http://www.vanoord.com">www.vanoord.com</a> )	13
Figure 2-19 Sketch of post-piled jacket (Baert, 2014)	14
Figure 2-20 Sketch of swaged connection ( <a href="http://www.leenaars-bv.nl">www.leenaars-bv.nl</a> )	14
Figure 2-21 Borkum Riffgrund II Offshore Wind Farm jackets being transported from the manufacturing facility to the assembly terminal ( <a href="http://renews.biz">renews.biz</a> )	15
Figure 2-22 Borkum Riffgrund II Offshore Wind Farm jackets and suction buckets at the assembly terminal ( <a href="http://www.rhenus.group">www.rhenus.group</a> )	15
Figure 2-23 Suction bucket jacket being picked up by heavy lift jack-up vessel ( <a href="http://www.maritimejournal.com">www.maritimejournal.com</a> )	16
Figure 2-24 Suction bucket jacket being installed by heavy lift jack-up vessel ( <a href="http://www.mynewsdesk.com">www.mynewsdesk.com</a> )	16
Figure 2-25 Pump technology for suction bucket jacket ( <a href="http://www.framo.com">www.framo.com</a> )	16

Figure 2-26 Tripod for Alpha Ventus Offshore Wind Farm being welded, transition piece integrated (www.wikiwand.com)	17
Figure 2-27 Tripod substructures, transition piece not integrated (a) tripod for the Borkum West II Offshore Wind Farm being welded (www.trianel-borkum.de) (b) tripods for the Global Tech I Offshore Wind Farm (www.offshorewind.biz)	17
Figure 2-28 Pre-piling template for the Borkum West II Offshore Wind Farm tripods (twd.nl)	18
Figure 2-29 Borkum West II Offshore Wind Farm tripod being installed (www.trianel-borkum.de)	18
Figure 2-30 Borkum West II Offshore Wind Farm tripod fully installed (www.trianel-borkum.de)	19
Figure 2-31 Tripod installation (a) tripods for the Global Tech I Offshore Wind Farm being shipped to site on board a heavy-lift jack-up vessel (www.offshorewind.biz) (b) tripod being installed at the Global Tech I Offshore Wind Farm (www.rechargenews.com)	19
Figure 2-32 Pile being hammered into the seabed at the Alpha Ventus Offshore Wind Farm (www.menck.com)	19
Figure 2-33 Wind farms featuring tripiles (a) Bard Offshore 1 Offshore Wind Farm (www.power- technology.com) (b) Hooksiel prototype (www.renewableenergyworld.com)	20
Figure 2-34 Piles being installed at the Bard Offshore 1 Wind Farm (www.power-technology.com)	20
Figure 2-35 Tripiles in Bard's manufacturing base in the German port of Emden (www.windpowermonthly.com)	21
Figure 2-36 Tower connection to gravity-based substructure (a) ways to anchor tower bottom flange into concrete (b) detail of the "bolt cage" system (Stavridou, Efthymiou, & Baniotopoulos, 2015)	22
Figure 2-37 Concrete foundations being cast (Jeppsson, Larsen, & Larsson, 2008)	23
Figure 2-38 Tower bolts to be cast into the foundation (Jeppsson, Larsen, & Larsson, 2008)	23
Figure 2-39 Concrete foundations being towed to Lillgrund site (Jeppsson, Larsen, & Larsson, 2008)	23
Figure 2-40 Concrete substructures being lowered into position (Jeppsson, Larsen, & Larsson, 2008)	24
Figure 2-41 Concrete substructure cross-section (Jeppsson, Larsen, & Larsson, 2008)	24
Figure 2-42 Kincardine Offshore Wind Farm semi-submersible foundations being transported to assembly base (www.projectcargojournal.com)	25
Figure 2-43 Wind turbines being mounted on semi-submersible foundations for Kincardine Offshore Wind Farm (www.principlepower.com)	25
Figure 2-44 Kincardine Offshore Wind Farm assembled units being towed to project site (www.offshorewind.biz)	26
Figure 2-45 Semi-submersible foundation being installed for Kincardine Offshore Wind Farm (a) assembled unit being hooked up to the already installed mooring spread (www.cnn.com) (b) anchor handling tug supply vessel (AHTS) assisting the mooring of the assembled units (www.oedigital.com)	26
Figure 2-46 Spar buoys being transported from the manufacture base off the project's assembly base (www.offshorewind.biz)	27
Figure 2-47 Spar buoys being upended (www.ptil.no)	27
Figure 2-48 Turbines being assembled at project's assembly base (www.businessinsider.com)	27
Figure 2-49 Turbine being mated with spar substructure (www.saipem.com)	28
Figure 2-50 Assembled structures being towed to the project's site (www.businessinsider.com)	28
Figure 2-51 Hornsea Met Mast (www.keystoneengr.com)	30
Figure 2-52 Illustration of jack-up foundation for wind turbine (Horwath, et al., 2021)	31
Figure 2-53 Mono-bucket substructure and turbine components being loaded onto jack-up vessel (www.offshorewind.biz)	31
Figure 2-54 Illustration of Provence Grand Large TLP substructure (www.provencegrandlarge.fr)	32
Figure 2-55 Illustration of the ITI Energy barge (Jonkman & Matha, A Quantitative Comparison of the Responses of Three Floating Platforms, 2009)	32
Figure 3-1 Comparison of wave profiles suggested by linear (solid line) and non-linear (intermittent line) wave theories (Καραμπάς, Κρεστενίτης, & Κουτίτας, 2015)	38



Figure 4-1 Wind turbine location (a) distant view (b) close-up view ( <a href="http://www.google.com/maps">www.google.com/maps</a> )	44
Figure 4-2 Spatial distribution of mean annual offshore wind power density at 80m height above sea level in the Aegean and Ionian Seas for the period 1995–2009 (Soukissian, et al., 2017)	44
Figure 4-3 Spatial distribution of mean offshore wind power density in (a) winter, (b) spring, (c) summer and (d) autumn at 80m above sea level in the Aegean and Ionian Seas, period 1995–2009 (Soukissian, et al., 2017)	45
Figure 4-4 Bathymetry in the area ( <a href="http://webapp.navionics.com">webapp.navionics.com</a> )	45
Figure 4-5 Geometry of the substructure and transition piece in SAP2000	47
Figure 4-6 Rotor-Nacelle Assembly of the NREL Offshore 5-MW Baseline Wind Turbine (Zhao, Yang, & He, 2012)	48
Figure 4-7 Model of the substructure and tower in SAP2000 (a) in “Extrude” view (b) in “Standard” view	50
Figure 4-8 Illustration of wind loads acting on the non-submerged part of the structure (Source: <a href="http://www.scielo.org">www.scielo.org</a> )	51
Figure 4-9 Approximation of actual wind profile with linear sections	53
Figure 4-10 Fetch calculation in the study area for North-West wind	54
Figure 4-11 Geotechnical properties of the seabed soil (Passon, 2006)	55
Figure 4-12 P-y curves for indicative depths below the mudline	56
Figure 4-13 Model of the entire structure in SAP2000	57
Figure 4-14 Model of the pile in SAP2000	58
Figure 5-1 Time histories produced for the hub-height fore-aft wind speed	62
Figure 5-2 Time histories produced for the hub-height side-to-side wind speed	62
Figure 5-3 Tower top fore-aft shear force progress with time under (a) DLC 1.3, (b) DLC 1.6	63
Figure 5-4 Tower top side-to-side shear force progress with time under (a) DLC 1.3, (b) DLC 1.6	63
Figure 5-5 Tower top axial force progress with time under (a) DLC 1.3, (b) DLC 1.6	63
Figure 5-6 Tower top roll moment progress with time under (a) DLC 1.3, (b) DLC 1.6	64
Figure 5-7 Tower top pitch moment progress with time under (a) DLC 1.3, (b) DLC 1.6	64
Figure 5-8 Tower top yaw moment progress with time under (a) DLC 1.3, (b) DLC 1.6	64
Figure 5-9 Demand / capacity ratios for the members of the tower under different load combinations	65
Figure 5-10 Demand / capacity ratios for the members of the tower for various snapshots of the time-history, hub-height wind speed equal to 7m/s under (a) DLC 1.3, (b) DLC 1.6	66
Figure 5-11 Demand / capacity ratios for the members of the tower for various snapshots of the time-history, hub-height wind speed equal to 11.4m/s under (a) DLC 1.3, (b) DLC 1.6	66
Figure 5-12 Demand / capacity ratios for the members of the tower for various snapshots of the time-history, hub-height wind speed equal to 20m/s under (a) DLC 1.3, (b) DLC 1.6	66
Figure 5-13 Global coordinate system in (a) 3d view and (b) plan view	67
Figure 5-14 Axial force (a), shear force (b), bending moment (c) diagrams, and deformed shape (d) of the three piles under the most extreme design load combination (DLC 1.3, V=11.4m/s, load propagation along the negative x axis)	69
Figure 5-15 Axial force (a), shear force (b), bending moment (c) diagrams, and deformed shape (d) of the tripod under the most extreme design load combination (DLC 1.3, V=11.4m/s, load propagation along the negative x axis)	70
Figure A-0-1 FAST control volumes for bottom-fixed systems (Jonkman & Jonkman, 2016)	77
Figure A-0-2 FAST control volumes for floating systems (Jonkman & Jonkman, 2016)	79
Figure A-0-3 Example of TurbSim grid implementation (Jonkman B. J., 2012)	79



# LIST OF TABLES

Table 2-1 Major offshore wind farms featuring bottom-fixed substructures	28
Table 2-2 Major offshore wind farms featuring floating substructures	29
Table 2-3 Acceptable depth and type of soil for each type of foundation (Horwath, et al., 2021)	30
Table 3-1 Wind turbine classes (Source: (DNV-GL, 2016))	33
Table 3-2 Design Load Cases for Ultimate Strength Analysis	41
Table 3-3 Design Load Cases for Fatigue Analysis	41
Table 4-1 Basic properties of the NREL Offshore 5-MW Baseline Wind Turbine (Jonkman, Butterfield, Musial, & Scott, 2009)	46
Table 4-2 Coordinates of substructure and transition piece nodes	47
Table 4-3 Length and section properties of substructure and transition piece members	48
Table 4-4 Geometry of tower members	49
Table 4-5 Variation of drag coefficient with Reynold's number (Roshko, 1961)	52
Table 4-6 Water fetch for each one of the main wind directions	53
Table 4-7 Fetch calculation in the study area for North-West wind	54
Table 4-8 Implementation of the Apparent Fixity approach	59
Table 5-1 Design load combinations checked in the context of the present work	61
Table 5-2 Demand / capacity ratios for the members of the tripod under different load combinations	68



# 1 INTRODUCTION

## 1.1 OVERVIEW

Wind power has been used for centuries to pump water, grind corn and flour and saw wood. Today, wind turbines are used to produce clean electricity and are expected to play a crucial role in the global energy sector's shift from carbon-heavy fossil fuels such as oil, gas and coal, to renewable energy sources. Both academic and business research make progress towards this goal, while states are expected to facilitate the process by introducing a less robust regulatory framework, which currently constitutes a bottleneck in many cases.

Figure 1-1 illustrates the main components of a modern, horizontal axis, upwind wind turbine. The blades and hub make up the rotor. The nacelle contains the gearbox, the low-speed and high-speed shafts, the generator, the controller and the brake. The gearbox blocks the rotor if the wind is outside the wind speed range in which the wind turbine is allowed by the manufacturer to work, whereas the controller enables its operation in this range. An anemometer measures wind speed and transmits the respective data to the controller. The anemometer also perceives wind direction and, in the case of upwind wind turbines, communicates with the yaw drive to ensure that the rotor is constantly facing the wind. Downwind wind turbines do not need this feature, as wind itself blows the rotor downwind. In case of emergency, the brake forces the rotor to stop.

Horizontal axis wind turbines work predominantly on the lift principle. As wind blows, lift force is generated, the blades move and cause the rotor to rotate. The low-speed main shaft transmits this rotation to the high-speed shaft through the gearbox. The generator then converts this mechanical energy to electrical energy, which in turn is fed into the grid.

The power generated by the wind turbine varies depending on the hub-height wind speed. A typical wind turbine power curve is given in Figure 1-2. The wind turbine starts to work and produce power at the cut-in hub-height wind speed. While the hub-height wind speed is between the cut-in and rated wind speeds (Control Region II), maximal power production is the control objective. As the wind turbine reaches the rated wind speed and the power supply capacity of the generator is reached, the turbine transits into Control Region III. In this region, which is delimited by the rated and cut-out speeds, the ability of the blades to rotate around their axis (pitch) is utilized. The pitch angle controller controls the rotor rotation at nominal speed while the generator outputs rated power. The control objective in Control Region III is to limit power production, by limiting both torque and rotor speed of the generator, in

order to ensure that constant rated power is obtained. The wind turbine stops working at the cut-out hub-height wind speed (Apata & Oyedokun, 2020).

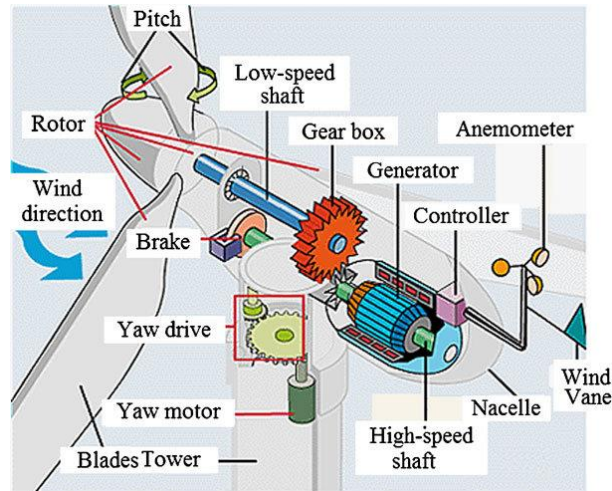


Figure 1-1 Main parts of a horizontal axis wind turbine (www.energy.gov)

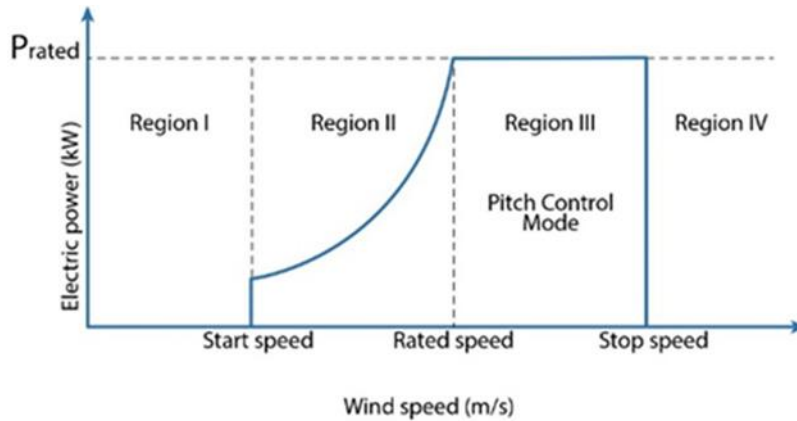


Figure 1-2 Typical wind turbine power curve (Source: [www.researchgate.net](http://www.researchgate.net))

As wind characteristics are more suitable for power production over the sea than they are on land (higher velocities and more uniform flow profile), and there are larger unexploited areas available offshore, wind turbines already occupy coastal and offshore grounds. The growing demand for renewable energy, together with the development of new substructure technologies, both bottom-fixed and floating, drive wind turbines further and further from the shore. Figure 1-3 depicts the historical trend of the global-weighted average offshore wind turbine capacities, hub heights, and rotor diameters.

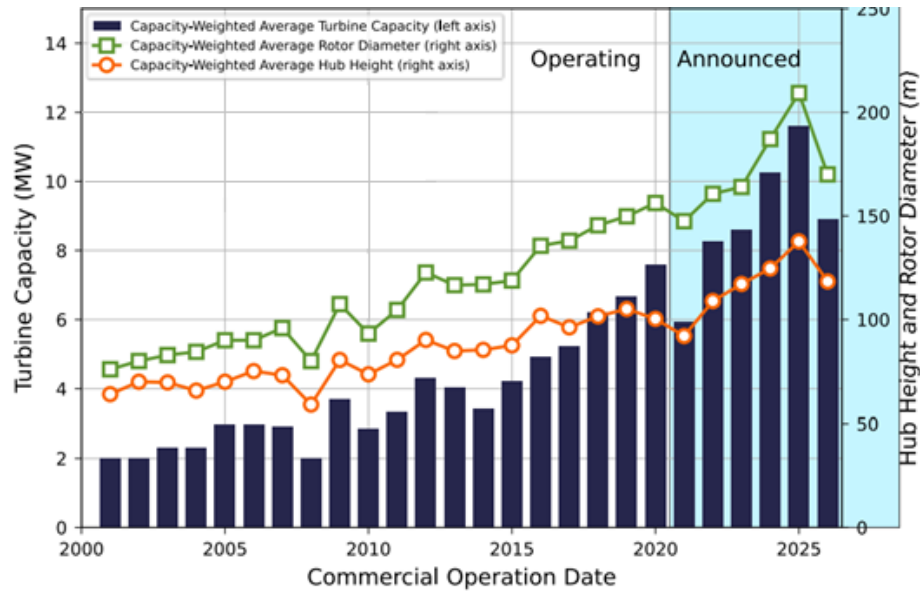


Figure 1-3 Global average offshore wind turbine capacity, hub heights, and rotor diameters (Musial, et al., 2021)

The installation of an offshore wind farm poses many challenges during both the design and the construction phases, and therefore its feasibility is based on the optimization of a long list of parameters. The wind regime in the area under examination is among the most significant ones since it determines the benefit from the potential installation of an offshore wind farm. The prevailing wind speeds, propagation direction, turbulence levels, annual and inter-annual variability have to be extensively studied. The prevailing wave regime as well as history of seismic activity in the area are additional major factors, since they constitute two of the most critical loads on the structure, following the wind action. Bathymetry is another aspect to be taken into account; seabed depths and slope determine the expedience of installing an offshore wind farm, as well as indicate which substructure types could be employed. Lastly, marine flora and fauna that could either be affected by the installation works or disturbed by the operation of the turbines should be recorded, and any resulting environmental restrictions should be identified.

## 1.2 THESIS OUTLINE

The present master's thesis aims to investigate the most recent stage of technological development of offshore wind turbines. It is also among the objectives to make use of some of the tools available for the modeling, design and structural analysis of an offshore wind turbine in the context of a case study; FAST, a software package specialized in the dynamic response of wind turbines, and the general-purpose finite element software SAP2000.

Research on the state of the art of offshore wind turbines is presented in Chapter 2. This section encompasses description of the available substructure and foundation systems, enumeration of the necessary vessels and other equipment used for transportation and installation, as well as research on some construction matters, such as the tower-transition piece connection and sequence of assembly of components. Chapter 3 comprises the theoretical background regarding wind turbine classification and consideration of loads, on which the subsequent analysis was based. Chapter 4 addresses a case study, the preliminary design of an offshore wind turbine, including selection of a suitable site, specification of the physical and mechanical properties of the turbine, determination of the exact geometry and dimensioning of the load-bearing part of the structure, and approximation of the wind and wave regime.

Results with regards to loading of the structure under each analysis as well as performance of the various members against strength checks are given in Chapter 5.



## **2 STATE OF THE ART OF OFFSHORE WIND TURBINES**

### **2.1 TECHNOLOGIES WIDELY APPLIED IN PRACTICE**

#### **2.1.1 BOTTOM-FIXED SYSTEMS**

The most commonly employed bottom-fixed systems comprise the monopile, jacket, tripod, tripile and gravity-based substructures.

##### **2.1.1.1 MONOPILE**

In the case of a monopile, a hollow cylindrical steel tube serves as both substructure and foundation. Soil resistance at the bottom end of the monopile and side friction between the pile walls and the soil act jointly to bear safely the vertical loads. The horizontal loads are carried by the monopile's resistance to bending, and by the lateral resistance of the soil surrounding the embedded length of the monopile (Horwath, et al., 2021).

The pile and the tower carrying the turbine are joined together through a transition piece mounted on top of the pile. The transition piece is a tube with a slightly larger diameter than that of the pile, and the two are mated through a grouted connection. At the top end of the transition piece, a flange is welded. The tower is then bolted to this flange.

At the beginning of the offshore wind industry, it was not possible to achieve the verticality tolerance dictated by wind turbine specifications (Golightly, 2014) once the pile had been driven; hence, a grouted transition piece was included to connect the tower to the monopile. The vertical alignment was achieved subsequently, by the grout being given a suitable misalignment. In addition to addressing this problem, the transition piece became a very useful component to mount all appurtenances upon, such as boat landings, anodes, cable hang-offs and platforms, as it was not being driven, and therefore it was not subject to the high accelerations implied by installation.

However, the transition piece is a weak spot of the monopile substructure. Over the years, the grout cracks and crumbles due to vibrations caused by the dynamic loads from wind and waves, and must be repaired. This risk can be mitigated in the three following ways. First, the grouted section can be reinforced with shear keys, circumferential weld beads on the outside of the monopile and the inside of

the transition piece (Figure 2-1 a). Therewith, the sliding resistance between the grout and the steel is increased so that no relative displacement occurs. Second, the monopile and transition piece can be mated with a conical joint in the area of the grouted section (Figure 2-1 b). If the steel-grout slip resistance is exceeded, minor displacement of the grout will occur. This settlement will introduce compressive contact stresses between the steel and the grout, which along with some friction, will provide sufficient resistance against further settlement (DNV-GL, 2016). Third, the flange connection between the tower and the foundation pile can be designed to sustain the impact of the pile driver. For example, the monopiles in Luchterduinen Offshore Wind Farm do not have a transition piece, the tower is mounted directly on the monopile (Figure 2-2). Upon completion of the pile driving process, secondary structures, such as the boat landing and the platform, are welded on support points designed to bear the accelerations caused by the pile driving.

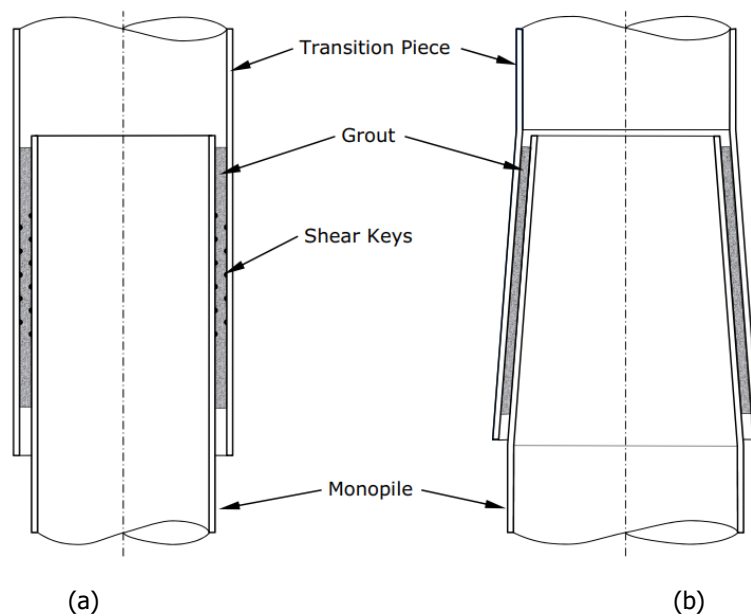


Figure 2-1 Grouted connection between monopile and transition piece (a) cylindrical with shear keys (b) conical without shear keys (DNV-GL, 2016)

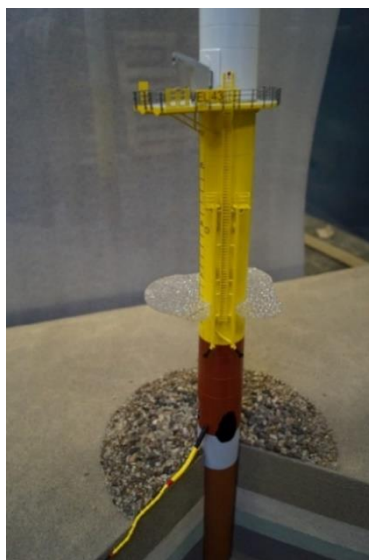


Figure 2-2 Model of a wind turbine at the Luchterduinen Offshore Wind Farm ([www.dubbelman-ridderkerk.nl](http://www.dubbelman-ridderkerk.nl))

The monopile foundation is manufactured onshore and transported to the designated location. Several monopiles and transition pieces can be transported at a time. With caps fitted on both ends, the monopiles can be made floating and towed by a tug to the site (Figure 2-3). Alternatively, they can be transported on a barge or on the deck of the installation vessel (Figure 2-4). As monopiles are typically transported horizontally, they first have to be upended using an upending frame, or a crane mounted on the installation vessel (Figure 2-5). When it comes to installation, either a jack-up vessel or a heavy lift crane vessel can be used (Figure 2-6). After the exact location of the bottom end is determined, the monopile is lowered and set down on the seabed. Slight penetration of the monopile takes place due to its self-weight, depending as well on the soil properties. It is installed through pile driving, by means of a hydraulic impact hammer or a vibratory hammer (Figure 2-7). Before and during the pile-driving process, pile-handling tools like gripper devices are also used for positioning and maintaining the monopile vertical (Figure 2-8).



Figure 2-3 Monopile transportation by tug at the Anholt Offshore Wind Farm ([windpoweroffshore.com](http://windpoweroffshore.com))



(a)



(b)

Figure 2-4 Monopile transportation (a) on a barge at the Borkum Riffgrund II Offshore Wind Farm ([www.wagenborg.com](http://www.wagenborg.com)) (b) on the deck of the installation vessel at the Dudgeon Offshore Wind Farm ([www.offshorewind.biz](http://www.offshorewind.biz))



(a)



(b)

Figure 2-5 Monopile upending (a) upending frame at the Kriegers Flak Offshore Wind Farm ([ocean-energyresources.com](http://ocean-energyresources.com)) (b) crane of an installation vessel uplifting a monopile at the Triton Knoll Offshore Wind Farm ([www.seaway7.com](http://www.seaway7.com))



(a)



(b)

Figure 2-6 Monopile installation (a) jack-up vessel at the Gode Offshore Wind Farm 1+2 ([www.deme-group.com](http://www.deme-group.com)) (b) heavy lift crane vessel at the Dudgeon Offshore Wind Farm ([www.offshorewind.biz](http://www.offshorewind.biz))



(a)



(b)

Figure 2-7 Pile installation (a) hydraulic impact hammer at the Gemini Offshore Wind Farm ([www.gemini.com](http://www.gemini.com)) (b) vibratory hammer at the Riffgat Offshore Wind Farm ([www.cape-holland.com](http://www.cape-holland.com))



Figure 2-8 Monopile gripper ([www.schuttevaer.nl](http://www.schuttevaer.nl))

Alternatively, when hammering the monopile down is not possible due to unsuitable soil characteristics, the piles can be drilled into the seabed. The holes are drilled by a drilling rig mounted on the installation vessel (Fig. 2-9). The piles are lifted from the transportation barge or vessel by crane and are allowed to sink into the drilled socket. The monopile is then grouted into position and the concrete is allowed to cure. When it is securely fixed into the drilled hole, the transition piece and the rest of the wind turbine components are put into place. This method was used in the cases of Blyth and Saint-Nazaire Offshore Wind Farms.



Figure 2-9 Seabed drilling rig ([www.bauer.de](http://www.bauer.de))

A combination of pile driving and relief drilling is sometimes necessary, as in the cases of Barrow (monopiles), Gwynt y Môr (monopiles) and Beatrice (jackets with piles) Offshore Wind Farms. Relief drilling is used when a pile hits early refusal during driving or requires unacceptable levels of energy to achieve further penetration. In this case, the drill is driven into the pile, it clamps itself on the inside and drills down to the pile tip or a certain distance beyond to remove obstacles, such as rocks and soil, and relieve the pile from the inside friction. After recovery of the drill, pile driving resumes until the pile reaches its final depth. The aim of drilling out the core at the interior of the monopiles is the reduction of both frictional and end resistance. By drilling the soil out, the friction acting on the internal surface of the monopile is eliminated over the drilled-out length. If refusal has occurred, the pile bore must be driven at a sufficient distance ahead of the pile toe to enable stress release and facilitate further

displacement of the annulus underneath the base of the pile during subsequent pile driving (Brunner & Beyer, 2008) (Offshore Wind, 2017).

Upon installation of the monopile, the transition piece is slowly lowered into position (Figure 2-10). Grouting equipment is used to join the monopile and transition piece together. Subsequently, the turbine tower is craned into position and bolted to the flange fitted on top of the transition piece. After all the tower pieces have been bolted together, the nacelle is mounted on top, and the generator is connected. Each turbine blade is then attached to the hub on the nacelle (Figure 2-11). Alternatively to this sequence of actions, the turbine components can be transported and assembled out at sea on special seajacking ships (Figure 2-12). During the final step, the wind turbine is connected to the offshore substation, which in turn feeds into the grid (Woodhatch, 2017).



Figure 2-10 Transition piece being lowered into position at the Gemini Offshore Wind Farm ([www.gemini.com](http://www.gemini.com))



Figure 2-11 Blade installation at the Borkum Riffgrund II Offshore Wind Farm ([www.jandenul.com](http://www.jandenul.com))



Figure 2-12 Pre-assembly of nacelle and blades for the Thornton Bank Offshore Wind Farm ([www.repower.com](http://www.repower.com))

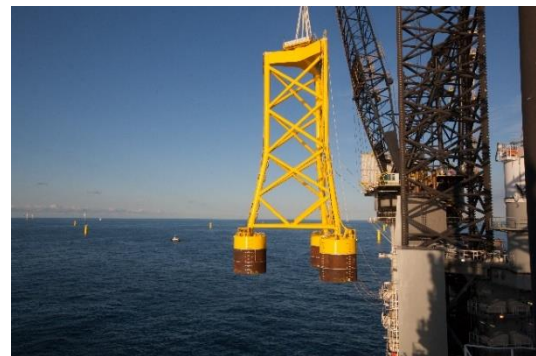
### 2.1.1.2 JACKET

Jackets are three or four-legged structures, with hollow cylindrical legs at the corners and smaller-diameter horizontal cross pieces and diagonal struts welded between the legs to provide rigidity. The legs are constructed with hollow cylindrical steel members of significantly smaller diameter in comparison to the monopiles. According to common engineering practice, the jackets are fixed in place using pipe piles or suction caissons, which transfer the vertical loads to the seabed. Horizontal forces create an overturning moment, which is counteracted by a combination of compression and tension in the piles or suction caissons. The self-weight of the jacket and the wind turbine also resists the overturning forces (Horwath, et al., 2021). The bolted connection between the transition piece and the tower is achieved with a flange, which is welded to the top and bottom of the hollow cylindrical segments respectively.

Some offshore wind jacket foundations are fabricated in two sections (Figure 2-13 a), e.g., the ones for Beatrice and Block Island Wind Farms; a larger, lower section consisting of rolled tubes welded together as the main frame and support trusses and a transition piece connected to a smaller, upper section of welded tubes. In other cases, the platform and transition piece are welded on the full jacket structure during the final assembly stage (Figure 2-13 b), e.g., the suction bucket jacket prototype installed at Borkum Riffgrund 1 Offshore Wind Farm and the jackets of the Seagreen 1 Offshore Wind Farm (Offshore Renewable Energy Catapult Ltd., 2020).



(a)



(b)

Figure 2-13 Jacket manufacture (a) in two pieces for the Block Island Offshore Wind Farm ([www.blockislandtimes.com](http://www.blockislandtimes.com)) (b) in one piece for the Borkum Riffgrund 1 Offshore Wind Farm ([www.offshorewindindustry.com](http://www.offshorewindindustry.com))

For piled jacket designs, piling can be done prior or subsequent to placing the substructure on the seabed, respectively known as pre-piling (Figure 2-14) and post-piling (Figure 2-19). In both cases, the jacket installation involves more steps and is slower than that of a monopile.

The pre-piling equipment comprises a piling template, a system to upend the piles and a hammer. Firstly, a template is placed on the seabed (Figure 2-15). Each pile is upended and lowered into the template, subsequently driven by a hydraulic hammer (Figure 2-16). The template secures that the piles are installed vertically and maintain the same center-to-center distance as the legs of the jacket substructure. When all piles are installed, the template is removed. Secondly, the jacket substructure is placed onto the pre-installed piles (Figure 2-17) by means of jacket stab-ins (Figure 2-18). Finally, the piles and jacket stab-ins are grouted together. The substructure rests initially on the foundation piles by means of a pile stopper. After grouting, the pile stopper is removed, so that the substructure is borne by the grout junction. Since the stab-in usually inserts the pile till below the mud line, the piles must be preliminary dredged to enable a smooth entering of the stab-in. In addition, the pile should be cleaned, typically with steel brushes and water jets), to remove possible marine growth and dirt, ensuring a

successful grout connection. A respective inspection before installing the jacket is recommended (Baert, 2014).

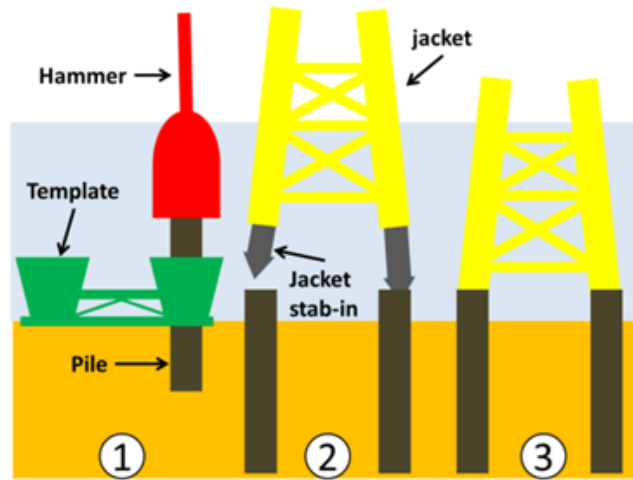


Figure 2-14 Pre-piling principle (Baert, 2014)



Figure 2-15 Pre-piling template being installed for the Beatrice Offshore Wind Farm (renews.biz)



Figure 2-16 Piles being installed for the Beatrice Offshore Wind Farm (www.beatricewind.com)





Figure 2-17 Jackets being installed on piles for the East Anglia One Offshore Wind Farm  
([www.heavyliftnews.com](http://www.heavyliftnews.com))

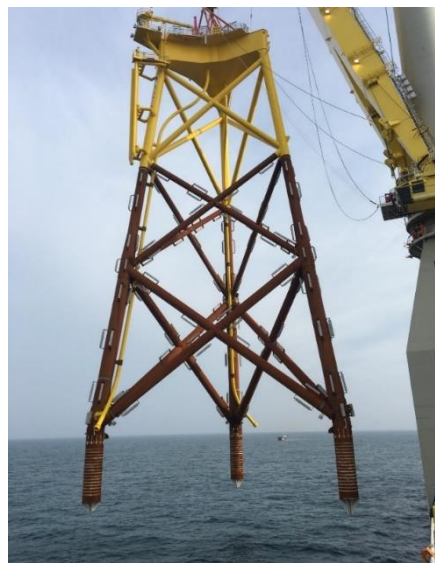


Figure 2-18 East Anglia One Offshore Wind Farm jacket with stab-ins to be mated with pre-installed piles  
([www.vanoord.com](http://www.vanoord.com))

Post-piling (Figure 2-19) implies the reverse of the process illustrated in Figure 2-14. The substructure is initially positioned on the desired position on the seabed, and serves itself as a template for the pile driving. The piles are then stabbed into the seabed through sleeves welded on each jacket leg, and driven with a hammer until the pile top reaches the same level as the top of the jacket leg sleeve. Finally, the pile and jacket leg sleeve are grouted together (Baert, 2014). The post-piling method has not been employed for a jacket so far.

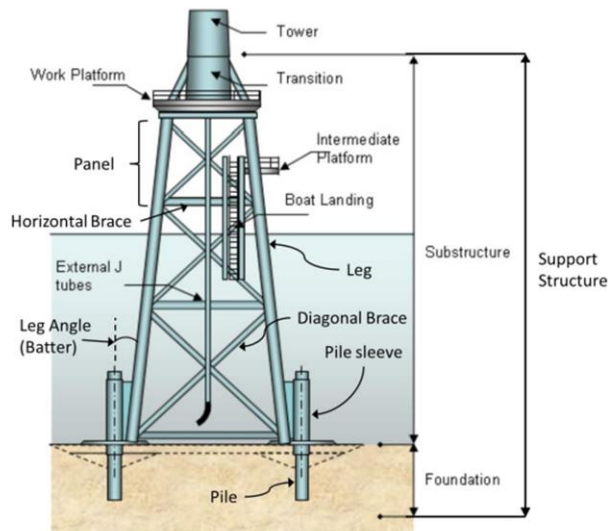


Figure 2-19 Sketch of post-piled jacket (Baert, 2014)

Grouted connections in jacket structures, either between jacket legs and preinstalled piles, or between jacket sleeves and post-installed piles, shall always be designed and constructed with shear keys (DNV-GL, 2018). Pile swaging is a concept that comes from the oil and gas industry and could potentially be adopted for the jacket-pile connection, allowing for a grout-free connection. In that case, the pile steel is pressed into slots of the pile sleeve by means of hydraulic pressure (Figure 2-20).

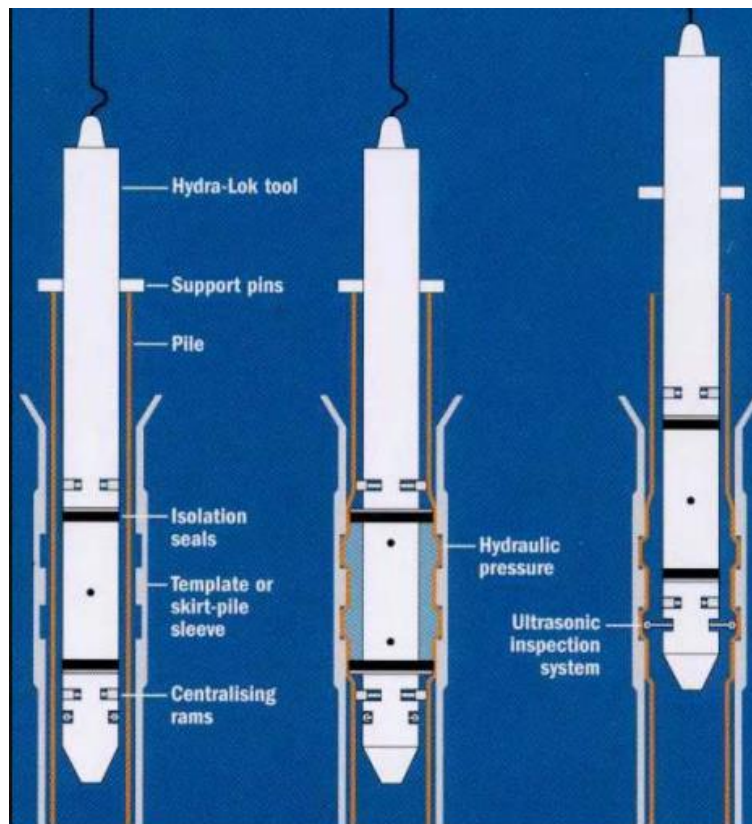


Figure 2-20 Sketch of swaged connection (www.leenaars-bv.nl)

An alternative to foundation piles is the suction bucket foundations, which are welded to the bottom of the jacket. Suction buckets are installed by pumping out water from the upside-down buckets. This

creates a vacuum, which presses them down into the seabed. Foundations, jacket, and transition piece are then installed together as a single unit. Besides lower costs due to the increased installation speed compared to the traditionally piled jacket, this concept enables easier decommissioning and practically noise free installation, thus significantly reducing any environmental risks as well.

This method has been applied in Borkum Riffgrund II Wind Farm. The jackets were manufactured in Poland and transported to Cuxhaven on barges, three at a time (Figure 2-21). A crawler crane lifted the jackets and placed them onto the previously positioned buckets (Figure 2-22). The assembled units were then transported by a self-propelled modular transporter across the heavy-duty berth to be placed in a specially prepared storage area until a heavy lift jack-up vessel transported them to the site (Figure 2-23) and completed their installation (Figure 2-24). The pump skids used for the installation of the suction buckets were pre-rigged to the foundations (Figure 2-25). A launch and recovery system attached to the installation vessel enabled them to remain attached to the buckets until the jacket substructure was securely fixed on the seabed, then return to the vessel.

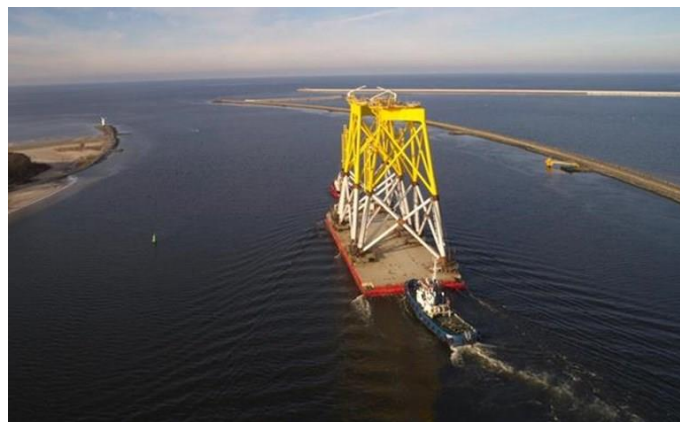


Figure 2-21 Borkum Riffgrund II Offshore Wind Farm jackets being transported from the manufacturing facility to the assembly terminal (renews.biz)



Figure 2-22 Borkum Riffgrund II Offshore Wind Farm jackets and suction buckets at the assembly terminal (www.rhenus.group)



Figure 2-23 Suction bucket jacket being picked up by heavy lift jack-up vessel ([www.maritimejournal.com](http://www.maritimejournal.com))



Figure 2-24 Suction bucket jacket being installed by heavy lift jack-up vessel ([www.mynewsdesk.com](http://www.mynewsdesk.com))

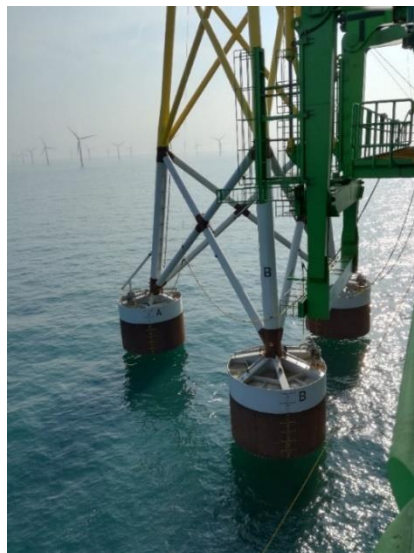


Figure 2-25 Pump technology for suction bucket jacket ([www.framo.com](http://www.framo.com))

### 2.1.1.3 TRIPOD

A tripod foundation shares some common characteristics with the jacket foundation and some with the monopile. It has a pyramid-shaped space frame constructed from hollow cylindrical steel members. A diagonal brace connects each leg to a cylindrical central column that is similar to a monopile, except that the central column does not enter the seabed. Secondary hollow cylindrical structural members connect the three legs together and provide additional support for the central column, which rises above the waterline to provide a base for the turbine tower (Horwath, et al., 2021).

As in the case of jackets, the bolted connection between the tower and the tripod's transition piece is achieved with a flange, which is welded to the top and bottom of the hollow cylindrical segments and bolted traditionally. However, when a tripod is used, the use of a transition piece is not strictly necessary. This is the case of the Alpha Ventus Wind Farm, where the central steel shaft of the tripod itself makes the transition to the wind turbine tower, to reduce the installation time and associated costs (Figure 2-26). The J-tube, boat lander and platform may be connected to the upper part of the tripod. Alternatively, the transition piece may be welded on the tripod substructure at a later stage, which was the case in the Borkum West II and Global Tech I Offshore Wind Farms (Figure 2-27).



Figure 2-26 Tripod for Alpha Ventus Offshore Wind Farm being welded, transition piece integrated ([www.wikiwand.com](http://www.wikiwand.com))



(a)



(b)

Figure 2-27 Tripod substructures, transition piece not integrated (a) tripod for the Borkum West II Offshore Wind Farm being welded ([www.trianel-borkum.de](http://www.trianel-borkum.de)) (b) tripods for the Global Tech I Offshore Wind Farm ([www.offshorewind.biz](http://www.offshorewind.biz))

The three-legged tripod base transfers the vertical loads to the seabed through piles or suction caissons. As in the case of the jacket foundation, horizontal forces create an overturning moment, which is resisted by a combination of compression and tension forces transferred from the piles or caissons to the seabed.

The bracing that connects the central column and the legs enables the reduction of the central column's diameter in comparison to that of a monopile (Horwath, et al., 2021).

Like a jacket foundation, piles or suction caissons at the corners of the tripod's triangular base anchor the foundation to the seabed. Piling can be performed either prior (Borkum West II) or subsequently (Alpha Ventus & Global Tech I) to the installation of the substructure. The tripod can have either vertical or inclined pile sleeves (DNV-GL, 2018). The possibility of installing a wind turbine atop a tripod substructure by means of the suction bucket foundation method is currently under examination. However, various meteorological masts have been installed on suction-bucket-foundation tripods, such as the HeMOSU-2 meteorological mast in the Southwest Offshore Wind Project in South Korea, and the CLP Met Mast constructed as part of the Hong Kong Offshore Wind Farm Project.

The principle for pre-piling described in chapter 2.1.1.2., is also possible in the case of a tripod, the only difference being that the tripod-pile mating is made via tripod leg sleeves instead of stab-ins. Firstly, a template is placed on the seabed (Figure 2-28). The piles are hoisted, upended, and lowered into the template, then driven by a hydraulic hammer. When all piles are installed, the template is removed. Secondly, the tripod substructure is placed onto the pre-installed piles by means of pile sleeves (Figure 2-29). Finally, the pile and jacket leg sleeves are grouted together (Figure 2-30).



Figure 2-28 Pre-piling template for the Borkum West II Offshore Wind Farm tripods (twd.nl)



Figure 2-29 Borkum West II Offshore Wind Farm tripod being installed (www.trianel-borkum.de)



Figure 2-30 Borkum West II Offshore Wind Farm tripod fully installed ([www.trianel-borkum.de](http://www.trianel-borkum.de))

During an installation with the post piling method, the tripod is initially placed on the seabed. Its positioning is carried out by a heavy lift vessel (Figure 2-31). The foundation piles are then driven through the pile sleeves at the corners of the tripod by means of a hydraulic hammer (Figure 2-32). The pile driving is usually carried out by the heavy lift vessel as well. Alternatively, it can be performed by a smaller crane vessel or a jack-up. When the pile top has reached the same height level as the pile sleeve, they are grouted together (van Wijngaarden, 2013).



(a)



(b)

Figure 2-31 Tripod installation (a) tripods for the Global Tech I Offshore Wind Farm being shipped to site on board a heavy-lift jack-up vessel ([www.offshorewind.biz](http://www.offshorewind.biz)) (b) tripod being installed at the Global Tech I Offshore Wind Farm ([www.rechargenews.com](http://www.rechargenews.com))

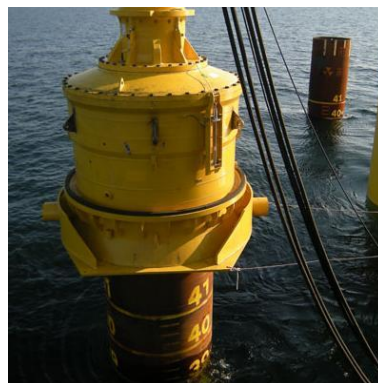


Figure 2-32 Pile being hammered into the seabed at the Alpha Ventus Offshore Wind Farm ([www.menck.com](http://www.menck.com))

#### 2.1.1.4 TRIPILE

A tripile foundation consists of three steel pile legs joining the transition piece above the waterline and therewith, forming a space frame that supports the wind turbine tower and turbine. Alternatively, the three piles could be jointed below the waterline to support a tower that rises above the water surface. Tripile foundations incorporate features of both the monopile and the tripod substructures. The legs are similar to monopiles but smaller in diameter. The three legs distribute the load over a larger footprint, similarly to the mechanism of the tripod foundation. The three piles transfer the vertical loads to the seabed. As with a tripod foundation, horizontal forces create an overturning moment that is resisted by the stiffness of the three piles on the one hand, a combination of compression and tension forces carried by the piles to the seabed on the other hand (Horwath, et al., 2021). Tripile foundations are currently installed only at two wind farms: BARD Offshore 1 and the single-turbine prototype Hooksiel (Figure 2-33).

Tripiles are anchored in the seabed using a pile-driving template (Figure 2-34). The three steel tubes are then joined together by a crosspiece (Figure 2-35) to carry the wind turbine. At the center of the transition piece, there is a connection flange for the wind turbine tower to be fitted onto. The pile-crosspiece connection is typically grouted, but could potentially be swaged as well.



(a)



(b)

Figure 2-33 Wind farms featuring tripiles (a) Bard Offshore 1 Offshore Wind Farm ([www.power-technology.com](http://www.power-technology.com))  
(b) Hooksiel prototype ([www.renewableenergyworld.com](http://www.renewableenergyworld.com))



Figure 2-34 Piles being installed at the Bard Offshore 1 Wind Farm ([www.power-technology.com](http://www.power-technology.com))





Figure 2-35 Tripiles in Bard's manufacturing base in the German port of Emden ([www.windpowermonthly.com](http://www.windpowermonthly.com))

#### 2.1.1.5 GRAVITY-BASED FOUNDATION

Gravity-based structures are the most common type of foundation for onshore wind turbines and were therefore chosen for early offshore wind turbines situated in very shallow waters. They consist of wide, heavy bases that lie on the seabed and support the cylindrical central column that rises above the waterline. The base is most commonly made of reinforced concrete, but steel designs are also used. The gravity base supports the vertical loads of the wind turbine by direct contact pressure with the seabed and therefore requires soils with a high bearing capacity. The overturning moment created by horizontal forces is counterbalanced by the weight of the base and the rest of the turbine structure (Horwath, et al., 2021).

Wind turbines with gravity-based foundations have three main subsystems: the tower, the caisson and the foundation bed. The caisson consists of a hollow concrete container and infill aggregates to reach the design weight of the support structure. The deformable foundation bed includes gravel mound, backfill layer, and natural ground to resist against the external forces and energy transmitted from the tower and the caisson (Nguyen, Lee, & Kim, 2019).

In order to enable sufficient bearing resistance, the seabed requires preparation prior to the installation of the concrete gravity base, which is not the case for the installation of monopiles and jackets. First, the upper seabed layer is removed using a dredger or a back-hoe excavator placed on a barge or other vessel up to a level where undisturbed soil is encountered. The dredged material, if suitable for filling the support structures, is disposed of nearby by split-hopper barges for later use. In a different case, it is disposed of at sea at a registered disposal site. Secondly, gravel is deposited in the hole to form a firm level base. Upon completion of installation, the gravity structure, and maybe nearby placed cables, are protected against development of scour by installation of a filter layer and armor stones, or other material like sandbags and concrete mattresses (Esteban, Couñago, López-Gutiérrez, Negro, & Vellisco, 2015).

Offshore gravity-based structures can be built using in-situ concrete as well as precast element solutions and are typically constructed onshore and towed to their final position offshore. Tanks or cells inside the gravity-based structure can be used to provide buoyancy during transportation to the project site. Two different techniques are used for transportation, either single transportation and installation of support structures by a heavy-lift vessel, or transportation of a number of support structures on a barge and use of a heavy-lift vessel for installation. Upon arrival at the project site, the gravity-based structure is set down by flooding the cells with water. To have sufficient ballast, cells can be filled with sand, rock, or other materials (Esteban, Couñago, López-Gutiérrez, Negro, & Vellisco, 2015) (DNV-GL, 2018).

The bottom flange of the tower is anchored to the concrete by means of pretensioned bolts. There are basically two different connecting systems: the steel pipe with a flange which is embedded in concrete, and the so called "bolt cage" where several long bolts are embedded in concrete (Figure 2-36). The bolt cage, which consists of a double rowed circular array of threaded steel bolts, is usually preferred in practice. A retainer ring, fitted to the tower flange dimensions, is used to hold the individual bolts in position. When the foundation is completed, the lower tower section is placed on the bolts protruding out of the concrete surface and then bolted with nuts and washers (Stavridou, Efthymiou, & Baniotopoulos, 2015).

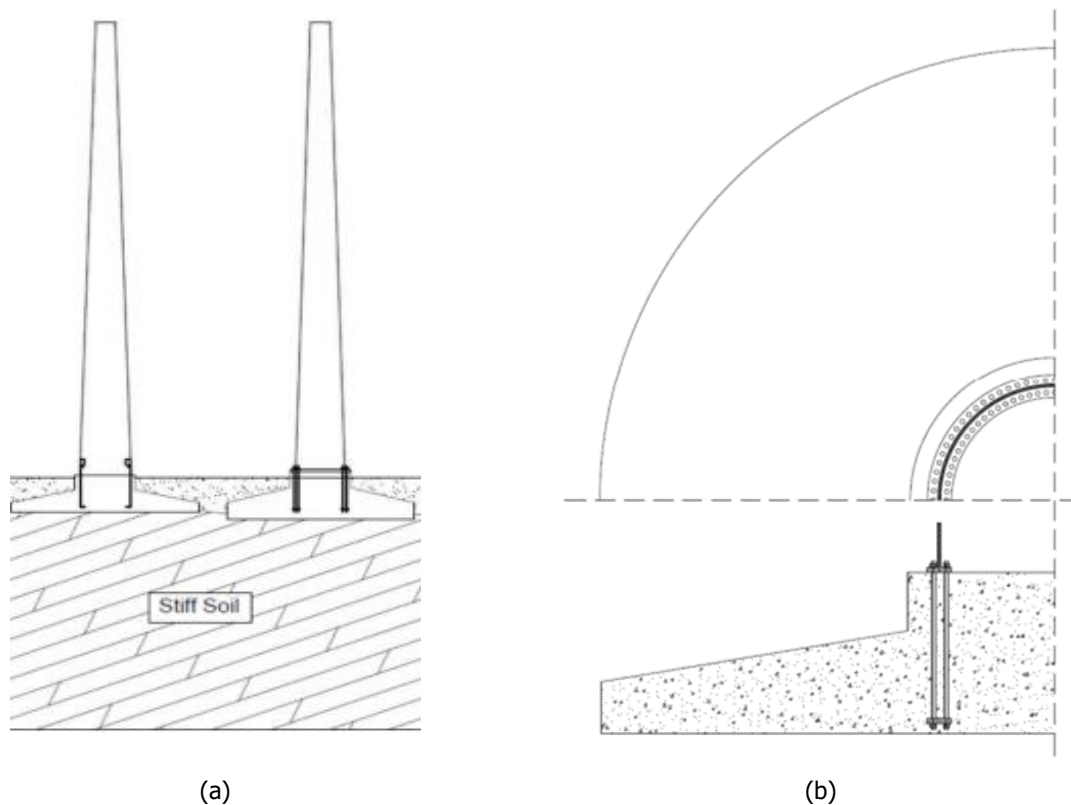


Figure 2-36 Tower connection to gravity-based substructure (a) ways to anchor tower bottom flange into concrete (b) detail of the "bolt cage" system (Stavridou, Efthymiou, & Baniotopoulos, 2015)

The Lillgrund Offshore Wind Farm in Sweden features 48 large concrete gravity-based foundations weighing around 1,400 tonnes each, and has a total capacity of 110MW. It was commissioned in December 2007 and continues to be Sweden's largest offshore wind farm. When it was commissioned, it was the third-largest wind farm in the world. The concrete foundations are placed in water depths ranging from 6m to 11m.

The substructures were cast directly on barges in the port of Swinoujscie in Poland (Figure 2-37). Tower bolts and other secondary structures were cast into the foundation (Figure 2-38). After completion of four foundations, which was the maximum number per barge, the foundations were towed to the site (Figure 2-39). Simultaneously to the casting process taking place in Poland, the dredging work at Lillgrund was initiated. Upon completion of dredging, a layer of crushed rock was placed on the seabed to level the excavated area. The foundations were then positioned using a crane barge (Figure 2-40). Next steps included the installation of filter rock, fitting of J-tube extensions, and installation of ballast rock, and armor rock together with filter rock around the J-tube extensions (Figure 2-41). Thereafter, ballast fill was placed in the shaft of the foundation and a concrete slab was cast on the top of each foundation (Jeppsson, Larsen, & Larsson, 2008).



Figure 2-37 Concrete foundations being cast (Jeppsson, Larsen, & Larsson, 2008)



Figure 2-38 Tower bolts to be cast into the foundation (Jeppsson, Larsen, & Larsson, 2008)



Figure 2-39 Concrete foundations being towed to Lillgrund site (Jeppsson, Larsen, & Larsson, 2008)



Figure 2-40 Concrete substructures being lowered into position (Jeppsson, Larsen, & Larsson, 2008)

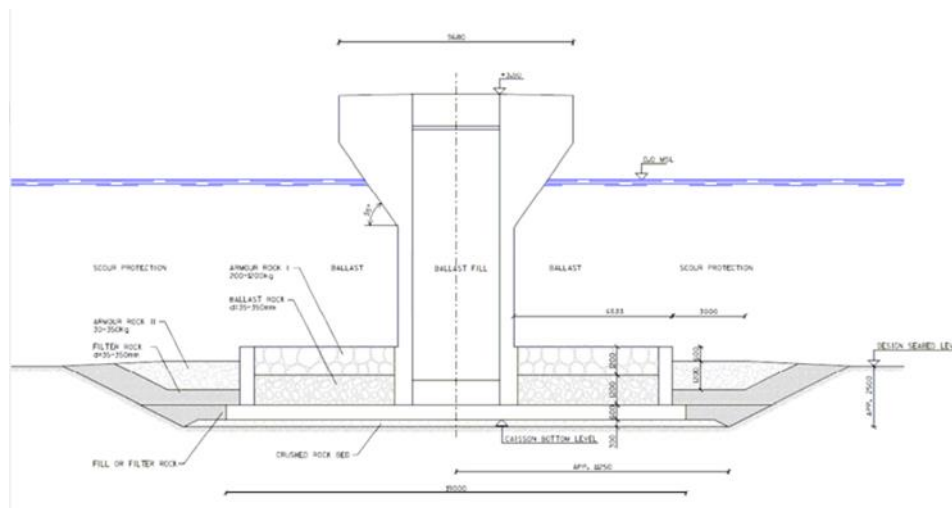


Figure 2-41 Concrete substructure cross-section (Jeppsson, Larsen, & Larsson, 2008)

## 2.1.2 FLOATING SYSTEMS

A key component of all floating designs is the anchoring system. The most commonly employed floating systems, spars and semi-submersibles, use catenary mooring systems with mooring lines at low tension to restrict the sway and surge motion of the floating wind turbine into the required limits. The mooring lines may be connected to deadweight anchors that sit on the seabed, drag anchors that are activated when pulled through the soil, dynamically embedded anchors, driven piles or suction caissons. Deadweight anchors made of concrete or steel have the greatest mass and the largest footprint. Drag anchors are made of steel and once activated, lie largely or entirely below the mudline. Dynamically embedded anchors use various systems to force the holding surfaces of the anchor deep into the seabed to increase its holding power. The mooring lines for spars and semi-submersibles may also be anchored with piles and suction caissons. Regardless of the anchor type, attaching a length of heavy ground chain or rode to the anchor is common practice (Horwath, et al., 2021).

### 2.1.2.1 SEMI-SUBMERSIBLE

Semi-submersibles have multiple submerged columns or hulls attached together with connecting braces. The hulls provide sufficient buoyancy to cause the structure to float and resist overturning (Horwath, et

al., 2021). The wind turbine is attached via a transition piece mounted on the upper surface of the substructure. The column and the tower are connected through a flange, which is either bolted or welded. A boat landing platform is installed on one or two of the columns.

Kincardine is the world's first floating wind power project to use wind turbines of more than 9MW capacity. The wind farm features a total of six offshore turbines including five V164-9.525MW turbines and one V80-2.0MW by MHI Vestas. The V80-2.0MW wind turbine has been operating on site since October 2018. The wind turbines are installed on triangular-shaped semi-submersible foundations. The foundations are moored in water depths in the range of 60m to 80m through four mooring lines each, which are secured on the seabed using drag-embedded anchors. The foundations are equipped with an automatic active ballast system that allows the platform to be always kept upright.

The foundations were fabricated in Spain and transported to Rotterdam by a semi-submersible barge, towed by a tug (Figure 2-42). In Rotterdam, the project's wind turbines were mounted onto the floating foundations at the quayside (Figure 2-43) in order to eliminate the need to use massive vessels and perform expensive operations offshore. The assembled units were then towed to the installation site southeast of Aberdeen (Figure 2-44). At the installation site, the turbine was hooked up to the already installed mooring system by a construction vessel in a water depth of approximately 70m (Figure 2-45). While two anchor handlers retained the floater in position, the hook-up construction vessel launched its ROV (remotely operated underwater vehicle) that connected the mandrel from the seabed to the receptacle on the floater. This was followed by pulling in the mooring lines with the winch of the floater.



Figure 2-42 Kincardine Offshore Wind Farm semi-submersible foundations being transported to assembly base ([www.projectcargojournal.com](http://www.projectcargojournal.com))



Figure 2-43 Wind turbines being mounted on semi-submersible foundations for Kincardine Offshore Wind Farm ([www.principlepower.com](http://www.principlepower.com))



Figure 2-44 Kincardine Offshore Wind Farm assembled units being towed to project site ([www.offshorewind.biz](http://www.offshorewind.biz))



(a)



(b)

Figure 2-45 Semi-submersible foundation being installed for Kincardine Offshore Wind Farm (a) assembled unit being hooked up to the already installed mooring spread ([www.cnbc.com](http://www.cnbc.com)) (b) anchor handling tug supply vessel (AHTS) assisting the mooring of the assembled units ([www.oedigital.com](http://www.oedigital.com))

#### 2.1.2.2 SPAR

Spars consist of a single ballasted vertical cylinder that supports the tower and extends well below the waterline. The submerged ballast keeps the structure upright (Horwath, et al., 2021). The ballast lowers the center of gravity so that it is below the center of buoyancy.

Hywind Scotland, world's first floating wind farm, features five floating cylindrical spar buoys moored to the seabed by means of a conventional 3-line mooring system made of steel chains, and suction anchors. The floating structure consists of a steel cylinder filled with ballast water and rock or iron ore. The structure has a design draft of 85m to 90m and a displacement of around 12,000tonnes. The diameter at the water line is about 9m to 10m, while the diameter of the submerged section of the buoy is 14m to 15m. Hywind uses a ballasted catenary layout with three mooring cables with 60tonnes sinkers hanging from the midpoint of each anchor cable to provide additional tension (Equinor, 2022).

The buoys were manufactured in the Fene shipyard in Spain, transported in a horizontal position on a semi-submersible heavy lift vessel (Figure 2-46) and unloaded off the project's onshore assembly base in Stord, Norway. Subsequently, each buoy was filled with water until the structure upended itself (Figure 2-47). Gravel and stone were then used to lower the structure to reach its design draft. The turbines and towers were assembled onshore in Stord (Figure 2-48) and transported off the coast of

Stord to be placed on their substructures by a semi-submersible crane vessel (Figure 2-49) and get connected to them through a bolted flange. Finally, the assembled units were towed to the installation site off Scotland by a tugboat (Figure 2-50).



Figure 2-46 Spar buoys being transported from the manufacture base off the project's assembly base ([www.offshorewind.biz](http://www.offshorewind.biz))



Figure 2-47 Spar buoys being upended ([www.ptil.no](http://www.ptil.no))



Figure 2-48 Turbines being assembled at project's assembly base ([www.businessinsider.com](http://www.businessinsider.com))

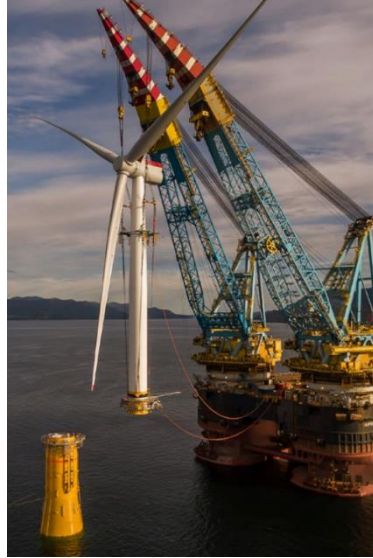


Figure 2-49 Turbine being mated with spar substructure (www.saipem.com)



Figure 2-50 Assembled structures being towed to the project's site (www.businessinsider.com)

## 2.2 LARGEST OFFSHORE WIND FARMS

All offshore wind farms with at least 400MW nameplate capacity that are currently operational are presented in Table 2-1, while all currently operational offshore wind farms featuring floating support structures for the wind turbines are presented in Table Table 2-2.

Table 2-1 Major offshore wind farms featuring bottom-fixed substructures

Wind farm	Country	Capacity (MW)	Year of commissioning	Type	Depth (m)
Hornsea 1	U.K.	1,218	2019	Monopile	20-40
Borssele 1 & 2	Netherlands	752	2020	Monopile	14-36
Borssele 3 & 4	Netherlands	731.5	2021	Monopile	16-38
East Anglia ONE	U.K.	714	2020	Jacket with piles	30-53
Walney Extension	U.K.	659	2018	Monopile	up to 54



Wind farm	Country	Capacity (MW)	Year of commissioning	Type	Depth (m)
London Array	U.K.	630	2013	Monopile	up to 25
Kriegers Flak	Denmark	605	2021	Monopile	up to 25
Gemini	Netherlands	600	2017	Monopile	28-36
Beatrice	U.K.	588	2019	Jacket with piles	55
Gode Wind (phases 1 & 2)	Germany	582	2017	Monopile	28-34
Gwynt y Môr	U.K.	576	2015	Monopile	15-30
Race Bank	U.K.	573	2018	Monopile	6-26
Greater Gabbard	U.K.	504	2012	Monopile	24-34
Hohe See	Germany	497	2019	Monopile	up to 40
Borkum Riffgrund 2	Germany	450	2019	Suction bucket jackets + monopiles	25-30
Horns Rev 3	Denmark	407	2019	Monopile	10-20
Dudgeon	U.K.	402	2017	Monopile	18-25
Veja Mate	Germany	402	2017	Monopile	39-41
Anholt	Denmark	400	2013	Monopile	15-19
BARD Offshore 1	Germany	400	2013	Tripile	40-44
Global Tech I	Germany	400	2015	Tripod with piles	38-41
Rampion	U.K.	400	2018	Monopile	19-40
Binhai North H2	China	400	2018	Monopile	14-18

Table 2-2 Major offshore wind farms featuring floating substructures

Wind farm	Country	Capacity (MW)	Year of commissioning	Type	Depth (m)
Kincardine Floating Offshore Wind Farm	Scotland	50	2021	Semi-sub	60-80
Hywind Scotland	Scotland	30	2017	Spar	95-120
Windfloat Atlantic	Portugal	25	2020	Semi-sub	60

### 2.3 TECHNOLOGY SELECTION CRITERIA

The predominant criteria considered when choosing which of the aforementioned designs to implement is the site depth and the soil conditions (Table 2-3). Of course, cost, manufacturing capacity, materials and equipment availability are other major decision criteria, however they are considered to be outside the scope of the present work.

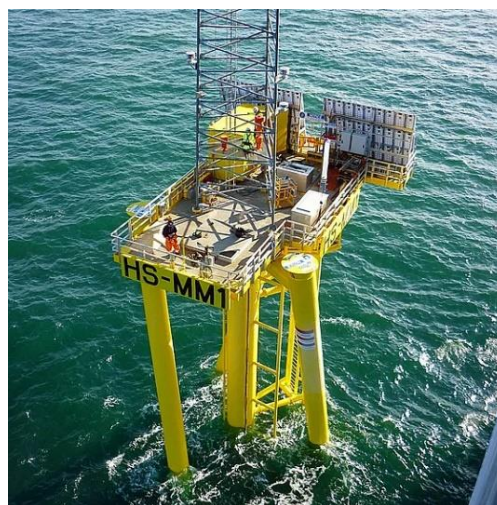
Table 2-3 Acceptable depth and type of soil for each type of foundation (Horwath, et al., 2021)

Substructure type	Max. depth	Type of soil
		<b>Fixed</b>
Monopile	50	Sands and clays preferred. Not suitable for shallow bedrock or strata with boulders, cobbles, or coarse gravel.
		With piles
Jacket	60	Stiff clays and medium to dense sands preferred. Possible in softer silts and clay, and in very soft sediments overlying stiffer soils or bedrock. Less well suited for locations with many boulders. (Soft-soil installations are possible with longer pile lengths.)
		With suction caissons
		Medium stiff clays and fine to medium sand preferred. Not suitable for strata with cobbles, boulders, or coarse gravel layers or in very soft soils.
Tripod	50	Same as jacket.
Tripile	40	Sands and clays preferred. Not suitable for shallow bedrock or strata with boulders, cobbles, or coarse gravel.
Gravity	40	Sand, medium to stiff clays, bedrock, and strata with cobbles, boulders, or coarse gravel. Not suitable for very soft soils or weak clays. Seabed preparation like dredging is typically required.
		<b>Floating</b>
Semi-sub		Medium stiff clays, fine to medium sands, coarse sands, and gravel.
Spar	220	Less well suited for locations with many boulders. Anchors available for any geological seabed condition.

## 2.4 CURRENTLY INVESTIGATED TECHNOLOGIES

Although technical knowledge from the offshore oil and gas industry can be directly adopted by the offshore wind industry, many differences can be found when comparing offshore wind structures to oil and gas structures. The larger wind loading contribution, the influence of dynamics and nonlinearities, shallow-water sites potentially leading to breaking waves, and the fact that wind turbines are “low risk structures” (unmanned, low pollution hazards) compared to oil and gas structures are the most prominent amongst others (Vorpahl, Schwarze, Fischer, & Seidel, 2013). Basic principles of many technologies that are currently under investigation, such as the twisted jacket and jack-up foundations, can be traced back to the oil and gas industry.

The Inward Battered Guide Structure (IBGS), or “twisted jacket” ([www.keystoneengr.com](http://www.keystoneengr.com)), is currently utilized to support two oil and gas platforms in the Gulf of Mexico, the Hornsea Meteorological Mast in the Hornsea Offshore Wind Farm (Figure 2-51) and elsewhere.

Figure 2-51 Hornsea Met Mast ([www.keystoneengr.com](http://www.keystoneengr.com))

Jack-up foundations have been used in the offshore oil and gas industry for decades as support structures for drilling rigs and platforms. Their application in the offshore wind industry is currently under discussion. A jack-up foundation consists of a floatable platform with three or four legs that can be raised and lowered relative to the platform (Figure 2-52). When lowered, the jack-up legs pierce the seabed under the weight of the structure, plus the weight of any additional temporary ballast water. Footings or spud cans on the legs can facilitate the load distribution from the legs to the soil. Once the legs are set, ballast water is drained, and the hull is jacked-up above the water surface to its operational height (Horwath, et al., 2021).

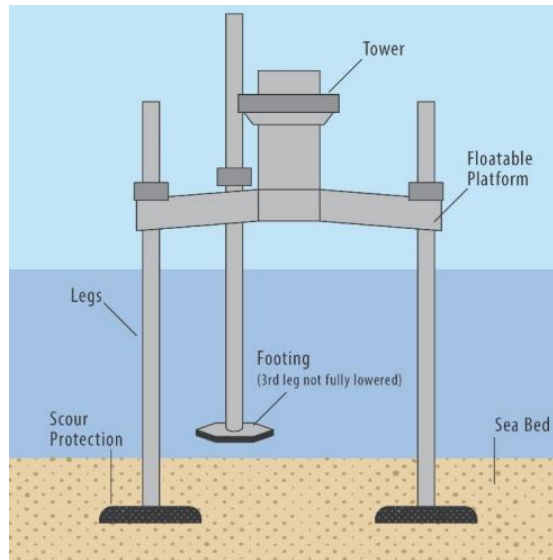


Figure 2-52 Illustration of jack-up foundation for wind turbine (Horwath, et al., 2021)

The mono-bucket substructure is essentially a single, large-diameter suction caisson. Although there are currently no large-scale commercial offshore wind projects that use this type of foundation, it has been used to support several meteorological masts, such as the one that used to serve Horns Rev 2 Wind Farm, and various wind turbine prototypes, such as the ones in Frederikshavn, Denmark and Wilhelmshaven, Germany (Horwath, et al., 2021). Deutsche Bucht is the first commercial offshore wind farm to feature mono-bucket foundations, as part of a pilot project designed to test the technology (Figure 2-53). More specifically, Deutsche Bucht features thirty-one monopiles and two mono-bucket foundations.



Figure 2-53 Mono-bucket substructure and turbine components being loaded onto jack-up vessel ([www.offshorewind.biz](http://www.offshorewind.biz))

Tension Leg Platforms (TLP's) are buoyant multihull steel floating platforms vertically moored to the seafloor by a group of tendons to minimize vertical movement of the structure. An additional downward and stabilizing force is induced by tension forces developed in the tendons. TLP's use tendons that maintain tension against the buoyancy of the wind turbine platform, most often utilizing piles or suction caissons for their greater and more reliable pullout resistance. Unlike drag anchors, piles or suction caissons utilized for TLP's are precisely positioned during installation (Horwath, et al., 2021). Although various prototypes of this technology are being developed, the platform will be employed on a commercial level for the first time as part of Provence Grand Large scheme off southern France, expectedly in 2023 (Figure 2-54). More specifically, three Siemens Gamesa turbines, each with a capacity of 8.4MW, will be installed atop TLP substructures.



Figure 2-54 Illustration of Provence Grand Large TLP substructure ([www.provencegrandlarge.fr](http://www.provencegrandlarge.fr))

The barge floater is another floating support structure for wind turbines, currently being studied by various developers, such as the ITI Energy barge (Jonkman & Matha, A Quantitative Comparison of the Responses of Three Floating Platforms, 2009) and Floatgen (<https://floatgen.eu/en>). Like the semi-submersible substructure, a barge platform is a waterplane-area stabilized structure (Figure 2-55). The main difference between the two, is that a semi-submersible has distributed buoyancy and consists of columns, while a barge is typically flat without interspaces.

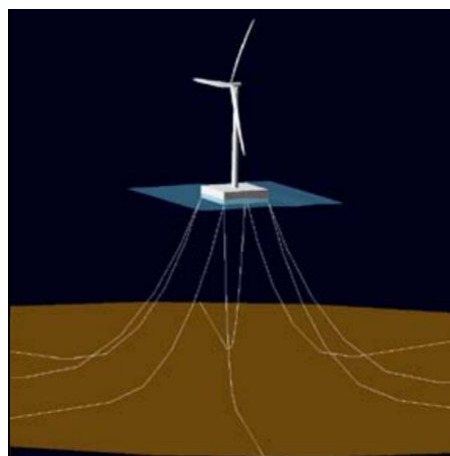


Figure 2-55 Illustration of the ITI Energy barge (Jonkman & Matha, A Quantitative Comparison of the Responses of Three Floating Platforms, 2009)

# 3 THEORETICAL BACKGROUND

## 3.1 WIND TURBINE CLASSIFICATION

Wind turbine classification allows structural engineers to demonstrate the feasibility of their design or design concept for generic offshore conditions without having extensive knowledge of the extreme waves and turbulence conditions. The basic parameters that define offshore wind turbine classes, are specified in Table 3-1, found in (DNV-GL, 2016). The design of an offshore wind turbine and its support structure depends though on more parameters than turbulence and extreme wave height and period. Wave spectra, long-term wave distribution, water depth, soil conditions and current profile have major influence on the design structural behavior and must therefore be carefully determined during the design process.

Table 3-1 Wind turbine classes (Source: (DNV-GL, 2016))

<b>Wind turbine class</b>	<b>I</b>	<b>II</b>	<b>III</b>
$V_{ref}$ (m/s)	50	42.5	37.5
$V_{ave}$ (m/s)	10	8.5	7.5
OA (high turbulence intensity)	$H_{ref}$ (m)	10	
	$T_{ref}$ (s)	12.5	
	$I_{ref}$ (-)	0.14	
	$t_a$ (m/s)	10	
	$t_b$ (-)	0.566	
	$A_c$ (m)	0.018	
OB (medium turbulence intensity)	$H_{ref}$ (m)	6	
	$T_{ref}$ (s)	10	
	$I_{ref}$ (-)	0.12	
	$t_a$ (m/s)	10.5	
	$t_b$ (-)	0.561	
OC (low turbulence intensity)	$A_c$ (m)	0.014	
	$H_{ref}$ (m)	2	
	$T_{ref}$ (s)	5.5	
	$I_{ref}$ (-)	0.1	
	$t_a$ (m/s)	11	
	$t_b$ (-)	0.566	
	$A_c$ (m)	0.011	

Where:

$V_{ref}$	maximum value of the 10-min mean of the extreme wind speed with a recurrence period of 50 years at hub height
$V_{ave}$	annual average wind speed over many years at hub height
$H_{ref}$	maximum value of the 3-hour average of the extreme sea state, with a recurrence period of 50 years
$T_{ref}$	Wave period corresponding to $H_{ref}$
$I_{ref}$	reference value of the wind speed turbulence intensity at 15m/s
$t_a$	turbulence offset factor
$t_b$	turbulence shape factor
$A_c$	Charnock's constant

A turbine designed according to a wind turbine class with a reference wind speed  $V_{ref}$ , is designed to withstand environmental conditions, for which the 10-min mean of the extreme wind speed with a recurrence period of 50 years at hub height is less than or equal to  $V_{ref}$ . In the DNV-GL standard,  $V_{ave}$  means the annual average of the wind speed over many years.

A support structure designed for a wave class with a reference significant wave height  $H_{ref}$  and period  $T_{ref}$ , is designed to withstand the environmental conditions in which the 3-hour average of the extreme sea state, in combination with a JONSWAP spectrum, with a recurrence period of 50 years is less than or equal to  $H_{ref}$  and  $T_{ref}$ , respectively. The design of support structures for offshore wind turbines shall be based on environmental conditions, which are characteristic at the specific site, at which the offshore wind turbine is to be installed. In some cases, generic design for the support structure or some of its parts is acceptable. The corresponding metocean conditions to be used for generic design may be derived using wave classes OA through OC (DNV-GL, 2016).

## 3.2 LOADS ACTING ON A WIND TURBINE

### 3.2.1 WIND

As wind turbines are subject to massive aerodynamic loads, they must be designed to withstand both normal and extreme wind conditions. Normal wind conditions are expected to occur frequently during normal operation of a wind turbine. Extreme wind conditions refer to extreme wind loads with a recurrence period of 1 or 50 years.

Normal wind conditions include the Normal Wind Profile (NWP) and the Normal Turbulence Model (NTM). The wind profile,  $V_z$ , denotes the average wind speed as a function of height  $z$  above mean sea level and is described by the power law given in Eq. (3-1). In the case of standard wind turbine classes (Table 3-1), the normal wind speed profile (NWP) is given by Eq. (3-2), where the power law exponent has been replaced by the value 0.2. The Normal Turbulence Model (NTM) is used to define turbulence under normal operation conditions. This model uses the normal wind profile model and turbulence with longitudinal component standard deviation,  $\sigma_{1,NTM}$ , given by Eq. (3-3) (IEC, 2005).

The extreme wind conditions include wind shear events, extreme wind speeds due to storms, and rapid changes in wind speed and direction. The extreme models described herein include the Extreme Wind Speed Model (EWM), the Extreme Operating Gust (EOG), and the Extreme Turbulence Model (ETM). The EWM is either a steady or a turbulent wind model, based on the reference wind speed,  $V_{ref}$ , and a fixed turbulence standard deviation,  $\sigma_{1,EWM}$ , given by Eq. (3-6). For the steady EWM, the extreme wind speed with a recurrence period of 50 years,  $V_{50,EWM,steady}$ , is computed as a function of height  $z$ , using Eq. (3-4). For the turbulent EWM, the corresponding 10-min average wind speed with a recurrence period of 50 years, extreme wind speed,  $V_{50,EWM,turb}$ , is given by Eq. (3-5). When it comes to the EOG, the hub-height gust magnitude  $V_{gust}$  is given by Eq. (3-7) for the standard wind turbine classes, and the longitudinal component standard deviation is the same as in the NTM. The Extreme Turbulence Model (ETM) uses the normal wind profile model and turbulence with longitudinal component standard deviation given by Eq. (3-8) (IEC, 2005).

$$V_z = V_{hub} * \left( \frac{z}{z_{hub}} \right)^a \quad (3-1)$$

$$V_{z,NWP} = V_{hub} * \left( \frac{z}{z_{hub}} \right)^{0.2} \quad (3-2)$$

$$\sigma_{1,NTM} = \sigma_{1,EOG} = I_{ref} * (0.75 * V_{hub} + 5.6) \quad (3-3)$$

$$V_{50,EWM,steady} = 1.4 * V_{ref} * \left( \frac{z}{z_{hub}} \right)^{0.11} \quad (3-4)$$

$$V_{50,EWM,turb} = V_{ref} * \left( \frac{z}{z_{hub}} \right)^{0.11} \quad (3-5)$$

$$\sigma_{1,EWM} = 0.11 * V_{hub} \quad (3-6)$$

$$V_{gust} = \min \left[ 1.35 * (0.8 * V_{50,EWM,steady} - V_{hub}), 3.3 * \frac{\sigma_{1,EOG}}{1 + 0.1 * \frac{D}{\Lambda_1}} \right] \quad (3-7)$$

$$\sigma_{1,ETM} = 2 * I_{ref} * \left[ 0.072 * \left( \frac{V_{ave}}{2} + 3 \right) * \left( \frac{V_{hub}}{2} - 4 \right) + 10 \right] \quad (3-8)$$

Where:

$V_z$	wind speed at height $z$ above mean sea level
$V_{hub}$	wind speed at hub height
$z$	vertical coordinate, measured positively upwards from mean sea level
$z_{hub}$	hub height
$V_{ref}$	maximum value of the 10-min mean of the extreme wind speed with a recurrence period of 50 years at hub height, values from Table 3-1
$V_{ave}$	annual average wind speed over many years at hub height, values from Table 3-1

$I_{ref}$	reference value of the wind speed turbulence intensity at 15m/s, values from Table 3-1
$a$	wind shear (or power law) exponent
$\sigma_1$	standard deviation of the longitudinal wind speed at hub height
$D$	rotor diameter
$\Lambda_1 = \begin{cases} 0.7 \cdot z_{hub}, & \text{if } z_{hub} \leq 60\text{m} \\ 42\text{m}, & \text{if } z_{hub} \geq 60\text{m} \end{cases}$	longitudinal turbulence scale parameter

### 3.2.2 WAVE

For offshore wind turbines, it is fundamental to determine the impact of wave loading on the structure. The wave regime is represented by the significant wave height  $H_s$  and the spectral peak period  $T_p$ . In the short term, i.e., over a 3-hour or 6-hour period, stationary wave conditions with constant values of  $H_s$  and  $T_p$  are assumed to prevail. For use in design load combinations, a number of reference sea states and corresponding wave heights are defined. The Normal, Severe and Extreme Sea States are described below.

The Normal Sea State (NSS) is characterized by a significant wave height, a peak period, and a wave direction. It is associated with a concurrent mean wind speed. The significant wave height  $H_{s,NSS}$  of the normal sea state is defined as the expected value of the significant wave height conditioned on the concurrent 10-minute mean wind speed. The normal sea state is used for calculation of both ultimate and fatigue loads.

Similarly, the Severe Sea State (SSS) is characterized by a significant wave height, a peak period, and a wave direction. This model associates a severe sea state with each mean wind speed, to calculate the ultimate loading of an offshore wind turbine during power production. For all 10-minute mean wind speeds at hub height ( $V_{hub}$ ) in the range of power production, the unconditional extreme significant wave height,  $H_{s,50yrs}$ , with a return period of 50 years may be used as a conservative estimate for  $H_{s,SSS}|V_{hub}$ .

The Extreme Sea State (ESS) considers combined environmental actions with return periods of 1 and 50 years. Both the extreme significant wave height ( $H_{s,50yrs}$  and  $H_{s,1yr}$ ) and the extreme individual wave height ( $H_{50yrs}$  and  $H_{1yr}$ ) should be checked during the design process.

Wind-wave misalignment, i.e., differences of the mean wind and wave directions can have an important influence on loads of offshore wind turbines and should therefore be considered. Co-directional wind and waves shall be assumed if this can be shown to be a conservative assumption.

Waves are irregular in shape, vary in height, length and speed of propagation, and may approach an offshore wind turbine from one or more directions simultaneously. A stochastic wave model represents the sea state as the superposition of many small individual frequency components, each of which is a periodic wave with its own amplitude, frequency and direction of propagation; the components have random phase relationships to each other. In some applications, periodic or regular waves can be used as an abstraction of a real sea for design purposes. A deterministic design wave shall be specified by its height, period and direction.

The correlation of wind conditions and waves is taken into account for the design of an offshore wind turbine. This correlation is considered in terms of the long-term joint probability distribution of relevant parameters, e.g. mean wind speed  $V_{10}$ , significant wave height  $H_s$  and peak spectral period  $T_p$ . The joint



probability distribution of these parameters is affected by local site conditions such as fetch and water depth. The distribution shall therefore be determined from suitable long-term measurements or by the use of a numerical hindcasting technique (IEC, 2020).

For the purposes of the present work, the SMB method (Sverdrup & Munk, 1947) has been used to predict the wave characteristics. In the absence of site-specific statistics regarding the wind speed distribution, wind blow duration is assumed to be unlimited and therefore wave development is assumed to be limited only by fetch. Eq. (3-9) - (3-11) describe the SMB method in the case of fully developed waves.

$$H_s = 0.283 * \frac{V_{10}^2}{g} * \tanh(0.0125 * \Phi^{0.42}) \quad (3-9)$$

$$T_p = 7.54 * \frac{V_{10}}{g} * \tanh(0.077 * \Phi^{0.25}) \quad (3-10)$$

$$\Phi = g * \frac{F}{V_{10}^2} \quad (3-11)$$

Where:

$V_{10}$	wind speed at 10m above mean sea level
$g$	acceleration of gravity, 9.81m/s <sup>2</sup>
$F$	fetch
$H_s$	significant wave height
$T_p$	peak wave period
$\Phi$	fetch coefficient

Fetch is the effective stretch of water, over which the wind blows at a certain speed and direction as it generates waves. To calculate it, radial lines are constructed from the point of measurement to the margins at intervals of 5°, such that the outermost radials form an angle of 45° with the wind direction. The fetch is determined by weighting the length of the radials to the corresponding cosine of the angles with respect to wind direction, as per Eq. (3-12) (Saville, McClendon, & Cochran, 1962). The process can be visualized in Figure 4-10.

$$F = \frac{\sum_{a=-45}^{a=+45} [R_i * (\cos a)^2]}{\sum_{a=-45}^{a=+45} \cos a} \quad (3-12)$$

Where:

$F$	fetch
$a$	angle
$R_i$	length of radial

5<sup>th</sup> order Stokes' wave theory is applied herein, which introduces the contribution of more harmonics to the model and is deemed to be a more reliable tool for the calculation of wave action on an offshore structure than the linear wave theory, is applied herein. Linear wave theory is a useful, foolproof tool;

however, it is widely based on assumptions as waves are in nature non-linear. The most fundamental assumption is the linearization of equations by elimination of the non-linear terms. However, when the ratio of wave height to water depth ( $H/d$ ) and/or the ratio of wave height to wavelength ( $H/\lambda$ ) reach high values, these terms can no longer be eliminated and this theory ceases to be valid. The non-linear wave approach suggests that the free surface elevation is not sinusoidal. The waves display horizontal asymmetry, with crests being sharper and troughs being flatter (Figure 3-1). Similarly, velocities differ from those specified by linear theory; particle velocities are higher below the crests, lower below the troughs (Καραμπάς, Κρεστενίτης, & Κουτίτας, 2015).

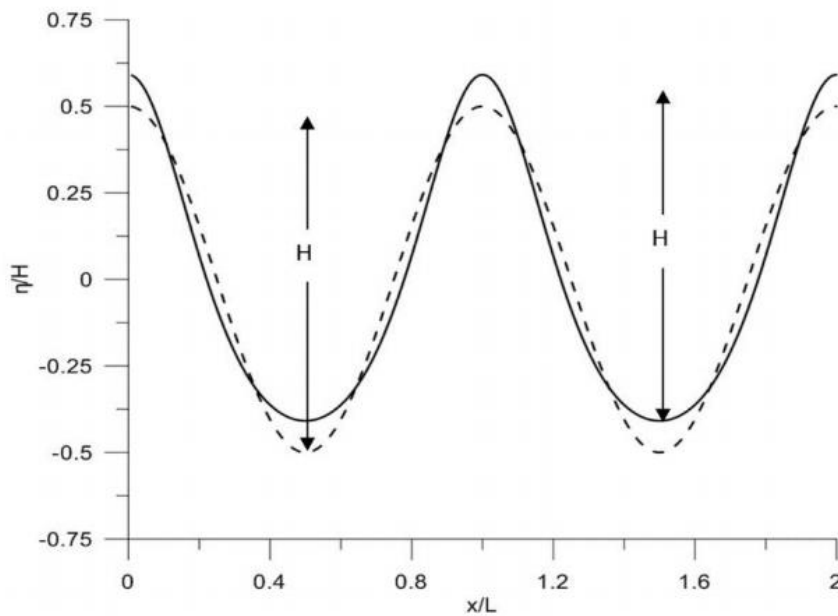


Figure 3-1 Comparison of wave profiles suggested by linear (solid line) and non-linear (intermittent line) wave theories (Καραμπάς, Κρεστενίτης, & Κουτίτας, 2015)

According to Stokes 5<sup>th</sup> order wave theory, the velocity potential, horizontal and vertical particle velocities and accelerations, dynamic component of pressure and sea surface elevation are given in Eq. (3-13) - (3-19) respectively (Skjelbreia & Hendrickson, 1961), (Massachusetts Institute of Technology, 2017).

$$\Phi = \frac{\lambda \cdot c}{2\pi} * \sum_{n=1}^5 D_n * \cosh \left[ \frac{2n\pi}{\lambda} * (z-d) \right] * \sin \left[ 2n\pi * \left( \frac{x}{\lambda} - \frac{t}{T} + \frac{a}{360} \right) \right] \quad (3-13)$$

$$u = - \frac{d\Phi}{dx} \quad (3-14)$$

$$w = - \frac{d\Phi}{dz} \quad (3-15)$$

$$a_x = \frac{du}{dt} + \frac{du}{dx} * u + \frac{du}{dz} * w \quad (3-16)$$

$$a_z = \frac{dw}{dt} + \frac{dw}{dx} * u + \frac{dw}{dz} * w \quad (3-17)$$

$$p_{\text{dyn}} = \rho * \left( \frac{d\Phi}{dt} - \frac{1}{2} * u^2 \right) \quad (3-18)$$

$$\eta = \frac{\lambda}{2\pi} * \sum_{n=1}^5 E_n * \cos \left[ 2\pi n * \left( \frac{x}{\lambda} - \frac{t}{T} + \frac{a}{360} \right) \right] \quad (3-19)$$

Where:

$\Phi$	velocity potential
$u$	horizontal particle velocity
$w$	vertical particle velocity
$a_x$	horizontal particle acceleration
$a_z$	vertical particle acceleration
$p_{\text{dyn}}$	dynamic component of pressure
$\eta$	sea surface elevation
$\lambda = g * \frac{T^2}{2\pi} * \tanh\left(\frac{2\pi}{\lambda} * d\right)$	wavelength (equation solved iteratively)
$c = \frac{\lambda}{T}$	wave celerity
$z$	vertical coordinate, measured positively upwards from mean sea level
$d$	water depth
$n$	order counter
$x$	horizontal coordinate
$t$	time
$T$	wave period
$a$	phase
$D_n$	$n^{\text{th}}$ order constant, see (Massachusetts Institute of Technology, 2017)
$E_n$	$n^{\text{th}}$ order constant, see (Massachusetts Institute of Technology, 2017)

The hydrodynamic loads on a cylindrical member along the direction of the incoming wave are herein calculated with the Morison equation (Journée & Massie, 2001). This semi-empirical method combines an inertial term, related to water particle acceleration, and a viscous drag term, related to water particle velocity. The inertial force component includes two terms; the first one is associated with the pressure field generated by the undisturbed waves (Froude-Krylov force). This term can be controlled using the  $C_p$  coefficient, with a value of 1 being the default. The second term is the scattering force associated with the disruption of the fluid by the presence of the structure. This term is controlled by the coefficient

of added mass,  $C_A$ . Eq. (3-20) gives the Morison equation for an infinitesimal strip of a submerged cylindrical member. The values of the drag and inertia coefficients suggested by the relative standard (American Petroleum Institute, 2007) are given by Eq. (3-21).

$$\frac{dF}{dz} = f_{\text{Inertia}} + f_{\text{Drag}} = \rho * (C_p + C_A) * \pi * \frac{D^2}{4} * \ddot{u} + \frac{1}{2} * \rho * C_D * D * u * |u| \quad (3-20)$$

Where:

F	total hydrodynamic force
z	vertical coordinate, measured positively upwards from mean sea level
$\rho$	saltwater density, 1,025kg/m <sup>3</sup>
D	member diameter
$\ddot{u}$	fluid particle horizontal acceleration
u	fluid particle horizontal velocity
$C_p$	Froude-Krylov coefficient
$C_A$	added mass coefficient
$C_D$	drag coefficient
$\begin{cases} C_M = 1.6 \text{ and } C_D = 0.65 \text{ for smooth members} \\ C_M = 1.2 \text{ and } C_D = 1.05 \text{ for rough members} \end{cases}$	(3-21)

Where:

$C_M = C_p + C_A$	inertia coefficient
$C_p$	Froude-Krylov coefficient
$C_A$	added mass coefficient
$C_D$	drag coefficient

The basic assumption of the Morison equation is that the submerged members on which the wave action is calculated do not affect the waves. This assumption is only valid as long as the structure is slender, which means that member diameters are relatively small compared to the wavelength, as per Eq. (3-22).

$$\frac{D}{\lambda} < \frac{1}{5} \quad (3-22)$$

Where:

D	member diameter
$\lambda$	wavelength

### 3.2.3 OTHER LOADS

Where relevant to the wind turbine site, additional loads have to be examined and taken into account. Marine growth increases the cross-sectional dimensions of structural elements and makes their surface rough, which alters the drag and inertia coefficients and therefore affects the hydrodynamic loading on

the members. Currents, both wind-generated ones and tidal ones, aggravate the hydrodynamic action on the substructure, affect the location and orientation of boat landings and fenders, and may create seabed scouring. In locations with special environmental conditions, such as extremely low or high temperatures, ice formation and seismic activity may be design-driving. Wake effects from neighboring wind turbines during power production should also be considered if applicable.

### 3.2.4 LOAD COMBINATIONS

Wind turbine design standards suggest that the design of an offshore wind turbine should be based on an onerous number of simulations that cover a comprehensive list of load combinations that the wind turbine may be found in during its lifespan (IEC, 2020). However, preliminary design can be based on selected load cases that cover fundamental events, which are expected during the wind turbine's life cycle, such as start-up and shutdown, extreme events of wind and / or wave action, power production and occurrence of fault. Such a selection should account for both ultimate strength analysis, as per Table 3-2, and fatigue analysis, as per Table 3-3 (Μηχανικοί Μελετών & Εφαρμογών Α.Ε., ΤΕΡΝΑ Ενεργειακή Α.Ε., Εργαστήριο Μεταλλικών Κατασκευών – Ε.Μ.Π., Εργαστήριο Υδραυλικής Μηχανικής-Π.Π., 2015).

Table 3-2 Design Load Cases for Ultimate Strength Analysis

Ultimate Strength Analysis				
Design Situation	No.	Wind	Wave	Partial Safety Factor
Power Production	1.3	ETM ( $V_{in} < V_{hub} < V_{out}$ )	NSS ( $H_s V_{hub}$ )	Normal ( $\gamma=1.35$ )
	1.6	NTM ( $V_{in} < V_{hub} < V_{out}$ )	SSS ( $H_{s,SSS}$ )	Normal ( $\gamma=1.35$ )
Power Production & Occurrence of Fault	2.1	NTM ( $V_{in} < V_{hub} < V_{out}$ )	NSS ( $H_s V_{hub}$ )	Normal ( $\gamma=1.35$ )
	2.3	EOG ( $V_{hub}=V_r \pm 2m/s$ and $V_{out}$ )	NSS ( $H_s V_{hub}$ )	Accidental ( $\gamma=1.1$ )
Start-up	3.2	EOG ( $V_{hub}=V_{in}, V_r \pm 2m/s$ and $V_{out}$ ) or ETM ( $V_{in} < V_{hub} < V_{out}$ )	NSS ( $H_s V_{hub}$ )	Normal ( $\gamma=1.35$ )
	6.1	EWM ( $V_{hub}=V_{ref}$ )	ESS ( $H_{s,50yrs}$ )	Normal ( $\gamma=1.35$ )
Parked	6.2	EWM ( $V_{hub}=V_{ref}$ )	ESS ( $H_{s,50yrs}$ )	Accidental ( $\gamma=1.1$ )

Table 3-3 Design Load Cases for Fatigue Analysis

Fatigue Analysis				
Design Situation	No.	Wind	Wave	Partial Safety Factor
Power Production	1.2	NTM ( $V_{in} < V_{hub} < V_{out}$ )	NSS Joint prob. distribution of $H_s, T_{pr}, V_{hub}$	Fatigue ( $\gamma=1.0$ )
Parked	6.4	NTM ( $V_{hub} < V_{in}$ and $V_{out} < V_{hub} < 0,7 V_{ref}$ )	NSS Joint prob. distribution of $H_s, T_{pr}, V_{hub}$	Fatigue ( $\gamma=1.0$ )
Parked and fault conditions	7.2	NTM ( $V_{hub} < V_{out}$ )	NSS Joint prob. distribution of $H_s, T_{pr}, V_{hub}$	Fatigue ( $\gamma=1.0$ )

Where:

ETM	Extreme Turbulence Model (section 3.2.1)
NTM	Normal Turbulence Model (section 3.2.1)
EWM	Extreme Wind Model (section 3.2.1)
EOG	Extreme Operating Gust (section 3.2.1)
NSS	Normal Sea State (section 3.2.2)

---

ESS	Extreme Sea State (section 3.2.2)
$V_{\text{hub}}$	wind speed at hub height
$V_{\text{in}}$	cut-in wind speed
$V_{\text{out}}$	cut-out wind speed
$V_r$	rated wind speed

# **4 CASE STUDY: CONCEPT DESIGN OF AN OFFSHORE WIND TURBINE WITH A TRIPOD SUBSTRUCTURE**

## **4.1 OVERVIEW OF METHODOLOGY**

For the analyses of the present study, two software packages were used, FAST<sup>1</sup> and SAP2000<sup>2</sup>. FAST, developed by the National Renewable Energy Laboratory (NREL), U.S. Department of Energy, is a state-of-the-art finite element tool that offers a multifaceted approach for the behavior of both the wind turbine and the structure it is mounted atop. A short description of the software and individual modules, as well the relative documentation is given in Annex A. The geometry and properties of the entire structure were modeled in FAST, and the software was used to simulate the operation of the turbine and the dynamic response of the tower and substructure, by producing time-series for the loads, namely the drag force on the transition piece and tower, and the three forces and three moments exerted by the turbine on the tower top. The full set of FAST modules used as part of the present work are indicatively given in Annex B for a particular load combination.

Additionally, a model of the load-bearing part of the structure, namely the tower and the structure supporting it, was built in SAP2000 to enable a more straightforward structural verification and optimization process of the support structure. As the full effect of the rotor-nacelle assembly, including mass, inertia and applied loads, has already been taken into account in FAST, snapshots from the time-histories output from FAST were selected and the corresponding load values were assigned to the structure in SAP2000, to run static analyses. Strength checks were performed for the members under the given loading, and demand / capacity ratios were examined. Wave action was modeled as a static loading on the structure in SAP2000, through the software's wave loading feature that automatically

---

<sup>1</sup> <https://www.nrel.gov/wind/nwtc/fastv8.html>

<sup>2</sup> <https://www.csiamerica.com/products/sap2000>

produces loads on the structure resulting from waves and buoyancy. The user input includes wave height, period and water depth.

## 4.2 SITE LOCATION

The selection of the most suitable location for installing an offshore wind farm is based on various parameters, such as the wind regime and wave regime in the area, potential impact from the wind farm on the surrounding environment, bathymetry and seabed soil characteristics, seabed slope, and history of seismic action. In the context of the present work, the location of the wind turbine is assumed to be off the north-west coast of Kasos Island (Figure 4-1). This specific location was selected because of the favorable characteristics of the wind regime in the area. More specifically, this region is among the ones displaying the highest wind power density in the Greek seas, both on annual (Figure 4-2) and seasonal (Figure 4-3) basis (Soukissian, et al., 2017). The depth in the area is suitable for installing a wind turbine atop a tripod substructure, as the depth fluctuates around 50m (Figure 4-4).

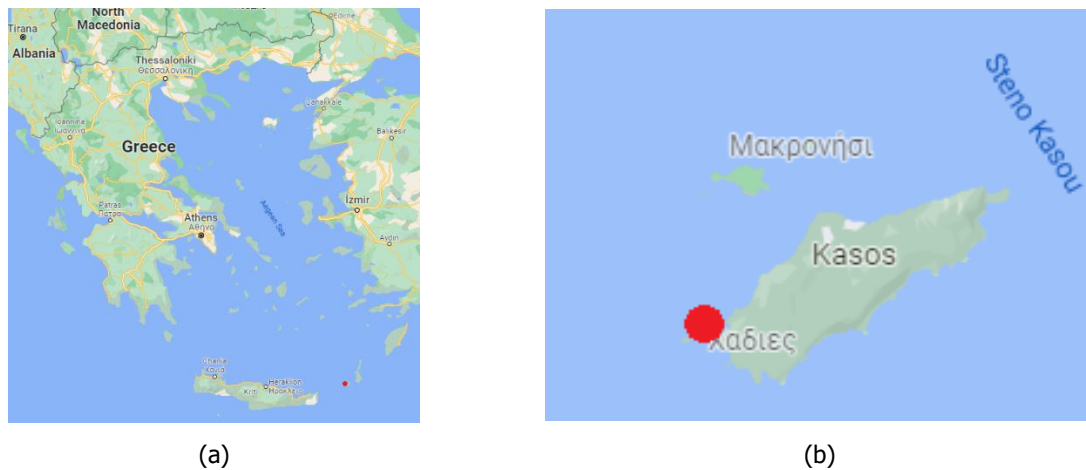


Figure 4-1 Wind turbine location (a) distant view (b) close-up view ([www.google.com/maps](http://www.google.com/maps))

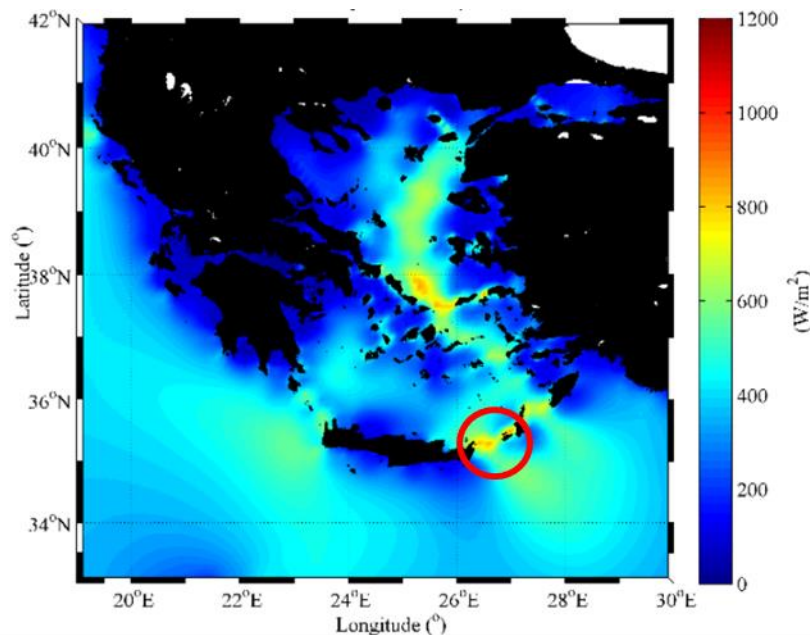


Figure 4-2 Spatial distribution of mean annual offshore wind power density at 80m height above sea level in the Aegean and Ionian Seas for the period 1995–2009 (Soukissian, et al., 2017)



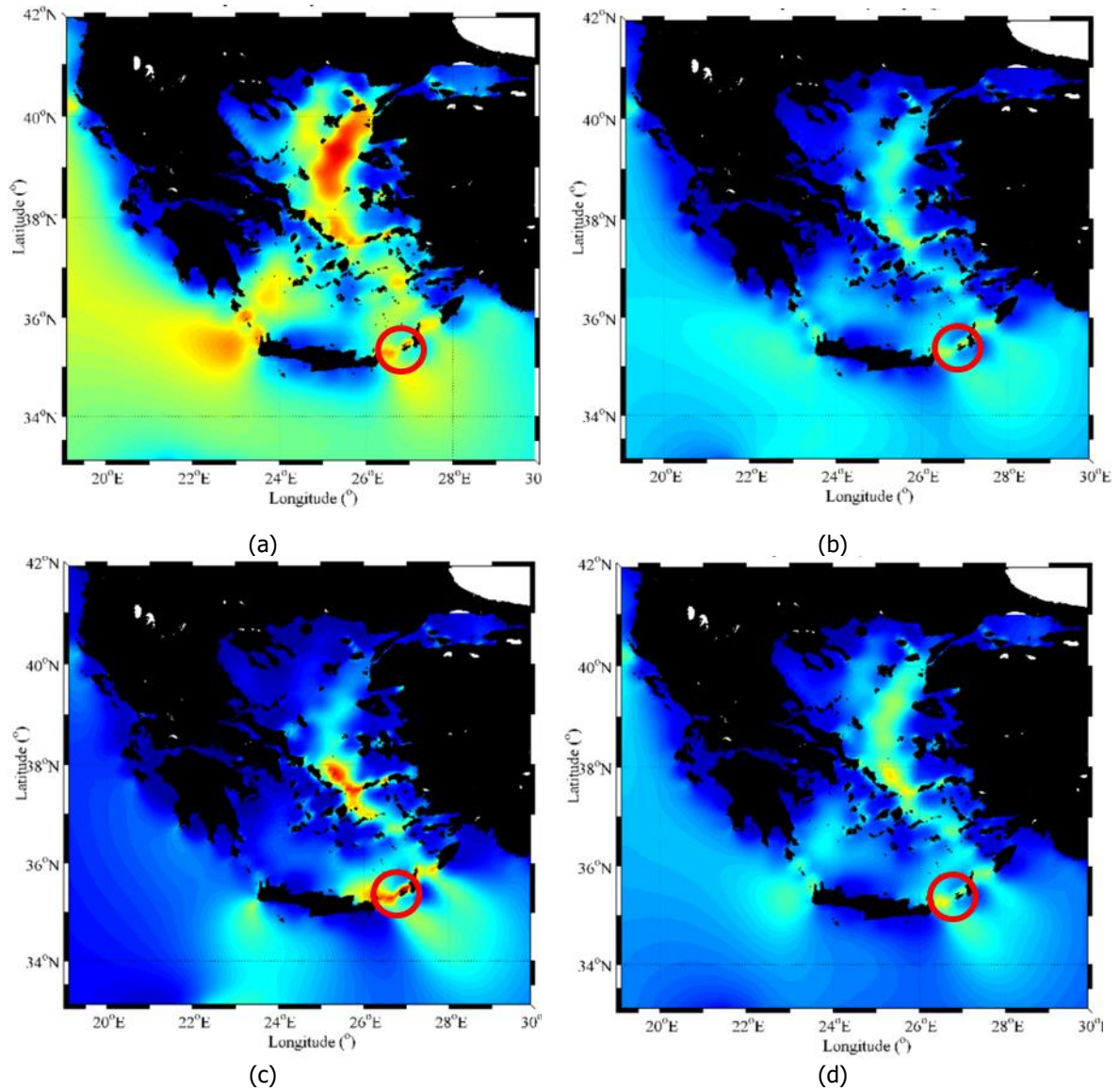


Figure 4-3 Spatial distribution of mean offshore wind power density in (a) winter, (b) spring, (c) summer and (d) autumn at 80m above sea level in the Aegean and Ionian Seas, period 1995–2009 (Soukissian, et al., 2017)



Figure 4-4 Bathymetry in the area (webapp.navionics.com)

### 4.3 BASIC PROPERTIES OF THE TURBINE

The turbine used for the purposes of the present work is the "NREL Offshore 5-MW Baseline Wind Turbine". The detailed specifications of this turbine were established by the National Renewable Energy Laboratory (NREL), as part of conceptual studies it conducted regarding offshore wind technology. This wind turbine is representative of typical utility-scale land-based and sea-based multi-megawatt turbines, and suitable for deployment in deep waters. Some of its fundamental properties are given in Table 4-1.

Table 4-1 Basic properties of the NREL Offshore 5-MW Baseline Wind Turbine (Jonkman, Butterfield, Musial, & Scott, 2009)

<b>Property</b>	<b>Value</b>
Rating	5MW
Rotor Orientation	Upwind
Configuration	3 blades
Control	Variable Speed, Collective Pitch
Drivetrain	High Speed, Multiple-Stage Gearbox
Rotor Diameter	126m
Hub Diameter	3m
Cut-In, Rated, Cut-Out Wind Speed	3m/s, 11.4m/s, 25m/s
Cut-In, Rated Rotor Speed	6.9rpm, 12.1rpm
Rated Tip Speed	80m/s
Overhang, Shaft Tilt, Precone	5m, 5°, 2.5°
Rotor Mass	110tonnes
Nacelle Mass	240tonnes
Coordinate Location of Overall Center of Mass	(-0.2m, 0.0m, 64.0m)

### 4.4 SUBSTRUCTURE AND TRANSITION PIECE GEOMETRY

As far as the tripod is concerned, the geometry used as part of NREL's OC3 Project was reproduced for the purposes of the present work (Jonkman & Musial, 2010), (Camp, 2008). The whole tripod is submerged, more specifically it extends from -45m, up to the mean sea level. The transition piece extends from the mean sea level up to +20m.

The configuration of the tripod and transition piece is depicted in Figure 4-5 and described in Table 4-2 and Table 4-3. The comprehensive list of nodes that were used by the FAST software for meshing the substructure and the transition piece can be found in the SubDyn module, which is included in Annex B; only the nodes required to describe the geometry are included in Figure 4-5 and Table 4-2. Both the transition piece and the substructure members are built with S355 structural steel.

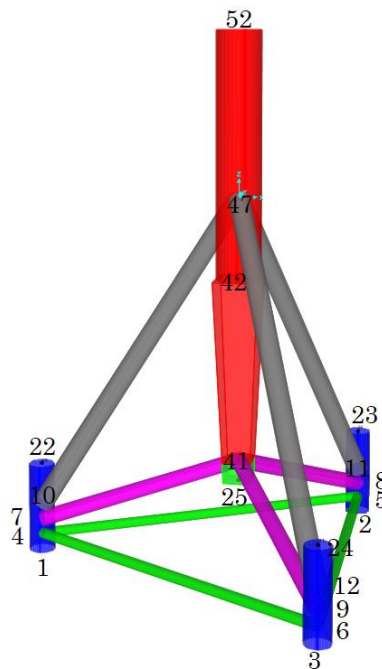


Figure 4-5 Geometry of the substructure and transition piece in SAP2000

Table 4-2 Coordinates of substructure and transition piece nodes

Node number	x	y	z
1	-24.8025	0.0000	-45.0000
2	12.4005	21.4785	-45.0000
3	12.4005	-21.4785	-45.0000
4	-24.8025	0.0000	-42.9793
5	12.4005	21.4785	-42.9793
6	12.4005	-21.4785	-42.9793
7	-24.8025	0.0000	-41.1426
8	12.4005	21.4785	-41.1426
9	12.4005	-21.4785	-41.1426
10	-24.8025	0.0000	-39.3061
11	12.4005	21.4785	-39.3061
12	12.4005	-21.4785	-39.3061
22	-24.8025	0.0000	-34.0706
23	12.4005	21.4785	-34.0706
24	12.4005	-21.4785	-34.0706
25	0.0000	0.0000	-34.7133
41	0.0000	0.0000	-32.1883
42	0.0000	0.0000	-10.0000
47	0.0000	0.0000	0.0000
52	0.0000	0.0000	20.0000

Table 4-3 Length and section properties of substructure and transition piece members

Member category	Member length (m)	Outer diameter (m)	Wall thickness (mm)
Pile sleeve	10.931	3.150	30.0
Member connecting each pile sleeve to the central pillar	26.368	1.875	15.0
Tripod leg	46.477	2.475	20.0
Member connecting two pile sleeves	42.958	1.200	15.0
Tapered part of the central pillar	24.713	3.142 @ Node 25 3.400 @ Node 41 5.500 @ Node 42	30.0
Cylindrical part of the central pillar	10.000	5.500	50.0
Transition piece	20.000	5.500	50.0

#### 4.5 TOWER GEOMETRY

The tower extends from +20m, where it is connected to the transition piece by means of a bolted flange, up to +98m above mean sea level. The hub lies at +100.4m, namely 2.4m higher than the yaw bearing tower top – a sketch of the rotor nacelle assembly (RNA) of the NREL Offshore 5-MW Baseline Wind Turbine is given in Figure 4-6.

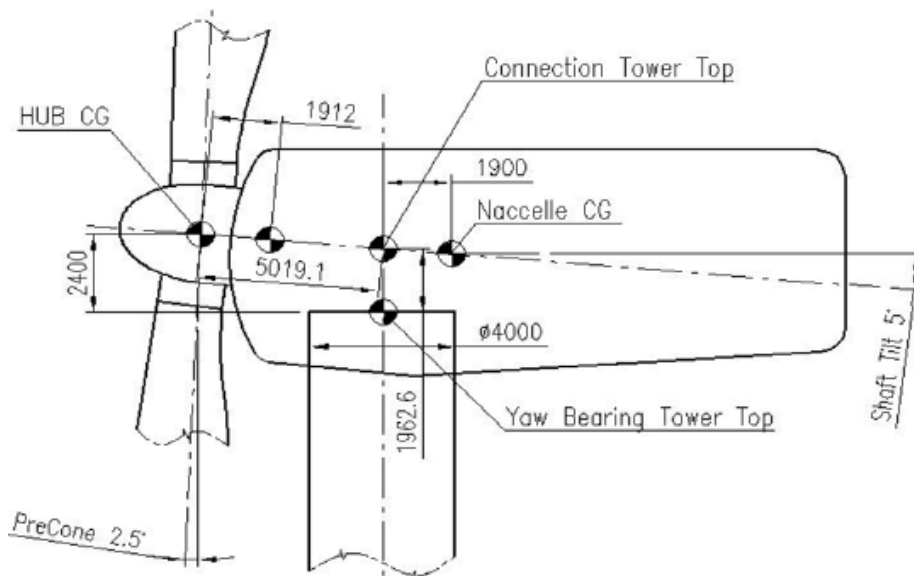


Figure 4-6 Rotor-Nacelle Assembly of the NREL Offshore 5-MW Baseline Wind Turbine (Zhao, Yang, & He, 2012)

The tower is cylindrical, with a diameter of 5.5m constant over its 78m length. It is manufactured in 9m-long sections that bear flanges at both ends and get bolted together either on site, either prior to the entire tower's transportation to the site. Each one of these sections consists of three 3m-wide steel plates, bent to the required ovality and welded together. The thickness of the plates is decreasing towards the tower top, due to the lower strength requirement and the consequent need to save material. The geometry of the cross-sections chosen for the tower elements are given in Table 4-4. The tower members are built with S355 structural steel.

Table 4-4 Geometry of tower members

<b>Tower member</b>	<b>Start height (m)</b>	<b>End height (m)</b>	<b>Diameter (m)</b>	<b>Thickness (mm)</b>
1	20	23	5.500	35
2	23	26	5.500	34.2
3	26	29	5.500	33.4
4	29	32	5.500	32.6
5	32	35	5.500	31.8
6	35	38	5.500	31
7	38	41	5.500	30.2
8	41	44	5.500	29.4
9	44	47	5.500	28.6
10	47	50	5.500	27.8
11	50	53	5.500	27
12	53	56	5.500	26.2
13	56	59	5.500	25.4
14	59	62	5.500	24.6
15	62	65	5.500	23.8
16	65	68	5.500	23
17	68	71	5.500	22.2
18	71	74	5.500	21.4
19	74	77	5.500	20.6
20	77	80	5.500	19.8
21	80	83	5.500	19
22	83	86	5.500	18.2
23	86	89	5.500	17.4
24	89	92	5.500	16.6
25	92	95	5.500	15.8
26	95	98	5.500	15

The model of the substructure and tower, which was built in the finite element program SAP2000, is depicted in Figure 4-7. In SAP2000, extruded members created using the Section Designer feature, such as the tapered part of the substructure's central pillar, are displayed as the rectangular bounding box that encloses the object.

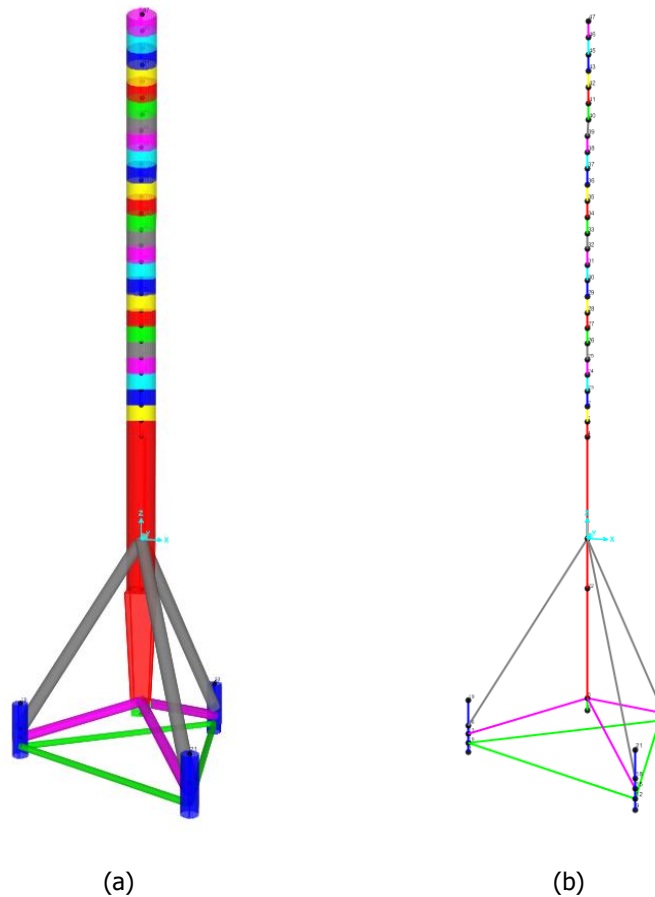


Figure 4-7 Model of the substructure and tower in SAP2000 (a) in "Extrude" view (b) in "Standard" view

## 4.6 LOADS

### 4.6.1 WIND

As it has already been mentioned, wind turbine classification as to its resilience to wind action is determined based on the wind speed maxima that can be withstood by the turbine. At an early design stage, in the absence of site-specific wind statistics, a rough approximation of the wind regime can be made. To that end, (EN 1991-1-4, 2010) was used in the context of the present work. This standard defines the fundamental value of the basic wind velocity,  $V_{b,0}$ , as the characteristic 10-minutes mean wind velocity, with a recurrence period of 50 years, irrespective of wind direction and time of year, at 10m above mean sea level or above ground level in open terrain. According to the Greek National Annex, this value is given by Eq. (4-1). The basic wind velocity accounts for wind direction and season effects, and is calculated by Eq. (4-2).

$$V_{b,0} = \begin{cases} 33\text{m/s for islands / coastal areas} \\ 27\text{m/s for the rest of the country} \end{cases} \quad (4-1)$$

$$V_b = V_{b,0} * C_{\text{season}} * C_{\text{dir}} = \begin{cases} 33\text{m/s for islands / coastal areas} \\ 27\text{m/s for the rest of the country} \end{cases} \quad (4-2)$$

Where

$V_{b,0}$	fundamental value of the basic wind velocity
$V_b$	basic wind velocity
$c_{dir}=1$ according to the Greek National Annex	wind direction factor
$c_{season}=1$ according to the Greek National Annex	season factor

The reference wind speed,  $V_{ref}$ , the basic quantity on which the turbine classification is based, is defined as the 10-min mean of the extreme wind speed with a recurrence period of 50 years at hub height. The Extreme Wind Model is used to calculate this quantity based on the aforementioned basic wind velocity,  $V_b$ , namely the corresponding wind velocity at 10m above mean sea level. On the assumption that the wind flow is steady, Eq. (3-4) yields  $V_{ref}=30.38\text{m/s}$ , whereas if the wind flow is assumed to be turbulent, Eq. (3-5) yields  $V_{ref}=42.53\text{m/s}$ . Therefore, based on the maximum value of wind speed expected in the area, the wind turbine shall be designed as class II.

The wind loading on the load-bearing part of the structure has two components, both of which are depicted in Figure 4-8. First, the wind causes a distributed load along the transition piece and tower. Second, the turbine, through both its presence and its operation, exerts three forces (x, y and z axes) and three moments (around x, y and z axes) on the tower top. Five of these turbine loads, are depicted in Figure 4-8. Shear force on the y axis only appears in the case of turbulent wind profile and is in all cases of much smaller magnitude than that on the x axis, which coincides with wind direction. For each case of wind characteristics input by the user, FAST produces time-series for both the distributed load and the forces and moments on the tower top caused by the turbine.

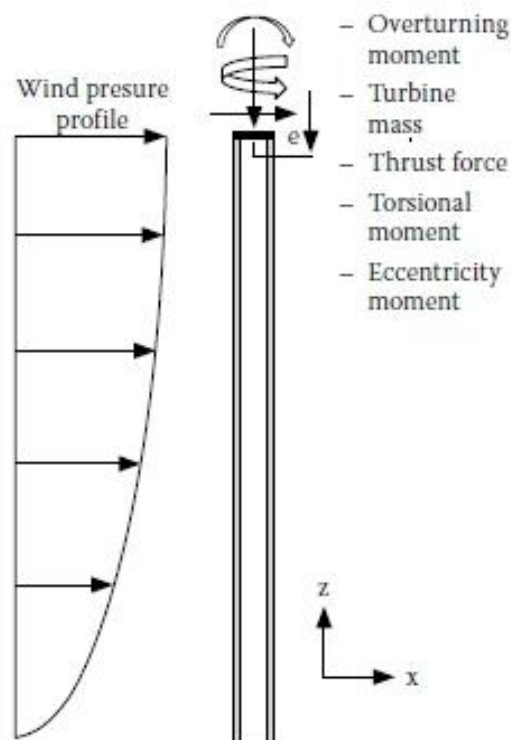


Figure 4-8 Illustration of wind loads acting on the non-submerged part of the structure (Source: www.scielo.org)

Aerodynamic forces on the tower are considered by calculating the drag force per unit length normal to the tower axis, as per Eq. (4-3). For each case of wind characteristics (velocity, turbulence) fed in by the user, FAST produces time-series of the drag force per unit length on specified tower nodes of the

tower. In the present work, eight nodes, located at altitudes of +20m, +32m, +44m, +56m, +68m, +80m, +92m, +98m, were selected. In FAST's aerodynamics module, AeroDyn v15, unless the source code is altered accordingly, the drag coefficient is in all cases considered to be equal to unity. In the absence of such an option, a Reynolds' number-dependent drag coefficient ( $C_{drag}$ ) is subsequently fitted to each one of the drag force values, as per Table 4-5. Linear interpolation is used to approximate a drag coefficient that corresponds to a Reynold's number value in between the given ones.

$$f_{Drag} = \frac{1}{2} * \rho * C_{drag} * D * V_z^2 \quad (4-3)$$

Where:

P	wind density, 1.225kg/m <sup>3</sup>
$C_{drag}$	drag coefficient
D	tower cross-section diameter
$V_z$	wind speed at height z

Table 4-5 Variation of drag coefficient with Reynold's number (Roshko, 1961)

Reynolds' number *10 <sup>6</sup> (-)	$C_{drag}$ (-)
0.01	1.11
0.02	1.20
0.122	1.20
0.200	1.17
0.300	0.90
0.400	0.54
0.500	0.31
1.000	0.38
1.500	0.46
2.000	0.53
2.500	0.57
3.000	0.61
3.500	0.64
4.000	0.67
5.000	0.70
10.000	0.70

For reasons of simplification, the wind action is assumed to evolve linearly between each pair of nodes, thus resulting in one triangle along the transition piece and seven trapezoids along the tower. This simplification is depicted in Figure 4-9; the black intermittent line represents the actual wind loading, which in this specific case follows the turbulent Extreme Wind Model and corresponds to a velocity of 20m/s at hub height (100.4m). Each one of the colored solid lines represents linear approximation of the actual loading between a pair of the aforementioned tower nodes, based on the values output by FAST on the starting and ending node.

The surface area of the triangle and trapezoids is then integrated, to convert the wind loads distributed over the tower length into lumped forces on the adjacent nodes. For example, the lumped force assigned to the node located at +20m is the sum of the surface area of the triangle ranging from mean sea level to +20m and half the surface area of the trapezoid ranging from +20m to +32m. The lumped force



assigned to the node located at +32m is the sum of half the surface area of the trapezoid ranging from +20m to +32m and half the surface area of the trapezoid ranging from +32m to +44m, and so on. The lumped force assigned to the node located at +98m is half the surface area of the trapezoid ranging from +92m to +98m.

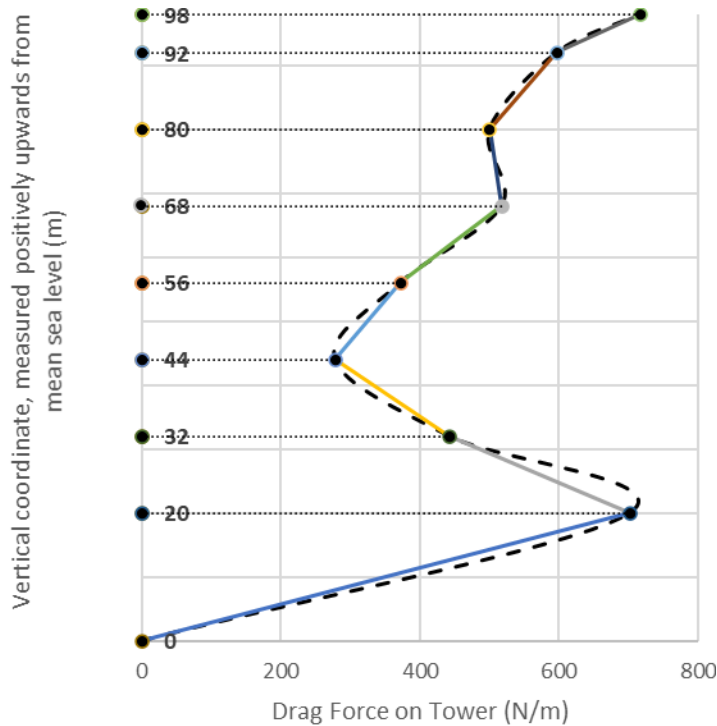


Figure 4-9 Approximation of actual wind profile with linear sections

Similarly, depending on the wind characteristics fed in by the user, FAST produces time-series for the three forces and three moments on the tower top caused by the turbine. Thus, in the SAP2000 model, the turbine is replaced by these equivalent six loads acting on the tower top and only the load-bearing part of the structure is considered.

#### 4.6.2 WAVE

As it can be ascertained by looking at Figure 4-1, the study area is mainly exposed to South, South-West, North-West and West winds and therefore waves. Fetch was calculated for all four of the aforementioned wind directions through Eq. (3-12). The respective results are given in Table 4-6.

Table 4-6 Water fetch for each one of the main wind directions

Wind direction	Fetch (km)
North-West	213.39
West	191.27
South-West	162.60
South	147.84

The wind turbine classification as to its resilience to wave action is based on the maximum fetch of the site, which in this case corresponds to the North-West wind, and equals 213.39km. Its calculation is depicted in Figure 4-10 and in Table 4-7. According to the SMB method, Eq. (3-9) - (3-11), the wave height and peak period corresponding to this fetch for  $V_{10}=33\text{m/s}$  as per Eq. (4-1), equal  $H_s=9.13\text{m}$  and  $T_p=11.92\text{s}$ . Therefore, based on the characteristics of the extreme wave expected in the area, the wind turbine shall be designed as class OA.

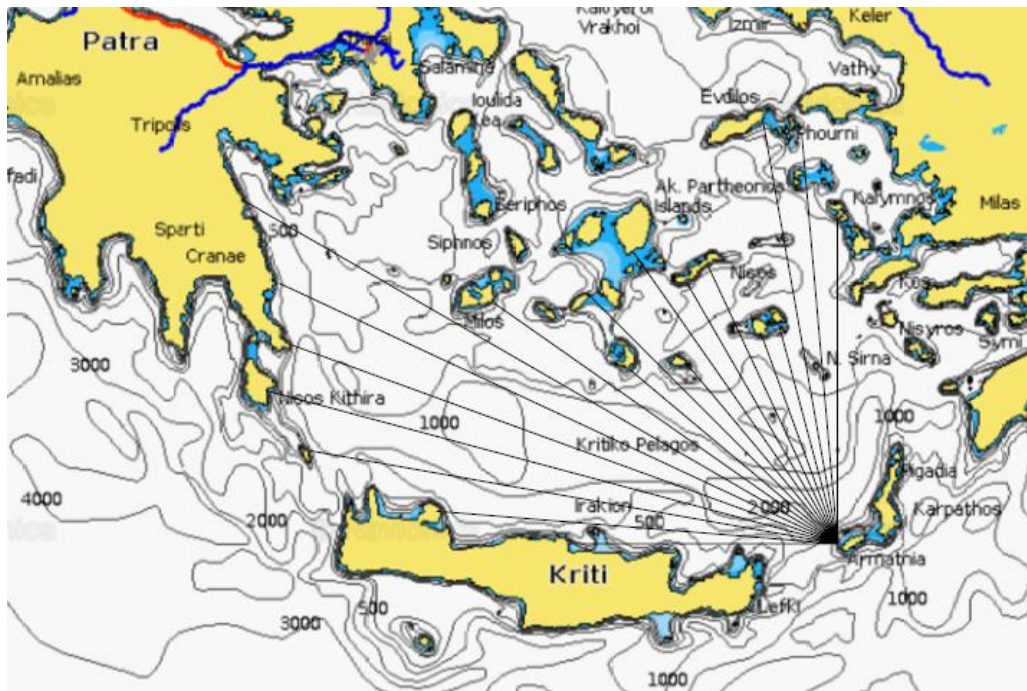


Figure 4-10 Fetch calculation in the study area for North-West wind

Table 4-7 Fetch calculation in the study area for North-West wind

North-West wind					
angle a (°)	angle a (rad)	cosa	cos <sup>2</sup> a	R (km)	R*cos <sup>2</sup> a
-45	-0.785	0.707	0.500	164.05	82,025.00
-40	-0.698	0.766	0.587	242.15	142,099.45
-35	-0.611	0.819	0.671	322.70	216,534.95
-30	-0.524	0.866	0.750	352.63	264,472.50
-25	-0.436	0.906	0.821	349.37	286,970.35
-20	-0.349	0.940	0.883	370.10	326,806.52
-15	-0.262	0.966	0.933	407.62	380,314.64
-10	-0.175	0.985	0.970	250.46	242,907.71
-5	-0.087	0.996	0.992	162.05	160,819.05
0	0.000	1.000	1.000	209.63	209,630.00
5	0.087	0.996	0.992	140.15	139,085.40
10	0.175	0.985	0.970	203.21	197,082.47
15	0.262	0.966	0.933	179.57	167,541.09
20	0.349	0.940	0.883	184.31	162,749.83
25	0.436	0.906	0.821	133.48	109,639.65
30	0.524	0.866	0.750	132.70	99,525.00
35	0.611	0.819	0.671	259.40	174,060.01
40	0.698	0.766	0.587	253.60	148,818.59
45	0.785	0.707	0.500	191.55	95,775.00
Sum		16.903			3,606,857.21
<b>Fetch (km)</b>	<b>213.39</b>				

#### 4.7 SOIL PROPERTIES

In the absence of site-specific geotechnical data, the seabed soil is assumed to be sandy for a depth of 35m below the mudline, then rocky. The sandy part is assumed to comprise three layers, the thickness and geotechnical properties of which are depicted in Figure 4-11. The sand profile chosen is based on previous work from the NREL (Passon, 2006). The soil response per unit length of the pile,  $P$ , to the pile deflection,  $y$ , under lateral loading is simulated with non-linear springs. In sandy soils,  $P$ - $y$  curves are dependent on the depth below the mudline, therefore each spring is described by its own  $P$ - $y$  curve, the shape of which is given by Eq. (4-4) - (4-7) (Χαλούλος, 2012), (American Petroleum Institute, 2007). The curves for five random depths below the mudline are indicatively given in Figure 4-12. Since the seabed is assumed to consist of rock below the depth of 35m, the joints at the bottom of the piles are modeled to be axially restrained, therefore no springs are placed in the vertical direction of the pile.

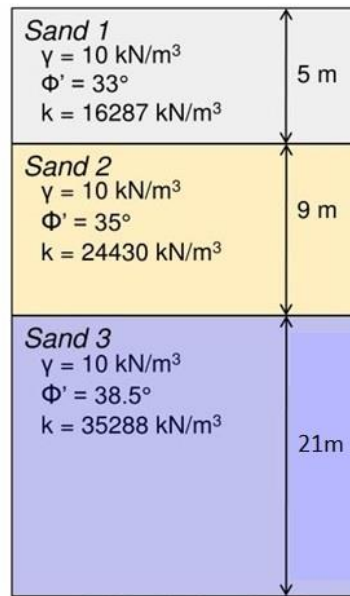


Figure 4-11 Geotechnical properties of the seabed soil (Passon, 2006)

$$P(z) = \frac{y}{\frac{1}{k_{ini} * z} + \frac{y}{p_{ult}}} \quad (4-4)$$

$$k_{ini} = k_{ini,0} * \left(1 - \frac{z/D}{1+z/D}\right) * \left(\frac{D}{0.6}\right)^{-0.35} \quad (4-5)$$

$$\frac{p_{ult}}{\gamma * z * D} = \begin{cases} \min\left(\frac{C_1 * (z/D) + C_2}{C_3}\right) & \text{if } \left(\frac{z}{D}\right) \leq \left(\frac{z}{D}\right)_{cr} \\ \min\left(\frac{C_1 * (z/D)_{cr} + C_2}{C_3}\right) & \text{if } \left(\frac{z}{D}\right) \geq \left(\frac{z}{D}\right)_{cr} \end{cases} \quad (4-6)$$

$$\left(\frac{z}{D}\right)_{cr} = 6.5 * \left(\frac{D}{0.6}\right)^{-0.64} \quad (4-7)$$

Where:

- $P$  soil response per unit length of the pile  
 $y$  pile deflection

$k_{ini}$	initial subgrade modulus
$z$	depth below the mudline
$p_{ult}$	soil ultimate bearing capacity
$k_{ini,0}$	initial subgrade modulus of the undisturbed soil
$D$	pile diameter
$\left(\frac{z}{D}\right)_{cr}$	critical ratio of depth below the mudline
$\gamma$	soil density
$C_1=0.115*10^{0.0405*\varphi}$	parameter
$C_2=0.571*10^{0.022*\varphi}$	parameter
$C_3=0.646*10^{0.0555*\varphi}$	parameter
$\varphi$	angle of internal friction

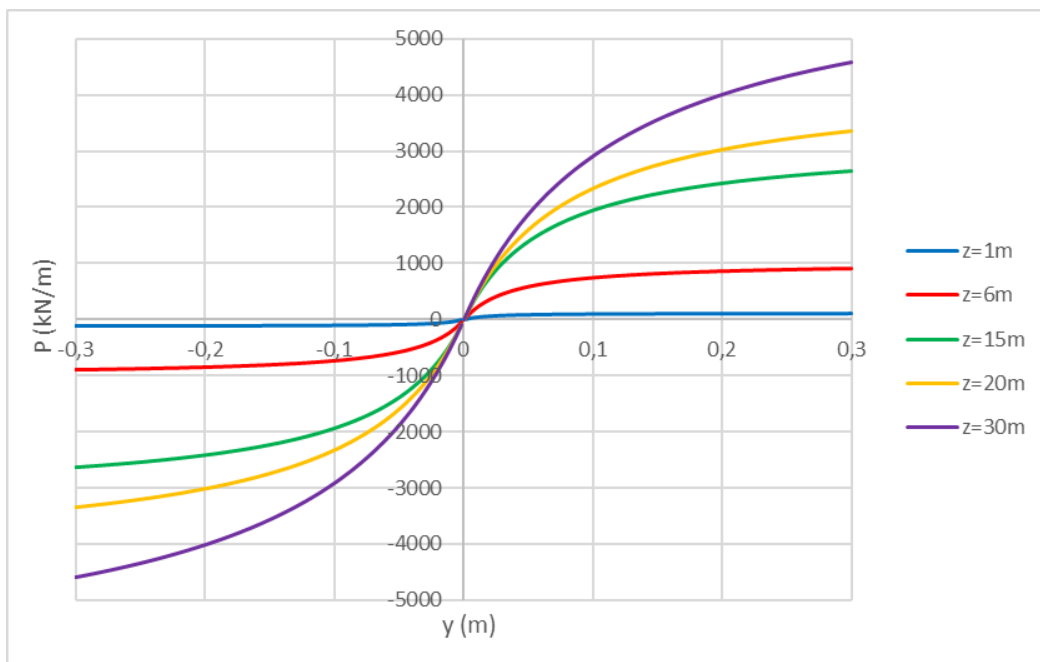


Figure 4-12 P-y curves for indicative depths below the mudline

## 4.8 FOUNDATION

The substructure is founded on three hollow cylindrical piles, each 35m long. Each foundation pile is connected with grout to the tripod through a pile sleeve; therefore, the pile diameter is the pile sleeve diameter (3.15m) reduced by twice the pile wall thickness (30mm) and twice the grout annulus (115mm),  $D=2.86\text{m}$ . The wall thickness of the cross-section of the pile is slightly less than that of the pile sleeve,  $t=25\text{mm}$ . The piles are built with S355 structural steel. A model of the entire structure including

the piles was built in SAP 2000 (Figure 4-13). The piles were modeled with beam elements, each 1m long, and the soil with non-linear springs described by P-y curves as per section 4.7 above.

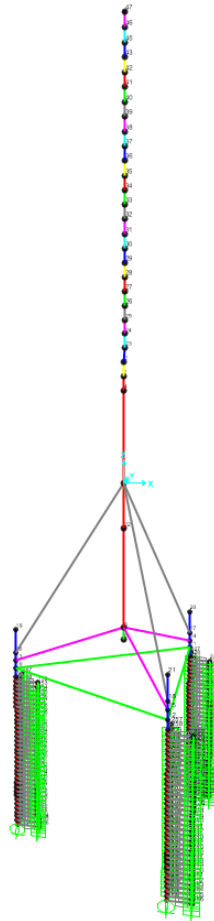


Figure 4-13 Model of the entire structure in SAP2000

As analysis is performed in SAP2000 by use of loads produced by FAST, the effect of the foundation on the response of the entire wind turbine system has to be considered in FAST as well. However, FAST's relative module, SubDyn, is currently limited to rigid connections between the bottom of the substructure and the seabed. The flexibility of the foundation and the effect of soil-structure interaction on the dynamic response of the bottom-fixed system can only be taken into consideration through the Apparent Fixity approach, which idealizes the pile as a cantilever beam specified with effective stiffness and length below the mudline. Certainly, this is a straightforward engineering approach and enables accurate modeling of the structural response only for a particular set of conditions; however, when the Apparent Fixity model is applied, it is common for the properties of the fictive beam to be suitably calibrated in such a manner that the mudline displacement and rotation are estimated accurately enough, when the structure is loaded by mudline shear force and bending moment representative of the loading under normal turbine operation conditions (Damiani, Jonkman, & Hayman, 2015).

The Apparent Fixity approach comprises three steps. First, shear and moment values at the mudline in the fore-aft direction are obtained from FAST simulations where the bottom joints of the tripod are clamped at the seabed. Second, a model of the pile in a finite element software package is used to determine the deflection and rotation at the top of the real pile for the given loads. Third, analytical relations are used to calculate the effective length and stiffness of a cantilever that would display the

same pile top deflection and rotation, when imposed to the same shear force and moment (Bush & Lance, 2009).

The method described above was followed for the purposes of the present work. Two analyses representative of the loading under normal turbine operation conditions were run in FAST for the fixed-base model (Figure 4-7). The first analysis was run for wind loads represented by the Extreme Turbulence Model, with a wind speed at hub height equal to 20m/s, and marine loads represented by a wave height equal to 2.69m and a peak period equal to 6.57s. The second analysis was run for uniform wind with the same speed, and the same wave height and peak period. From each analysis, four sets of concurrent internal tripod leg shear force  $F_x$  and bending moment  $M_y$  were selected from the respective time-series output by FAST; one of them corresponds to the worst loading, namely maximum values of force and moment, whereas the other three were picked randomly from the time-history. Subsequently, a model was created in SAP2000 exclusively for the pile with the actual properties (Figure 4-14). The aforementioned selected shear forces and moments were introduced as external loading on the top of the actual pile, in order to carry out static analyses and determine the resulting deflection and rotation. Finally, Eq. (4-8) - (4-9) were used to calculate the length and stiffness of the fictive cantilever that would display the same deflection and rotation when exposed to the same loading.

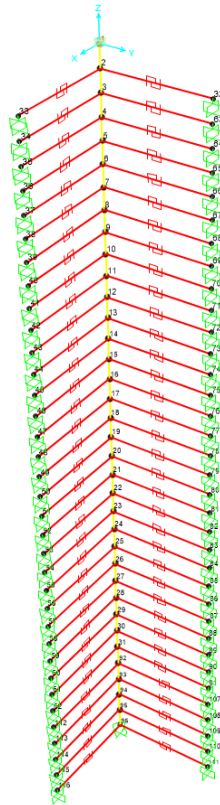


Figure 4-14 Model of the pile in SAP2000

$$w = w_F + w_M = \frac{FL^3}{3*EI} + \frac{ML^2}{2*EI} \quad (4-8)$$

$$\theta = \theta_F + \theta_M = \frac{FL^2}{2*EI} + \frac{ML}{EI} \quad (4-9)$$

Where:

$W_F$	deflection due to the shear force
$W_M$	deflection due to the bending moment
$\theta_F$	rotation due to the shear force
$\theta_M$	rotation due to the bending moment
F	shear force at the mudline
M	bending moment at the mudline
L	effective length
EI	effective stiffness

The three steps of the process followed are depicted in Table 4-8. To materialize the effective stiffness, the fictive beam's diameter is assumed to be constant and equal to that of the pile sleeves, whereas the wall thickness is treated as a variable. Young's modulus of steel is taken equal to 210GPa. The resulting Apparent Fixity properties are as follows:  $L_{AF}=15.60\text{m}$ ,  $D_{AF}=3.15\text{m}$ ,  $t_{AF}=0.028\text{m}$  (the mean values of the resulting length and wall thickness values are used).

Table 4-8 Implementation of the Apparent Fixity approach

<b>Shear and moment values output by FAST and input to SAP2000</b>								
<b>F (kN)</b>	2722.0	2687.0	-880.4	-1006.0	-752.1	1577.0	-978.1	2055.0
<b>M (kNm)</b>	6455.0	6716.0	-268.3	-1897.0	-27.7	377.7	-1419.0	2501.0
<b>Results from pile model in SAP2000</b>								
<b>w (m)</b>	0.0727	0.0723	-0.0150	-0.0202	-0.0121	0.0293	-0.0188	0.0450
<b><math>\theta</math> (rad)</b>	0.0072	0.0072	-0.0015	-0.0021	-0.0012	0.0028	-0.0019	0.0044
<b>Cantilever beam properties from analytical relations</b>								
<b><math>L_{eff}</math> (m)</b>	16.04	16.01	15.45	15.01	15.52	15.83	15.10	15.82
<b><math>EI_{eff}</math> (<math>10^8</math> kPa*m<sup>4</sup>)</b>	0.749	0.748	0.888	0.796	0.924	0.869	0.815	0.801
<b><math>t_{eff}</math> (m)</b>	0.0250	0.0249	0.0297	0.0266	0.0310	0.0290	0.0273	0.0268





# 5 RESULTS

## 5.1 SUMMARY OF THE ANALYSES PERFORMED

In the context of the present master’s thesis, the case of “Power Production” under ultimate strength analysis was examined, including design load cases 1.3 and 1.6. The wind and wave models dictated by each load case are presented in Table 3-2 and described in Chapter 3.2. To investigate the extent of wind speed’s effect on the loads arising on the tower and the substructure, three hub-height wind speeds were examined: the rated wind speed, 11.4m/s, a wind speed lower than the rated wind speed, 7m/s, and a wind speed higher than the rated wind speed, 20m/s. The wave characteristics corresponding to each design load combination are given in Table 5-1, while the partial safety factors are in all cases equal to 1.35, as per (IEC, 2020).

Table 5-1 Design load combinations checked in the context of the present work

Ultimate Strength Analysis					
Design Situation	Design Load Case No.	Wind (m/s)	Wave		Partial Safety Factor (-)
			H <sub>s</sub> (m)	T <sub>p</sub> (s)	
Power Production	1.3	7	0.52	3.00	Normal ( $\gamma=1.35$ )
		11.4	1.18	4.41	
		20	3.60	7.59	
	1.6	7	9.13	11.52	Normal ( $\gamma=1.35$ )
		11.4	9.13	11.52	
		20	9.13	11.52	

A 10-minutes long analysis was executed for each mean, hub-height wind speed and sea state. To ensure independence of the results from the initial conditions used for the dynamic simulations on FAST, the start-up transient was eliminated prior to post-processing the results. To that end, the first 20 seconds of the time-series output from the dynamic analysis were excluded. Subsequently, four snapshots were selected from each time-series and investigated statically. Each snapshot corresponds to the moment, at which one of the following quantities exerted on the tower top due to the operation of the turbine is maximized: tower top fore-aft shear force (along wind propagation axis), tower top roll moment (about wind propagation axis), tower top pitch moment (about axis perpendicular to wind propagation axis), and tower top yaw moment (torsional moment). The tower top axial force, which represents the turbine mass, and the tower top side-to-side shear force, which is caused by turbulence

and represents the wind flow perpendicular to the wind propagation axis, are not considered design driving and therefore, were not included in this process.

## 5.2 WIND FLOW DATA

Figure 5-1 and Figure 5-2 depict an indicative realization of the hub-height fore-aft and side-to-side wind speed time-histories respectively. These time-histories were produced by FAST's preprocessor TurbSim (refer to Annex A) and introduced to FAST as input data for the wind flow. By looking at the graphs, it can be visually verified that DLC 1.3, which simulates wind flow following the Extreme Turbulence Model, gives a more turbulent wind profile with higher peaks compared to DLC 1.6, which simulates wind flow following the Normal Turbulence Model.

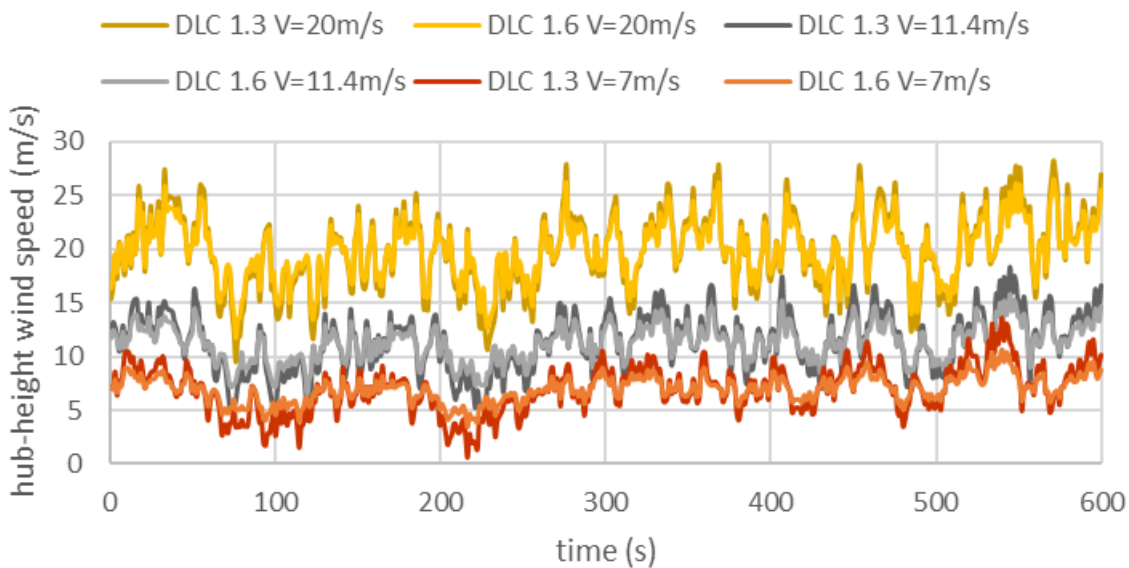


Figure 5-1 Time histories produced for the hub-height fore-aft wind speed

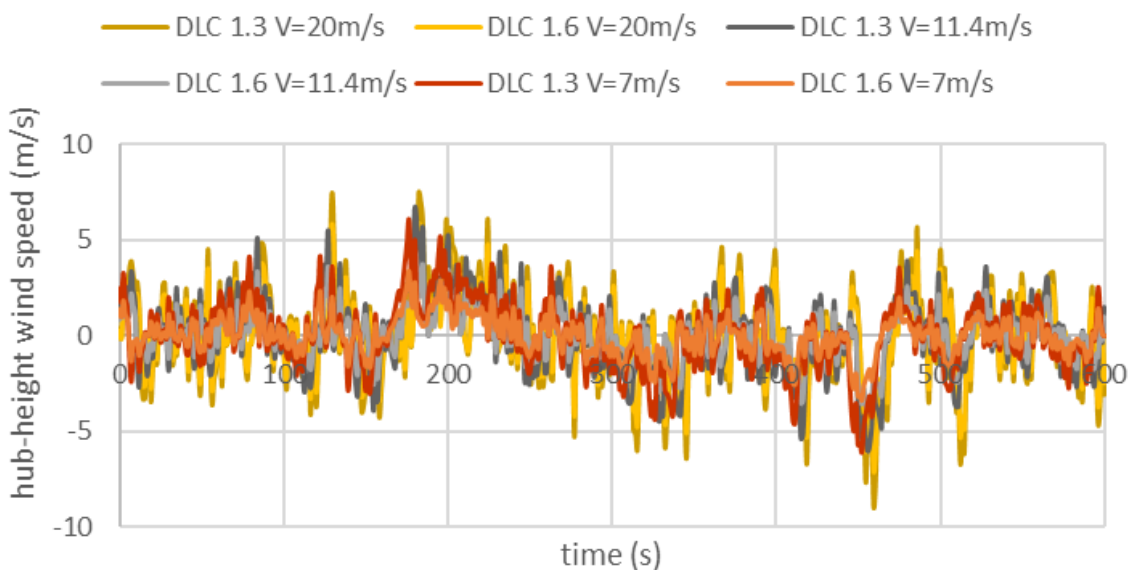


Figure 5-2 Time histories produced for the hub-height side-to-side wind speed

### 5.3 LOADS EXERTED BY THE TURBINE ON THE TOWER TOP

The time-series output by FAST for the three forces and three moments on the tower top resulting from one realization of each one of the aforementioned load combinations are illustrated in Figure 5-3 - Figure 5-8. Each chart encompasses three graphs, each one corresponding to one of the aforementioned wind speeds. The entire analysis time is included; thus the start-up transient can be visually identified (first 20 seconds). Notably, the values depicted in the graphs are multiplied by the partial safety factor at a later stage, when the loads are assigned to the SAP2000 model to check the overall performance of the structure.

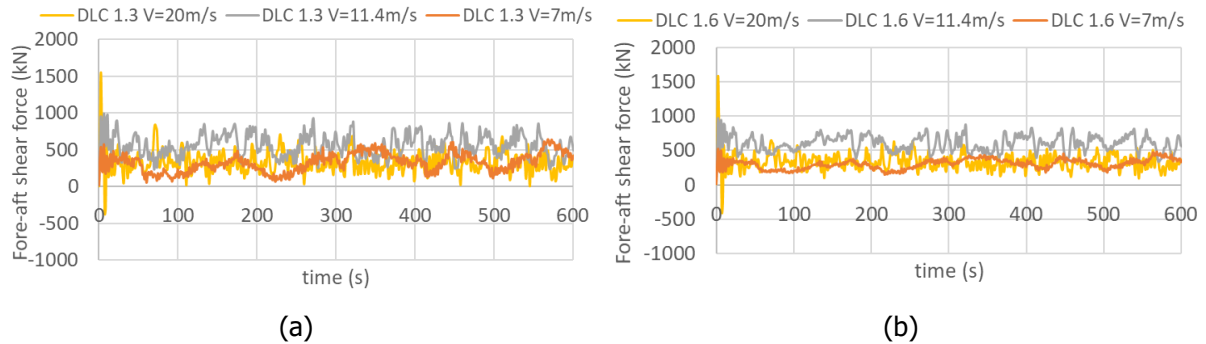


Figure 5-3 Tower top fore-aft shear force progress with time under (a) DLC 1.3, (b) DLC 1.6

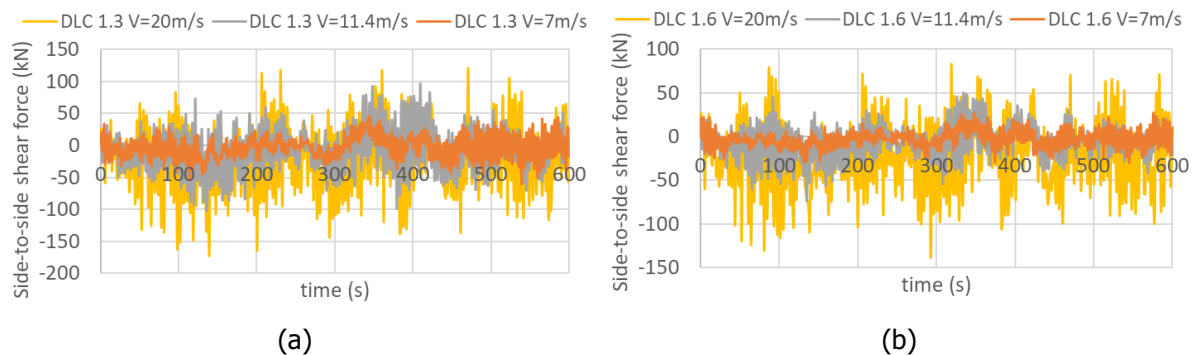


Figure 5-4 Tower top side-to-side shear force progress with time under (a) DLC 1.3, (b) DLC 1.6

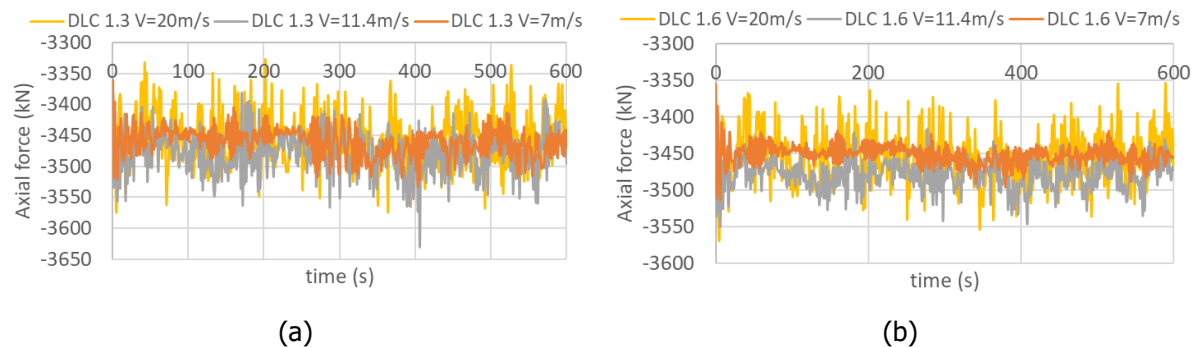


Figure 5-5 Tower top axial force progress with time under (a) DLC 1.3, (b) DLC 1.6

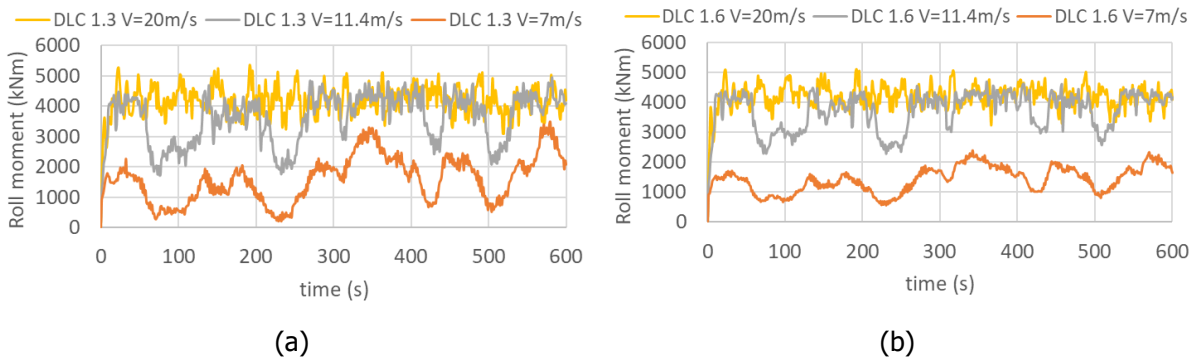


Figure 5-6 Tower top roll moment progress with time under (a) DLC 1.3, (b) DLC 1.6

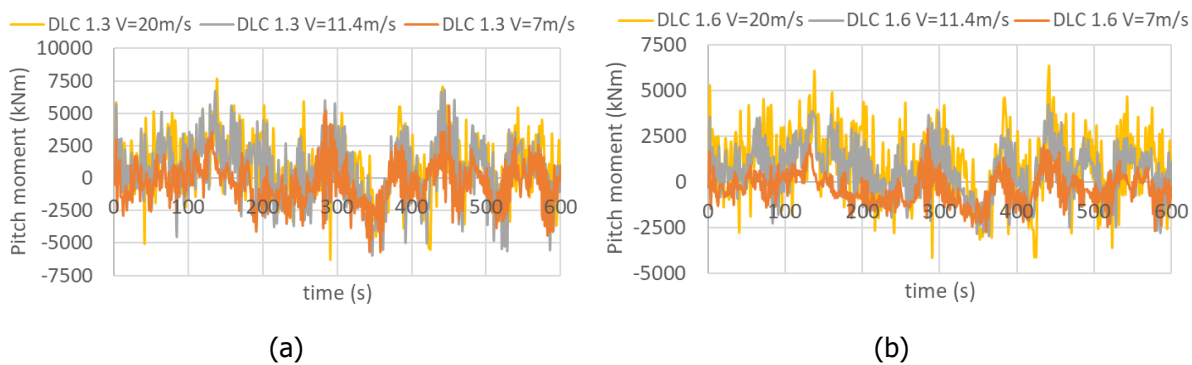


Figure 5-7 Tower top pitch moment progress with time under (a) DLC 1.3, (b) DLC 1.6

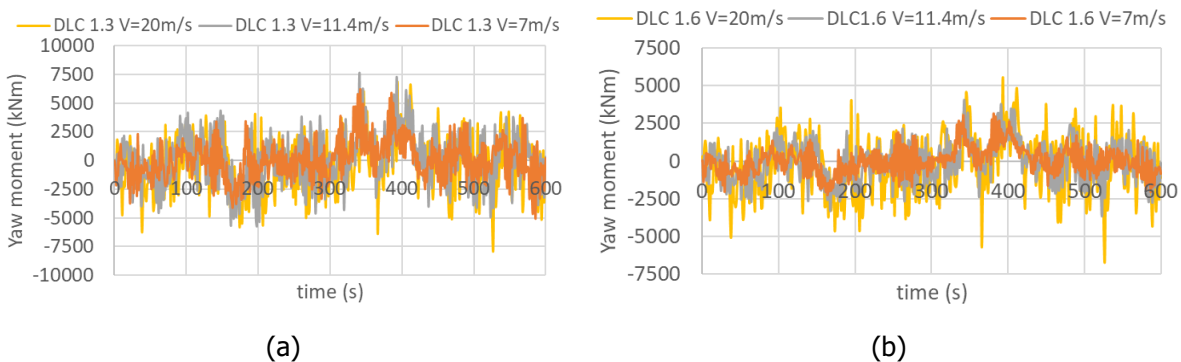


Figure 5-8 Tower top yaw moment progress with time under (a) DLC 1.3, (b) DLC 1.6

Comparing the side-to-side shear force, axial force, pitch moment and yaw moment values at the tower top level, it can be noted that these are comparable for all three wind speeds under the same turbulence model, with peaks progressively getting higher with the wind speed increase. However, this remark does not apply to the behavior of the tower top fore-aft shear force and roll moment.

Regarding the tower top fore-aft shear force charts, it can be deduced that the fore-aft shear force values are comparable for wind speeds equal to 7m/s and 20m/s under the same turbulence model. However, the respective value is significantly higher when the hub-height wind speed is equal to 11.4m/s, which is the rated wind speed. The mean tower top thrust force being highest at the rated wind speed can be attributed to the transition from Control Region II to Control Region III at this speed. This transition can be visualized in Figure 1-2, which constitutes a typical wind turbine power curve and portrays its operating regions.

Additionally, regarding the tower top roll moment charts, it is observed that the values increase with increasing hub-height wind speed. This can be explained by the fact that drivetrain torque increases with increasing thrust force on the rotor (HBM - Hottinger Brüel & Kjaer, 2022). Drivetrain torque is the quantity that affects predominantly the mean roll moment at the tower top level, with the side-to-side component of wind turbulence being a secondary factor (Duckwitz & Shan, 2014).

#### 5.4 DEMAND / CAPACITY RATIOS FOR THE TOWER

Figure 5-9 depicts the demand / capacity ratios for the tower members for each combination of the aforementioned wind speeds and design load cases. Notably, the maximum demand / capacity ratio for the uppermost member of the tower is 0.192, while for its downmost member it is estimated at 0.398. The descending trend of the demand / capacity ratio towards the tower top suggests that the tower could have been designed to be tapered rather than cylindrical. However, a decrease in diameter or thickness is not recommended at this stage, as there is no evidence that the considered design load cases are the most critical ones.

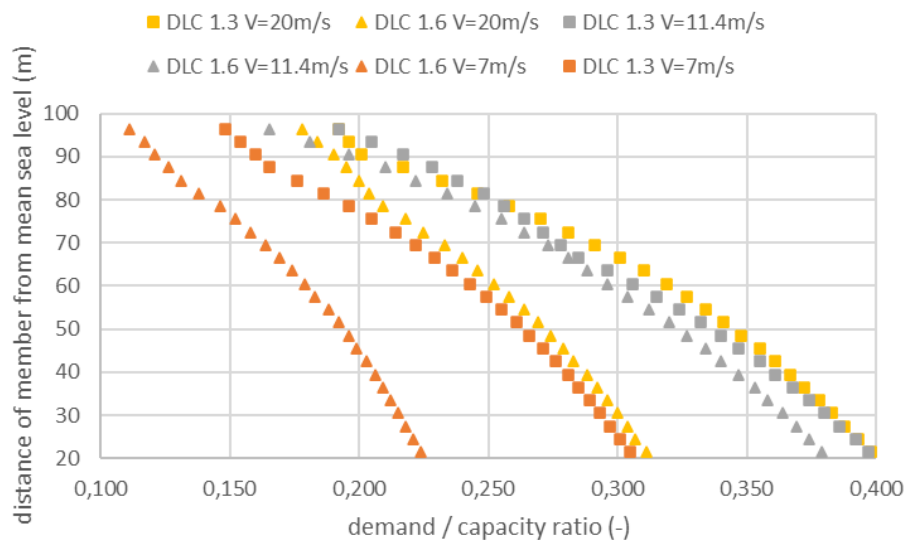


Figure 5-9 Demand / capacity ratios for the members of the tower under different load combinations

Additionally, it can be attested that the demand / capacity ratios for any wind speed are in all cases greater, when the wind flow follows the Extreme Turbulence Model, while lower values are documented when it follows the Normal Turbulence Model. This behavior can be explained by the fact that more turbulent wind flow leads to higher levels of fluid friction and increased viscosity.

Comparison of graphs depicting the analyses under the Normal Turbulence Model and different wind speeds yields that the member exploitation is higher for 20m/s than it is for 11.4m/s, which in turn results in higher exploitation ratios than the respective ones for 7m/s. However, comparison of graphs depicting the analyses under the Extreme Turbulence Model and different wind speeds, yields that the member exploitation ratios resulting from the analyses for 20m/s and 11.4m/s are comparable. In fact, maximum exploitation appears to be governed by the analyses for 11.4m/s for the uppermost members of the tower and dictated by the analyses for 20m/s for the intermediate members, whereas the resulting ratios for the two hub-height wind speeds are almost identical for the downmost members. The comparability of the strain in tower members for the rated wind speed and the much higher hub-height wind speed of 20m/s, can be attributed to the transition in control regions at the rated wind speed, similarly to what has already been discussed in Chapter 5.3.

Each one of the graphs in Figure 5-9 consists of the maxima of the demand / capacity ratios resulting from the static assignment of the loads corresponding to the time-history snapshots that the thrust force, and the three moments (roll, pitch, yaw) are maximized. In order to identify which one of these quantities is predominant for the structural design of the tower, the demand / capacity ratios at the aforementioned snapshots are given in Figure 5-10, Figure 5-11 and Figure 5-12. For all design load combinations, the maximum exploitation ratio for the members of the tower appears to be governed by either the tower top thrust force or the tower top pitch moment. In fact, the pitch moment appears to have a stronger influence on the uppermost members of the tower, whereas the thrust force has a stronger influence on the downmost members of the tower.

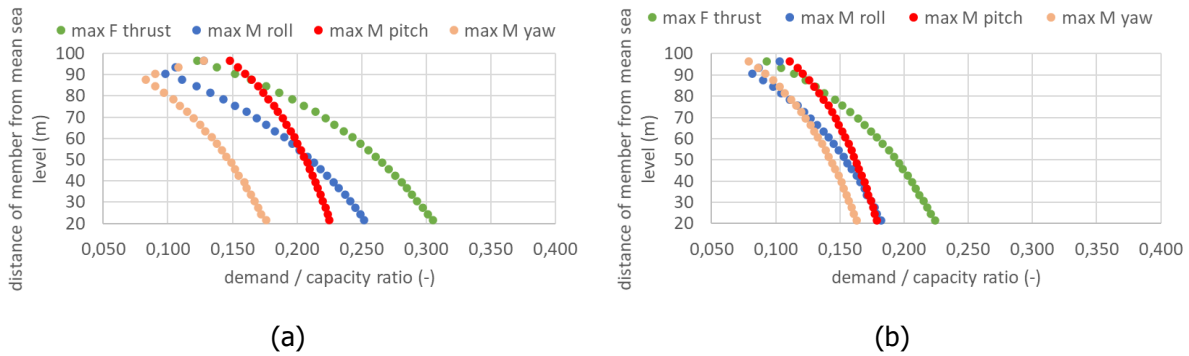


Figure 5-10 Demand / capacity ratios for the members of the tower for various snapshots of the time-history, hub-height wind speed equal to 7m/s under (a) DLC 1.3, (b) DLC 1.6

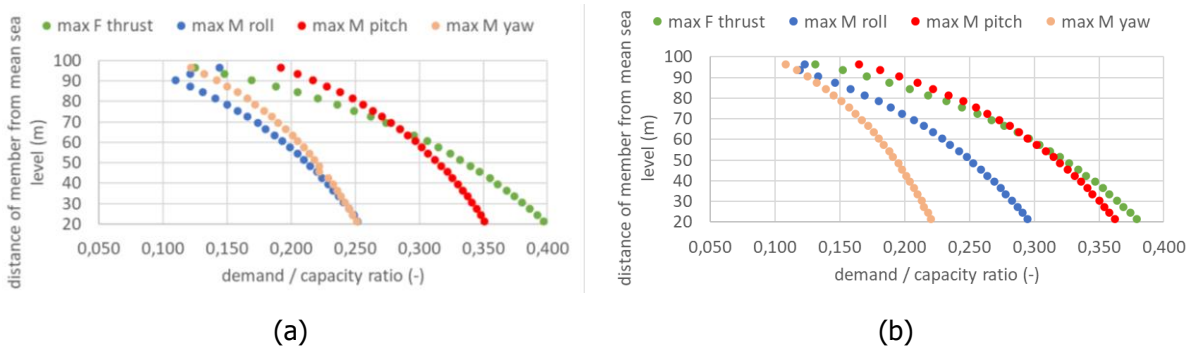


Figure 5-11 Demand / capacity ratios for the members of the tower for various snapshots of the time-history, hub-height wind speed equal to 11.4m/s under (a) DLC 1.3, (b) DLC 1.6

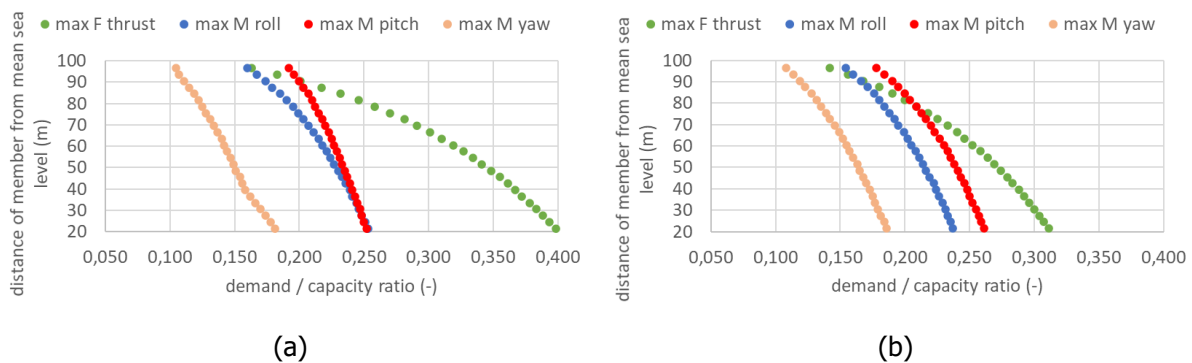


Figure 5-12 Demand / capacity ratios for the members of the tower for various snapshots of the time-history, hub-height wind speed equal to 20m/s under (a) DLC 1.3, (b) DLC 1.6

## 5.5 DEMAND / CAPACITY RATIOS FOR THE SUBSTRUCTURE AND FOUNDATION

Due to the special symmetry of the substructure (3 axes of symmetry on the xy plane) the transition piece and the tripod's member groups, namely the central pillar, members connecting the central pillar to the pile sleeves, tripod legs and members interconnecting sleeves, were investigated under loading in three wind and wave propagation directions: along the positive x axis, along the negative x axis, and along the negative y axis, as per the global coordinate system illustrated in Figure 5-13. Wind and waves were in all cases considered to be co-directional, which is expected to be the most unfavorable scenario for the structure overall.

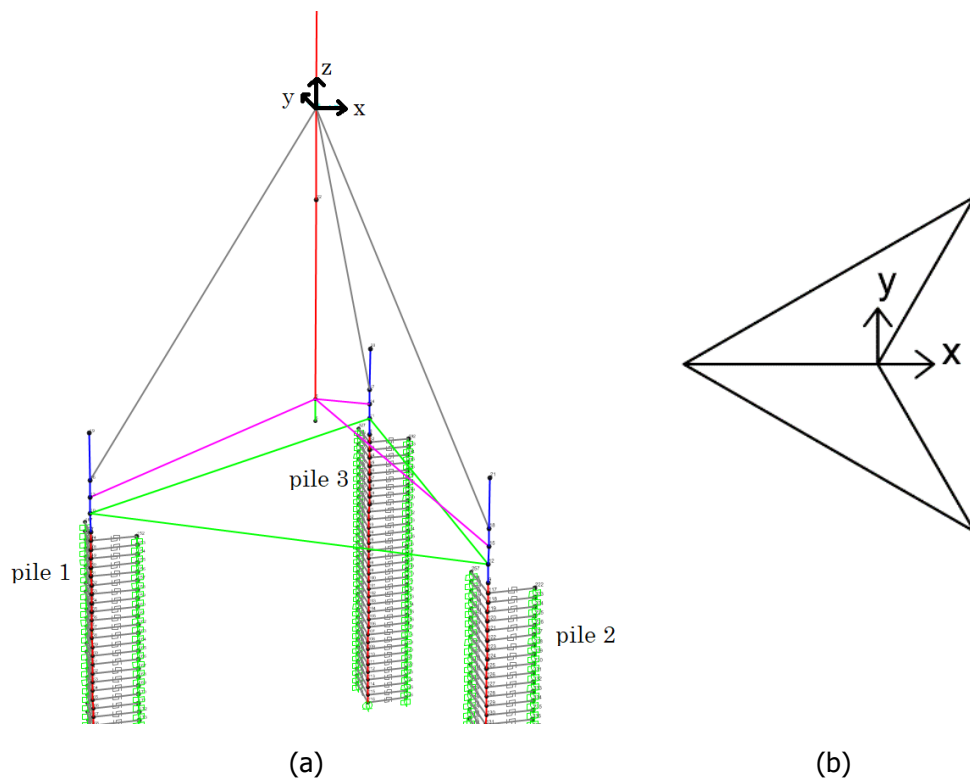


Figure 5-13 Global coordinate system in (a) 3d view and (b) plan view

Therefore, the analyses enumerated in 5.1 were ran for each one of these propagation directions. The maximum demand / capacity ratios resulting from each design load combination for each member category are given in Table 5-2. Notably, the demand / capacity ratios for the pile sleeves are not presented herein, as these members are to a significant degree subject to local buckling, a structural failure mechanism that has not been studied in the context of the present work.

Table 5-2 Demand / capacity ratios for the members of the tripod under different load combinations

Wind & Wave Propagation Direction	Design Load Combination	Maximum exploitation ratio for each member category					
		Transition piece	Central pillar	Member from central pillar to pile sleeve	Tripod leg	Member connecting sleeves	Pile
Along +x axis	DLC 1.6 V=7m/s	0.195	0.166	0.202	0.282	0.262	0.177
	DLC 1.6 V=11.4m/s	0.332	0.300	0.243	0.350	0.280	0.214
	DLC 1.6 V=20m/s	0.270	0.240	0.224	0.317	0.272	0.200
	DLC 1.3 V=7m/s	0.265	0.235	0.238	0.312	0.277	0.203
	DLC 1.3 V=11.4m/s	0.349	0.318	0.255	0.374	0.286	0.218
	DLC 1.3 V=20m/s	0.346	0.314	0.260	0.353	0.286	0.225
Along -x axis	DLC 1.6 V=7m/s	0.195	0.166	0.206	0.331	0.267	0.186
	DLC 1.6 V=11.4m/s	0.332	0.300	0.257	0.410	0.292	0.243
	DLC 1.6 V=20m/s	0.269	0.239	0.230	0.383	0.279	0.216
	DLC 1.3 V=7m/s	0.274	0.244	0.234	0.386	0.280	0.219
	DLC 1.3 V=11.4m/s	0.368	0.336	0.317	0.463	0.299	0.263
	DLC 1.3 V=20m/s	0.270	0.240	0.232	0.391	0.281	0.219
Along -y axis	DLC 1.6 V=7m/s	0.177	0.149	0.202	0.304	0.259	0.192
	DLC 1.6 V=11.4m/s	0.243	0.214	0.232	0.354	0.270	0.220
	DLC 1.6 V=20m/s	0.272	0.243	0.233	0.377	0.276	0.237
	DLC 1.3 V=7m/s	0.192	0.163	0.217	0.313	0.262	0.196
	DLC 1.3 V=11.4m/s	0.263	0.234	0.238	0.367	0.273	0.230
	DLC 1.3 V=20m/s	0.277	0.248	0.234	0.380	0.277	0.239
<b>Maximum exploitation ratio overall</b>		0.368	0.336	0.317	0.463	0.299	0.263

Comparison of the demand / capacity ratios for any combination of wind speed, member category and loads propagation direction yields that these are in all cases greater, when the wind action follows the Extreme Turbulence Model (DLC 1.3), compared to the cases where it follows the Normal Turbulence Model (DLC 1.6). This behavior contradicts the fact that DLC 1.6 is associated with much more severe wave action (Table 5-1), and it is therefore concluded, that the effect of wave loading on the substructure is less significant than that of wind.

Comparison of graphs of wind and wave propagation along either the positive or negative x axis, the same turbulence model and different wind speeds, indicates that the member exploitation is higher for 20m/s than it is for 7m/s, whereas the greatest exploitation appears for the rated wind speed, 11.4m/s. This observation does not apply when wind and waves propagate along the negative y axis, in which



case the demand / capacity ratios appear to grow progressively with the wind speed. This indicates that wave action is more unfavorable for the tripod at this propagation direction.

Overall, the maximum demand / capacity ratio for all member categories of the substructure and foundation appear for DLC 1.3, hub-height wind speed equal to 11.4m/s and load propagation along the negative x axis. The exploitation of these members being maximized for this load propagation direction can be attributed to the undertaking of the loading by exclusively the corresponding tripod leg (Figure 5-13). It is remarkable that the load combination of DLC 1.3 and  $V=11.4\text{m}$  constitutes one of the most unfavorable loading scenarios for the tower as well, as it was attested in Chapter 5.4.

Axial force, shear force and bending moment diagrams, along with the deformed shape of the substructure and piles for the most unfavorable load combination (DLC 1.3, hub-height wind speed equal to 11.4m/s, wind and wave propagation along the negative x axis), are given in Figure 5-14 and Figure 5-15 respectively. Pile numbering has been given in Figure 5-13.

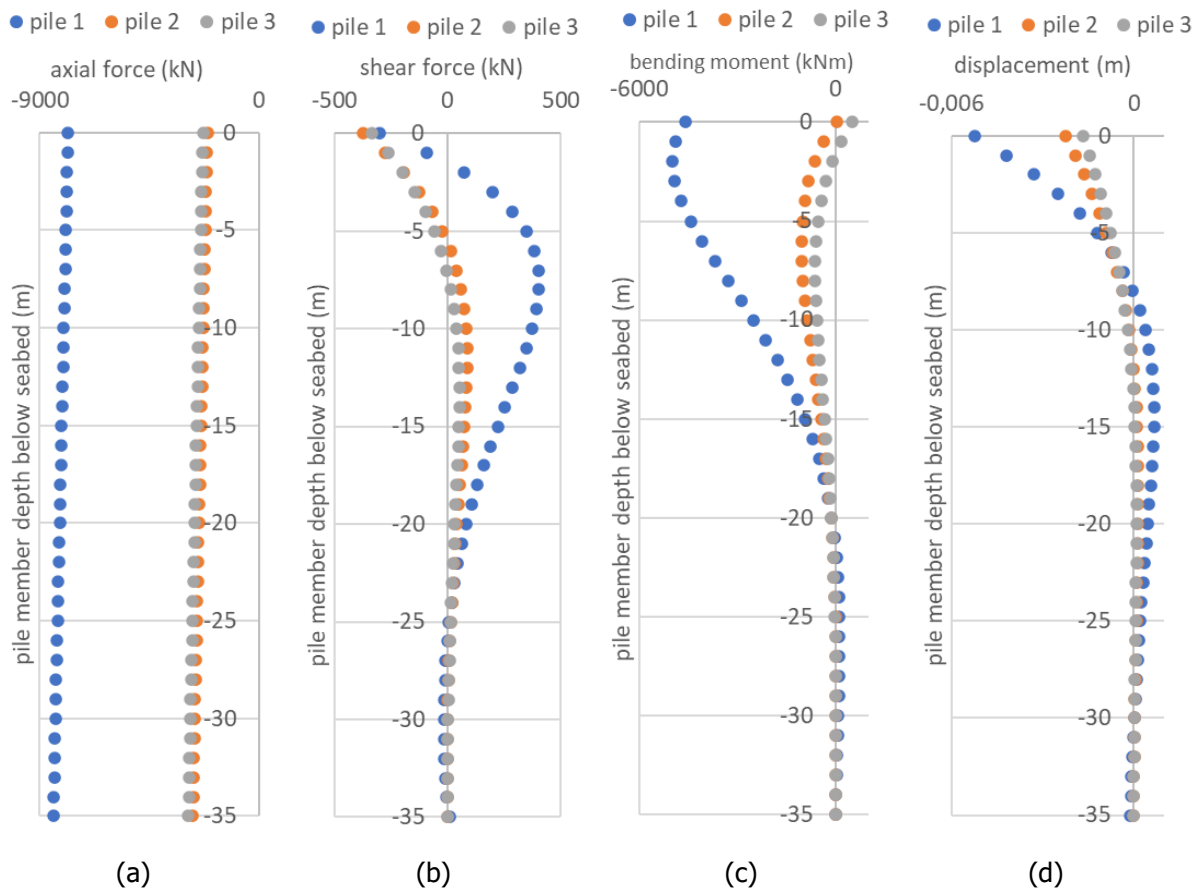


Figure 5-14 Axial force (a), shear force (b), bending moment (c) diagrams, and deformed shape (d) of the three piles under the most extreme design load combination (DLC 1.3,  $V=11.4\text{m/s}$ , load propagation along the negative x axis)

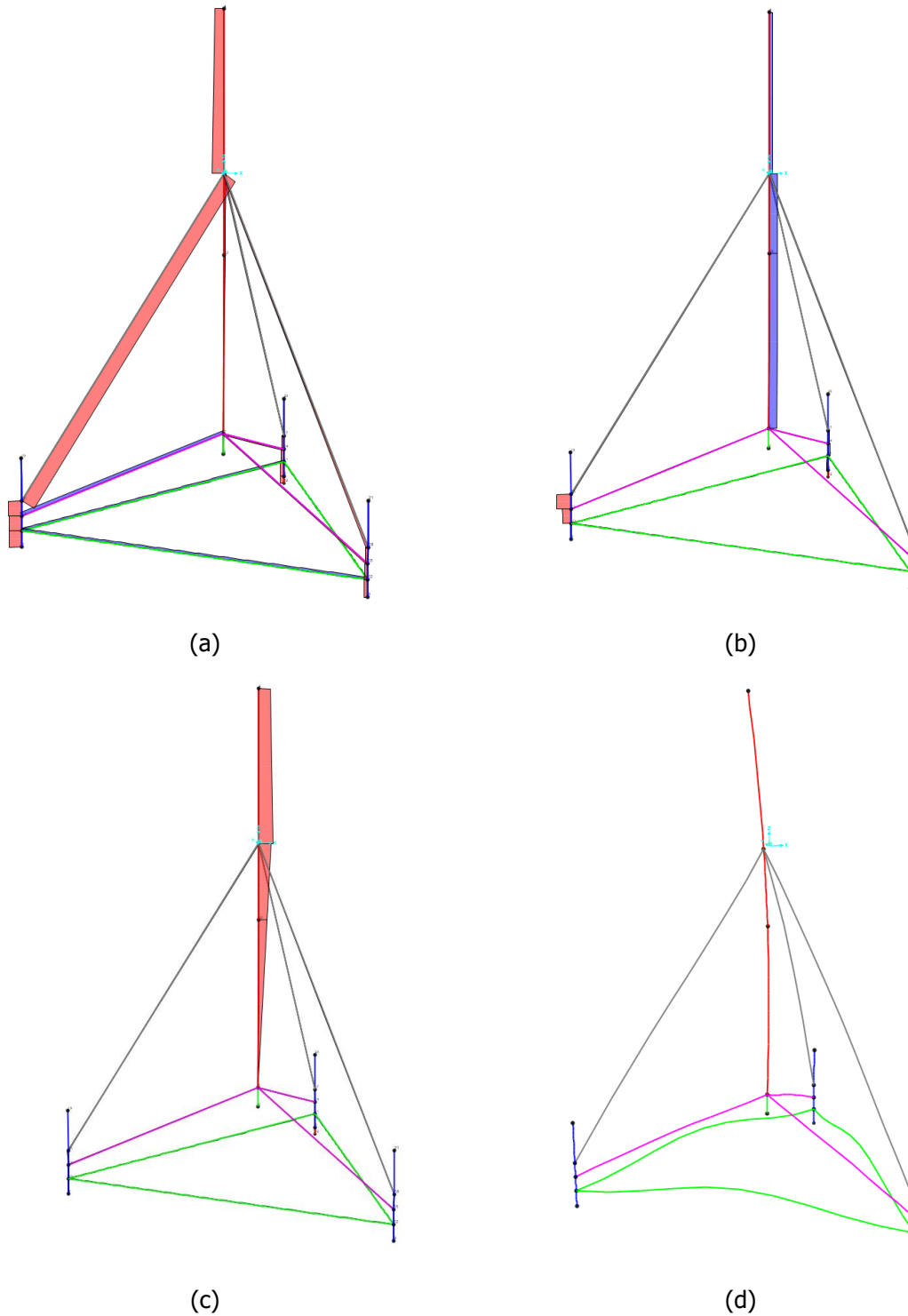


Figure 5-15 Axial force (a), shear force (b), bending moment (c) diagrams, and deformed shape (d) of the tripod under the most extreme design load combination (DLC 1.3,  $V=11.4\text{m/s}$ , load propagation along the negative x axis)

## 6 CONCLUSIONS AND SUGGESTED FURTHER WORK

The latest technological advancements in the industry of offshore wind emphasize on structural systems that can accommodate the larger installation depths, as well as construction practices to streamline the transportation and installation of increasingly large and heavy structures. Widely employed bottom-fixed systems include the monopile, jacket, tripod, tripile and gravity-based, while some floating systems have also been used, namely the spar and semi-submersible. Academic and commercial interest also focuses on introducing structures from the oil and gas industry, such as the twisted jacket, jack-up and tension leg platform.

An offshore wind turbine with a tripod substructure and pile foundation was used as a case study. The location of the structure, north-west coast of Kasos Island, was selected due to the high wind power density in the area and suitability of depth for the installation of a tripod. Subsequent to specifying the geometry of the structure and simulating the soil-pile interaction with non-linear springs, analyses were executed for the power production phase of the turbine and structural design checks were performed for the members. Wind and wave loads on the structure were estimated under Design Load Cases 1.3 (Extreme Turbulence Model and Normal Sea State) and 1.6 (Normal Turbulence Model and Severe Sea State), for three hub-height wind speeds: 7m/s, 11.4m/s (the rated wind speed), and 20m/s.

Design Load Case 1.3, for hub-height wind speed equal to 11.4m/s, and load propagation along the negative x axis proved to be the most unfavorable loading scenario for the structure overall. This can be attributed to the following observations. First, the demand / capacity ratios for any wind speed, are in all cases greater, when the wind flow follows the Extreme Turbulence Model rather than the Normal Turbulence Model. This can be explained by the increased fluid friction and viscosity that accompanies wind flow of higher turbulence levels. Second, the mean tower top thrust force is highest at the rated wind speed, potentially due to the transition in turbine control regions at this speed. Third, the undertaking of the loading by exclusively one tripod leg, renders load propagation along the negative x axis the most critical one.

As far as future work is concerned, the following suggestions can be made. First, the strength checks were performed in SAP2000, on a simplified model consisting of beam elements. A more elaborate model built with shell elements would provide further information regarding the structural design, for instance regarding local buckling. Additionally, the power production phase was indicatively selected and studied, in order to examine the behavior of the entire structure, while the turbine is working.

However, the configuration of the tripod has to be checked against a significant number of additional design situations, to cover among others the occurrence of fault, start-up and shut down phases, parked condition and maintenance. A considerable number of simulations has to be executed for each design situation, to address the stochastic nature of wind and wave action and represent reality as accurately as possible. Lastly, turbine performance analysis based on detailed statistical data of the wind regime in the area must precede site selection, in order for the output of the turbine to be the maximum possible.

## REFERENCES

- American Petroleum Institute. (2007). *Recommended Practice for Planning, Designing and Constructing Fixed Offshore Platforms - Working Stress Design*. Washington: American Petroleum Institute.
- Apata, O., & Oyedokun, D. (2020). An overview of control techniques for wind turbine systems. *Scientific African*.
- Baert, B. (2014). *Analysis of the Installation of a Series of Piles for Offshore Wind Turbine Foundations*. Rostock: University of Rostock.
- Bir, G. S. (2007). *User's Guide to BModes*. Golden, Colorado: National Renewable Energy Laboratory.
- Brunner, W. G., & Beyer, M. (2008). New Bauer Flydrill System, Drilling Monopiles at Barrow Offshore Wind Farm, U.K. *6th International Conference on Case Histories in Geotechnical Engineering*. Arlington, VA.
- Bush, E., & Lance, M. (2009). Foundation models for offshore wind turbines. *47th AIAA aerospace sciences meeting including the new horizons forum and aerospace exposition*. Orlando, Florida.
- Camp, T. (2008). OC3 internal communication from GH, tower definition\_NEW.xls.
- Damiani, R., Jonkman, J., & Hayman, G. (2015). *SubDyn User's Guide and Theory Manual*. Golden, Colorado: National Renewable Energy Laboratory.
- DNV-GL. (2016). *Recommended Practice - Analysis of grouted connections using the finite element method*. DNV-GL.
- DNV-GL. (2016). *Standard - Loads and site conditions for wind turbines*. DNV-GL.
- DNV-GL. (2018). *Standard - Support structures for wind turbines*. DNV-GL.
- Duckwitz, D., & Shan, M. (2014). Active tower damping and pitch balancing - design, simulation and field test. *Journal of Physics: Conference Series, The Science of Making Torque from Wind 2012*. 555, pp. 1-11. Oldenburg, Germany: IOP Publishing Ltd.
- EN 1991-1-4. (2010). *Eurocode 1: Actions on structures - Part 4: Wind actions*. European Committee for Standardization.
- Equinor. (2022). *How Hywind works*. Retrieved from Equinor: <https://www.equinor.com/en/what-we-do/floating-wind/how-hywind-works.html>

- Esteban, M. D., Couñago, B., López-Gutiérrez, J. S., Negro, V., & Vellisco, F. (2015). Gravity based support structures for offshore wind turbine generators: Review of the installation process. *Ocean Engineering*, *110*, 281-291.
- Golightly, C. (2014). Tilting of monopiles. Long, heavy and stiff; pushed beyond their limits. *Ground Engineering*.
- HBM - Hottinger Brüel & Kjaer. (2022). *Torque Measurement in Wind Turbines*. Retrieved from HBM - Hottinger Brüel & Kjaer: [https://www.hbm.com/fileadmin/mediapool/files/technical-articles-technotes-white-papers/2012/wind\\_turbines\\_en.pdf](https://www.hbm.com/fileadmin/mediapool/files/technical-articles-technotes-white-papers/2012/wind_turbines_en.pdf)
- Horwath, S., Hassrick, J., Grismala, R., Diller, E., Krebs, J., & Manhard, R. (2021). *Comparison of Environmental Effects from Different Offshore Wind Turbine Foundations*. U.S. Department of the Interior, Bureau of Ocean Energy Management, Office of Renewable Energy Programs.
- IEC. (2005). *Standard: Wind turbines Part 1: Design requirements*. IEC.
- IEC. (2020). *Standard: Wind energy generation systems Part 3-1: Design requirements for fixed offshore wind turbines*. IEC.
- Jeppsson, J., Larsen, P. E., & Larsson, Å. (2008). *Technical Description Lillgrund Wind Power Plant*. Vattenfall Vindkraft AB.
- Jonkman, B. J. (2012). *TurbSim User's Guide: Version 1.50*. Golden, Colorado: National Renewable Energy Laboratory.
- Jonkman, B., & Jonkman, J. (2016). *FAST v8.16.00a-bjj User Manual*. Golden, Colorado: National Renewable Energy Laboratory.
- Jonkman, J. M., Hayman, G. J., Jonkman, B. J., Damiani, R. R., & Murray, R. E. (2017). *AeroDyn v15 User's Guide and Theory Manual*. Golden, Colorado: National Renewable Energy Laboratory.
- Jonkman, J. M., Robertson, A. N., & Hayman, G. J. (2015). *HydroDyn User's Guide and Theory Manual*. Golden, Colorado: National Renewable Energy Laboratory.
- Jonkman, J., & Matha, D. (2009). A Quantitative Comparison of the Responses of Three Floating Platforms. *European Offshore Wind 2009 Conference and Exhibition*. Stockholm: National Renewable Energy Lab (NREL), U.S. Department of Energy.
- Jonkman, J., Butterfield, S., Musial, W., & Scott, G. (2009). *Definition of a 5-MW Reference Wind Turbine for Offshore System Development*. Golden, Colorado: National Renewable Energy Laboratory.
- Journée, J. J., & Massie, W. W. (2001). Wave forces on slender cylinders. In J. J. Journée, & W. W. Massie, *Offshore Hydromechanics*. Delft University of Technology.
- Massachusetts Institute of Technology. (2017). *Stokes wave theory*. Retrieved from Abaqus documentation: <https://abaqus-docs.mit.edu/2017/English/SIMACAETHERefMap/simathe-c-stokeswave.htm>
- Musial, W., Spitsen, P., Beiter, P., Duffy, P., Marquis, M., Cooperman, A., . . . Shields, M. (2021). *Offshore Wind Market Report: 2021 Edition*. Office of Energy Efficiency and Renewable Energy, U.S. Department of Energy.
- Nguyen, C.-U., Lee, S.-Y., & Kim, J.-T. (2019). Vibration-Based Damage Assessment in Gravity-Based Wind Turbine Tower under Various Waves. *Shock and vibration*.
- Offshore Renewable Energy Catapult Ltd. (2020). *U.K. Strategic Capability Assessment - Offshore Wind Foundations*. Offshore Wind Growth Partnership.

- Offshore Wind. (2017, March). *Bauer Renewables to Do Relief Drilling for Beatrice Piles*. Retrieved October 2021, from Offshore Wind: <https://www.offshorewind.biz/2017/03/02/bauer-renewables-to-do-relief-drilling-for-beatrice-piles/>
- Passon, P. (2006). *Memorandum: derivation and description of the soil-pile-interaction models*. IEA-Annex XXVIII Subtask 2.
- Platt, A., Jonkman, B., & Jonkman, J. (2016). *InflowWind User's Guide*. Golden, Colorado: National Wind Technology Center.
- Roshko, A. (1961). Experiments on the flow past a circular cylinder at very high Reynolds number. *Journal of Fluid Mechanics*, 10(3), 345-356.
- Saville, T., McClendon, E. W., & Cochran, A. L. (1962). Freeboard allowances for waves in inland reservoirs. *Waterways and Harbors*, 93-124.
- Skjelbreia, L., & Hendrickson, J. (1961). Fifth order gravity wave theory. *7th Conference Coastal Engineering*, (pp. 184-196). The Hague.
- Soukissian, T., Papadopoulos, A., Skrimizeas, P., Karathanasi, F., Axaopoulos, P., Avgoustoglou, E., . . . Katsafados, P. (2017). Assessment of offshore wind power potential in the Aegean and Ionian Seas based on high-resolution hindcast model results. *AIMS Energy*, 5(2), 268-289.
- Stavridou, N., Efthymiou, E., & Baniotopoulos, C. C. (2015). Verification of Anchoring in Foundations of Wind Turbine Towers. *American Journal of Engineering and Applied Sciences*.
- Sverdrup, H. U., & Munk, W. H. (1947). *Wind, sea and swell: Theory of relations for forecasting*. Washington, D.C.: U.S. Navy Department, Hydrographic Office.
- van Wijngaarden, M. (2013). *Concept design of steel bottom founded support structures for offshore wind turbines*. Delft: Delft University of Technology.
- Vorpahl, F., Schwarze, H., Fischer, T., & Seidel, M. (2013). Offshore wind turbine environment, loads, simulation, and design. *Wiley Interdisciplinary Reviews: Energy and Environment*, 2(5), 548-570.
- Woodhatch, M. (2017, April). *Offshore Wind Turbines – How do you install a wind turbine out at sea?* Retrieved November 2021, from Groundsure: <https://www.groundsure.com/resources/offshore-wind-turbines/>
- Zhao, Y., Yang, J., & He, Y. (2012). Preliminary Design of a Multi-Column TLP Foundation for a 5-MW Offshore Wind Turbine. *Energies*, 5(12), 3874-3891.
- Καραμπάς, Θ., Κρεστενίτης, Ι., & Κουτίτας, Χ. (2015). Στοιχεία Κυματομηχανικής. Στο *Ακτομηχανική - έργα προστασίας ακτών*. Αθήνα: Σύνδεσμος Ελληνικών Ακαδημαϊκών Βιβλιοθηκών.
- Μηχανικοί Μελετών & Εφαρμογών Α.Ε., ΤΕΡΝΑ Ενεργειακή Α.Ε., Εργαστήριο Μεταλλικών Κατασκευών – Ε.Μ.Π., Εργαστήριο Υδραυλικής Μηχανικής- Π.Π. (2015). *Σχεδιασμός θαλασσιών ανεμογεννητριών με βάση την επιτελεστικότητα*. Ερευνητικό Πρόγραμμα SEAWIND.
- Χαλούλος, Γ. Κ. (2012). *Αριθμητική διερεύνηση της σεισμικής απόκρισης πασσάλου υπό καθεστώς ρευστοποίησης και οριζόντιας μετατόπισης του εδάφους*. Αθήνα: Εθνικό Μετσόβιο Πολυτεχνείο.





## ANNEX A - SHORT DESCRIPTION OF FAST

The last public release of FAST, FAST v8.16.00a-bjj, was used to model the behavior of the offshore wind turbine and the structure it is mounted atop. FAST is a wind turbine multi-physics engineering tool that consists of various modules coupled together, each representing a different physics aspect of a bottom-fixed or floating wind turbine system (Figure A-0-1). The software has been set up and constantly further developed by the National Renewable Energy Laboratory (NREL), U.S. Department of Energy.

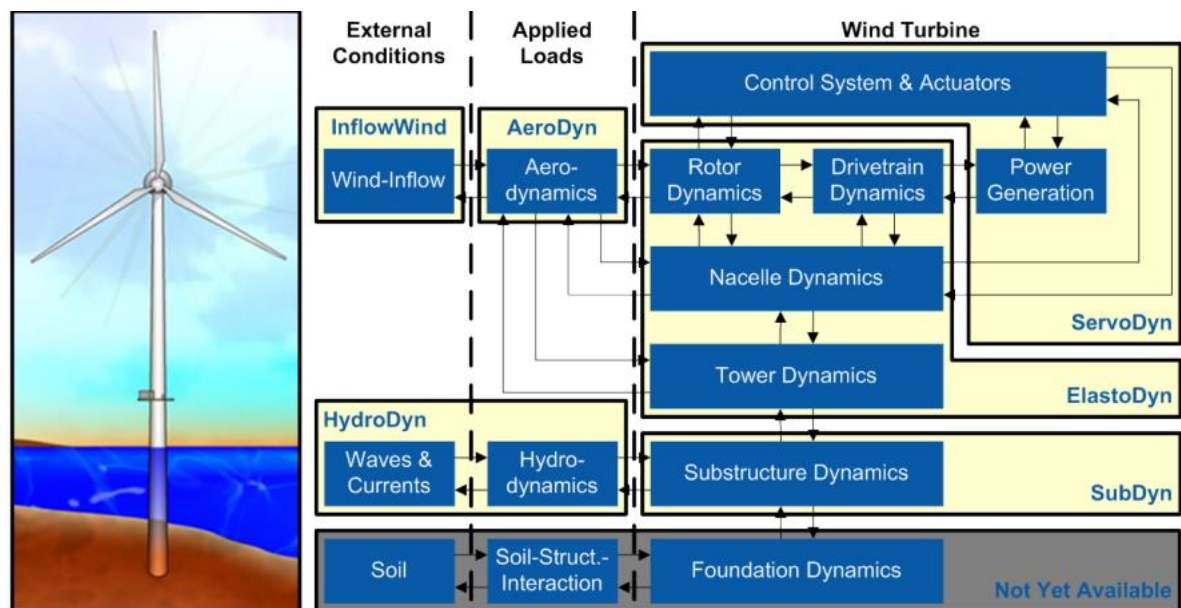


Figure A-0-1 FAST control volumes for bottom-fixed systems (Jonkman & Jonkman, 2016)

InflowWind is a module for producing and processing wind data. At each time step, InflowWind receives the coordinate position of various points from the driver code and returns the undisturbed wind-inflow velocities at these positions. Each wind velocity component is calculated as a function of the input coordinate positions and internal time-varying parameters, undisturbed from interaction with the wind turbine. Various types of wind profiles are supported: uniform, steady and turbulent (Platt, Jonkman, & Jonkman, 2016).

AeroDyn enables aero-elastic simulation of horizontal axis turbines by calculating aerodynamic loads on both the blades and tower. At each time step, AeroDyn receives from the driver code the instantaneous structural position, orientation, and velocities of analysis nodes in the tower, hub, and blades, as well as the undisturbed fluid velocities at the tower and blade nodes. This module then computes the aerodynamic loads on the blade and tower nodes and returns them to FAST (Jonkman, Hayman, Jonkman, Damiani, & Murray, 2017).

ServoDyn simulates the control and electrical drive mechanisms of the turbine; blade-pitch control, override pitch maneuvers, generator models, torque control, high-speed shaft brake, nacelle-yaw control, override yaw maneuvers, nacelle- and tower- based tuned-mass dampers (Jonkman & Jonkman, 2016).

ElastoDyn simulates the structural dynamics of the transition piece, tower, and rotor-nacelle assembly (RNA); blade bending, shear, extensional and torsion degrees of freedom (DOF's), support for non-straight, composite, and highly flexible blades, rotor-teeter DOF, generator azimuth and drivetrain torsion DOF's, nacelle-yaw DOF, tower-bending DOF's, rigid-body platform DOF's, fixed-bottom substructure DOF's, gravitational loading, gearbox friction (Jonkman & Jonkman, 2016).

HydroDyn calculates the hydrodynamic loads on the wind turbine substructure and is applicable to both bottom-fixed and floating offshore substructures. HydroDyn generates waves analytically for finite depth using first order (linear Airy) or first-order and second-order wave theory wave kinematics in the domain between the seabed and still-water level; no wave stretching is included. Waves generated internally within HydroDyn can be regular or irregular, unidirectional or multidirectional. Alternatively, wave kinematics can be generated externally and imported. Multiple approaches for hydrodynamic load calculation are available: a potential-flow theory solution, applicable to substructures or members of substructures that are large relative to a typical wavelength, a strip-theory solution, applicable to slender substructures or members, or a combination of the two. At each time step, HydroDyn receives from the driver code the position, orientation, velocities, and accelerations of the substructure, in order to compute the hydrodynamic loads and return them to FAST (Jonkman, Robertson, & Hayman, 2015).

SubDyn is a structural dynamics module for the substructures of bottom-fixed offshore wind turbines, namely monopiles, tripods and jackets. At each time step, loads and responses are transferred between SubDyn, HydroDyn, and ElastoDyn via the FAST driver code to enable hydro-elastic interaction. At the interface nodes, the transition piece's six degree-of-freedom displacements, velocities and accelerations are inputs to SubDyn from ElastoDyn; and the six reaction loads at the transition piece are outputs from SubDyn to ElastoDyn. SubDyn also outputs the local substructure displacements, velocities, and accelerations to HydroDyn in order to calculate the local hydrodynamic loads that become inputs for SubDyn. In addition, SubDyn can calculate member internal reaction loads, as requested by the user (Damiani, Jonkman, & Hayman, 2015).

SoilDyn, a soil-structure interaction module applicable to pile foundations is currently being developed by the NREL. This module will allow users to input soil stiffness and damping. Until such an option becomes publicly available, the flexibility of the foundation and the effect of soil-structure interaction on the dynamic response of a bottom-fixed offshore wind turbine can be considered through the Apparent Fixity approach, which has been described and used in the context of the present work, in Chapter 4.8.

The simulation of some floating systems in FAST, namely spar, semi-submersible, TLP platform and ITI barge, is also feasible. In that case, SubDyn is replaced by either MAP++, MoorDyn or FEAMooring, which are alternative modules to model the dynamics of the mooring system of the floating structure (Figure A-0-2). The rest of the modules enumerated and described above are still applicable, by making the necessary adjustments.

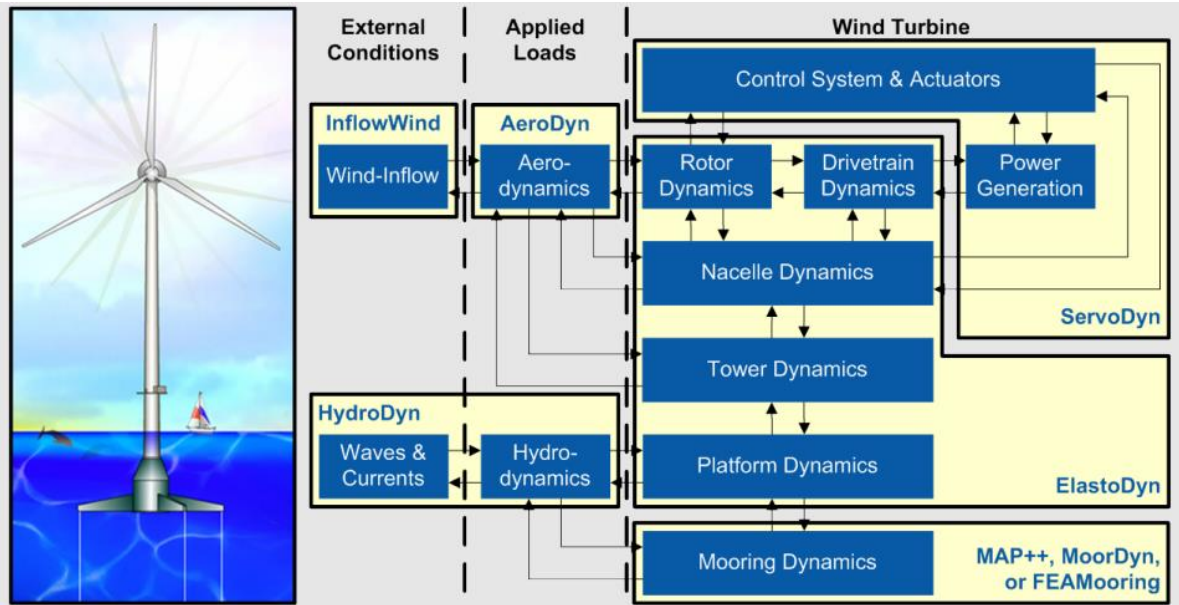


Figure A-0-2 FAST control volumes for floating systems (Jonkman & Jonkman, 2016)

FAST comes with a range of supporting engineering tools that include preprocessors to help build models, simulators to perform the analysis, postprocessors to analyze the results, and utilities to run and manage the processing tasks. Two of the available preprocessors were used as part of the present work, TurbSim and BModes.

TurbSim is a stochastic, full-field turbulence simulator to be used with the Inflow Wind module, in case the wind profile setting is set to "Turbulent". TurbSim is used to numerically simulate time series of three-component wind speed vectors at points in a two-dimensional vertical rectangular grid that is fixed in space (Figure A-0-3). Spectra of velocity components and spatial coherence are defined in the frequency domain. Spectral representation can be based on several different spectral models, including two models suggested by the IEC, the IEC Kaimal Model (IECKAI) and the IEC Von Karman Isotropic Model (IECVKM). The dimensions of the grid, namely height and width, are parameters to be input by the user, and must in all cases be at least 10% larger than the rotor diameter. The hub is in the horizontal center of the grid, and the turbine hub height plus assumed rotor radius determines the top of the grid (Jonkman B. J., 2012).

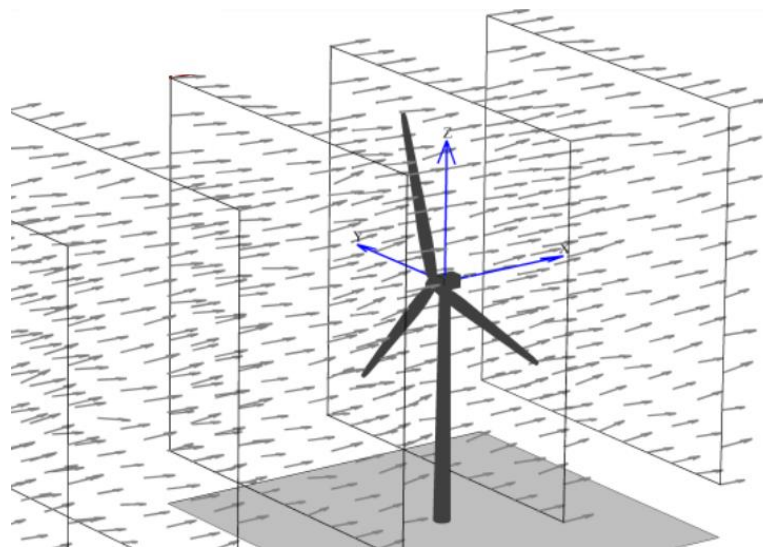


Figure A-0-3 Example of TurbSim grid implementation (Jonkman B. J., 2012)

BModes is a finite-element code that provides dynamically coupled modes for a beam. A sixth-order polynomial is then fitted to each mode, the coefficients of which are used as input to ElastoDyn. FAST needs blade and tower modes, as well as structural properties to compute modal integrals for its equations of motion, and uses uncoupled modes for fore-aft and side-to-side degrees of freedom of the blade and also for the fore and lateral motions of the tower. BModes computes flap-lag-torsion coupled modes that account for the torsion degrees of freedom, as well as the offsets of shear center, tension center, and center of mass, which can cause significant dynamic couplings (Bir, 2007). In the work presented herein, the blade geometry was not altered, therefore the default modes for blades were maintained. BModes was used to provide the first two fore-aft and first two side-to-side modes of the tower, for the tower distributed properties selected.

## **ANNEX B- FAST INPUT FILES**

Indicatively, the modules used as part of one particular FAST analysis are given below, including the text files required by the pre-processors TurbSim and BModes. The analysis corresponds to the Power Production Design Load Case 1.6 (please refer to Table 3-2). More specifically, the wind action follows the Normal Turbulence Model, with a wind speed at hub height equal to 11.4m/s. The sea conditions are described by still water, as the FAST analysis precedes the one in SAP2000, which is where the wave action is considered. Lastly, the apparent fixity length has been considered both in the SubDyn module, and in the calculation of tower mode shapes through the BModes pre-processor.



## MAIN INPUT FILE

----- FAST v8.16.\* INPUT FILE -----

FAST Certification Test #20: NREL 5.0 MW Baseline Wind Turbine with OC3 Tripod Configuration, for use in offshore analysis

----- SIMULATION CONTROL -----

False Echo - Echo input data to <RootName>.ech (flag)  
"FATAL" AbortLevel - Error level when simulation should abort (string) {"WARNING", "SEVERE", "FATAL"}  
600 TMax - Total run time (s)  
0.008 DT - Recommended module time step (s)  
2 InterpOrder - Interpolation order for input/output time history (-) {1=linear, 2=quadratic}  
1 NumCrctn - Number of correction iterations (-) {0=explicit calculation, i.e., no corrections}  
99999.9 DT\_UJac - Time between calls to get Jacobians (s)  
1E+06 UJacScfFact - Scaling factor used in Jacobians (-)

----- FEATURE SWITCHES AND FLAGS -----

1 CompElast - Compute structural dynamics (switch) {1=ElastoDyn; 2=ElastoDyn + BeamDyn for blades}  
1 CompInflow - Compute inflow wind velocities (switch) {0=still air; 1=InflowWind; 2=external from OpenFOAM}  
2 CompAero - Compute aerodynamic loads (switch) {0=None; 1=AeroDyn v14; 2=AeroDyn v15}  
1 CompServo - Compute control and electrical-drive dynamics (switch) {0=None; 1=ServoDyn}  
1 CompHydro - Compute hydrodynamic loads (switch) {0=None; 1=HydroDyn}  
1 CompSub - Compute sub-structural dynamics (switch) {0=None; 1=SubDyn}  
0 CompMooring - Compute mooring system (switch) {0=None; 1=MAP++; 2=FEAMooring; 3=MoorDyn; 4=OrcaFlex}  
0 CompIce - Compute ice loads (switch) {0=None; 1=IceFloe; 2=IceDyn}

----- INPUT FILES -----

"5MW\_Baseline/NRELOffshrBsline5MW\_OC3Tripod\_ElastoDyn\_try.dat" EDFile - Name of file containing ElastoDyn input parameters (quoted string)  
"5MW\_Baseline/NRELOffshrBsline5MW\_BeamDyn.dat" BDBldFile(1) - Name of file containing BeamDyn input parameters for blade 1 (quoted string)  
"5MW\_Baseline/NRELOffshrBsline5MW\_BeamDyn.dat" BDBldFile(2) - Name of file containing BeamDyn input parameters for blade 2 (quoted string)  
"5MW\_Baseline/NRELOffshrBsline5MW\_BeamDyn.dat" BDBldFile(3) - Name of file containing BeamDyn input parameters for blade 3 (quoted string)  
"5MW\_Baseline/NRELOffshrBsline5MW\_InflowWind\_Turb\_try.dat" InflowFile - Name of file containing inflow wind input parameters (quoted string)  
"5MW\_Baseline/NRELOffshrBsline5MW\_OC3Tripod\_AeroDyn15\_try\_LS.dat" AeroFile - Name of file containing aerodynamic input parameters (quoted string)  
"5MW\_Baseline/NRELOffshrBsline5MW\_OC3Tripod\_ServoDyn.dat" ServoFile - Name of file containing control and electrical-drive input parameters (quoted string)  
"5MW\_Baseline/NRELOffshrBsline5MW\_OC3Tripod\_HydroDyn\_try\_LS.dat" HydroFile - Name of file containing hydrodynamic input parameters (quoted string)

```

"5MW_Baseline/NRELOffshrBsline5MW_OC3Tripod_SubDyn_try_AF_LS.dat"  SubFile      - Name of file containing sub-structural input parameters (quoted
string)
"unused"  MooringFile  - Name of file containing mooring system input parameters (quoted string)
"unused"  IceFile        - Name of file containing ice input parameters (quoted string)
----- OUTPUT -----
False     SumPrint      - Print summary data to "<RootName>.sum" (flag)
    1  SttsTime    - Amount of time between screen status messages (s)
    1000 ChkptTime  - Amount of time between creating checkpoint files for potential restart (s)
    1.2  DT_Out     - Time step for tabular output (s) (or "default")
    0  TStart      - Time to begin tabular output (s)
    1  OutFileFmt  - Format for tabular (time-marching) output file (switch) {1: text file [<RootName>.out], 2: binary file [<RootName>.outb], 3: both}
True      TabDelim    - Use tab delimiters in text tabular output file? (flag) {uses spaces if false}
"ES10.3E2" OutFmt      - Format used for text tabular output, excluding the time channel. Resulting field should be 10 characters. (quoted string)
----- LINEARIZATION -----
False     Linearize   - Linearization analysis (flag)
    2  NLinTimes  - Number of times to linearize (-) [>=1] [unused if Linearize=False]
    30, 60  LinTimes   - List of times at which to linearize (s) [1 to NLinTimes] [unused if Linearize=False]
    1  LinInputs  - Inputs included in linearization (switch) {0=none; 1=standard; 2=all module inputs (debug)} [unused if Linearize=False]
    1  LinOutputs - Outputs included in linearization (switch) {0=none; 1=from OutList(s); 2=all module outputs (debug)} [unused if Linearize=False]
False    LinOutJac  - Include full Jacobians in linearization output (for debug) (flag) [unused if Linearize=False; used only if LinInputs=LinOutputs=2]
False    LinOutMod  - Write module-level linearization output files in addition to output for full system? (flag) [unused if Linearize=False]
----- VISUALIZATION -----
    0  WrVTK      - VTK visualization data output: (switch) {0=none; 1=initialization data only; 2=animation}
    2  VTK_type   - Type of VTK visualization data: (switch) {1=surfaces; 2=basic meshes (lines/points); 3=all meshes (debug)} [unused if WrVTK=0]
false   VTK_fields  - Write mesh fields to VTK data files? (flag) {true/false} [unused if WrVTK=0]
    15 VTK_fps     - Frame rate for VTK output (frames per second){will use closest integer multiple of DT} [used only if WrVTK=2]

```

## TURBSIM INPUT FILE

TurbSim Input File. Valid for TurbSim v1.50; 17-May-2010; Example file that can be used with simulations for the NREL 5MW Baseline Turbine; note that UsableTime has been decreased in this file so that the file distributed with the FAST CertTest isn't as large

-----Runtime Options-----

```

13428      RandSeed1    - First random seed (-2147483648 to 2147483647)
RanLux     RandSeed2    - Second random seed (-2147483648 to 2147483647) for intrinsic pRNG, or an alternative pRNG: "RanLux" or "RNSNLW"

```



False	WrBHHTP	- Output hub-height turbulence parameters in binary form? (Generates RootName.bin)
False	WrFHHTP	- Output hub-height turbulence parameters in formatted form? (Generates RootName.dat)
False	WrADHH	- Output hub-height time-series data in AeroDyn form? (Generates RootName.hh)
True	WrADFF	- Output full-field time-series data in TurbSim/AeroDyn form? (Generates RootName.bts)
False	WrBLFF	- Output full-field time-series data in BLADED/AeroDyn form? (Generates RootName.wnd)
True	WrADTWR	- Output tower time-series data? (Generates RootName.twr)
False	WrFMFFF	- Output full-field time-series data in formatted (readable) form? (Generates RootName.u, RootName.v, RootName.w)
False	WrACT	- Output coherent turbulence time steps in AeroDyn form? (Generates RootName.cts)
True	Clockwise	- Clockwise rotation looking downwind? (used only for full-field binary files - not necessary for AeroDyn)
0	ScaleIEC	- Scale IEC turbulence models to exact target standard deviation? [0=no additional scaling; 1=use hub scale uniformly; 2=use individual scales]

-----Turbine/Model Specifications-----

31	NumGrid_Z	- Vertical grid-point matrix dimension
31	NumGrid_Y	- Horizontal grid-point matrix dimension
0.05	TimeStep	- Time step [seconds]
630.0	AnalysisTime	- Length of analysis time series [seconds]
600.0	UsableTime	- Usable length of output time series [seconds] (program will add GridWidth/MeanHHWS seconds) [bjj: was 630]
100.4	HubHt	- Hub height [m] (should be > 0.5*GridHeight)
170.0	GridHeight	- Grid height [m]
170.0	GridWidth	- Grid width [m] (should be >= 2*(RotorRadius+ShaftLength))
0	VFlowAng	- Vertical mean flow (up) tilt angle [degrees]
0	HFlowAng	- Horizontal mean flow (skew) angle [degrees]

-----Meteorological Boundary Conditions-----

IECKAI	TurbModel	- Turbulence model ("IECKAI"=Kaimal, "IECVKM"=von Karman, "GP_LLJ", "NWTCUP", "SMOOTH", "WF_UPW", "WF_07D", "WF_14D", or "NONE")
"3"	IECstandard	- Number of IEC 61400-x standard (x=1,2, or 3 with optional 61400-1 edition number (i.e. "1-Ed2") )
"A"	IECturbc	- IEC turbulence characteristic ("A", "B", "C" or the turbulence intensity in percent) ("KHTTEST" option with NWTCUP, not used for other models)
NTM	IEC_WindType	- IEC turbulence type ("NTM"=normal, "xETM"=extreme turbulence, "xEWM1"=extreme 1-year wind, "xEWM50"=extreme 50-year wind, where x=wind turbine class 1, 2, or 3)
default	ETMc	- IEC Extreme turbulence model "c" parameter [m/s]
PL	WindProfileType	- Wind profile type ("JET"=Low-level jet, "LOG"=Logarithmic, "PL"=Power law, or "default", or "USR"=User-defined)
100.4	RefHt	- Height of the reference wind speed [m]

11.4	URef	- Mean (total) wind speed at the reference height [m/s]
default	ZJetMax	- Jet height [m] (used only for JET wind profile, valid 70-490 m)
default	PLExp	- Power law exponent [-] (or "default")
default	Z0	- Surface roughness length [m] (or "default")

-----Non-IEC Meteorological Boundary Conditions-----

default	Latitude	- Site latitude [degrees] (or "default")
0.05	RICH_NO	- Gradient Richardson number
default	UStar	- Friction or shear velocity [m/s] (or "default")
default	ZI	- Mixing layer depth [m] (or "default")
default	PC_UW	- Hub mean u'w' Reynolds stress [(m/s)^2] (or "default")
default	PC_UV	- Hub mean u'v' Reynolds stress [(m/s)^2] (or "default")
default	PC_VW	- Hub mean v'w' Reynolds stress [(m/s)^2] (or "default")
default	IncDec1	- u-component coherence parameters (e.g. "10.0 0.3e-3" in quotes) (or "default")
default	IncDec2	- v-component coherence parameters (e.g. "10.0 0.3e-3" in quotes) (or "default")
default	IncDec3	- w-component coherence parameters (e.g. "10.0 0.3e-3" in quotes) (or "default")
default	CohExp	- Coherence exponent (or "default")

-----Coherent Turbulence Scaling Parameters-----

"M:\coh_events\eventdata"	CTEventPath	- Name of the path where event data files are located
"Random"	CTEventFile	- Type of event files ("random", "les" or "dns")
true	Randomize	- Randomize disturbance scale and location? (true/false)
1.0	DistScI	- Disturbance scale (ratio of dataset height to rotor disk).
0.5	CTLy	- Fractional location of tower centerline from right (looking downwind) to left side of the dataset.
0.5	CTLz	- Fractional location of hub height from the bottom of the dataset.
10.0	CTStartTime	- Minimum start time for coherent structures in RootName.cts [seconds]

=====  
NOTE: Do not add or remove any lines in this file!  
=====

## INFLOW WIND INPUT FILE

----- InflowWind v3.01.\* INPUT FILE -----  
for FAST CertTests #20 and #25

```

-----
False      Echo      - Echo input data to <RootName>.ech (flag)
   3      WindType    - switch for wind file type (1=steady; 2=uniform; 3=binary TurbSim FF; 4=binary Bladed-style FF; 5=HAWC format; 6=User
defined)
   0      PropagationDir - Direction of wind propagation (meteorological rotation from aligned with X (positive rotates towards -Y) -- degrees)
   8      NWindVel    - Number of points to output the wind velocity (0 to 9)
  0, 0, 0, 0, 0, 0, 0, 0      WindVxiList - List of coordinates in the inertial X direction (m)
  0, 0, 0, 0, 0, 0, 0, 0      WindVyiList - List of coordinates in the inertial Y direction (m)
 20, 32, 44, 56, 68, 80, 92, 98      WindVzList - List of coordinates in the inertial Z direction (m)
===== Parameters for Steady Wind Conditions [used only for WindType = 1] =====
   8      HWindSpeed  - Horizontal windspeed (m/s)
  100     RefHt      - Reference height for horizontal wind speed (m)
   0.2    PExp       - Power law exponent (-)
===== Parameters for Uniform wind file [used only for WindType = 2] =====
"Wind/90m_12mps_twr.bts"  Filename    - Filename of time series data for uniform wind field. (-)
   100     RefHt      - Reference height for horizontal wind speed (m)
 125.88   RefLength  - Reference length for linear horizontal and vertical sheer (-)
===== Parameters for Binary TurbSim Full-Field files [used only for WindType = 3] =====
"TurbSim_DLC1.6_V11.4.bts"  Filename    - Name of the Full field wind file to use (.bts)
===== Parameters for Binary Bladed-style Full-Field files [used only for WindType = 4] =====
"unused"   FilenameRoot - Rootname of the full-field wind file to use (.wnd, .sum)
False      TowerFile  - Have tower file (.twr) (flag)
===== Parameters for HAWC-format binary files [Only used with WindType = 5] =====
"wasp\Output\basic_5u.bin"  FileName_u  - name of the file containing the u-component fluctuating wind (.bin)
"wasp\Output\basic_5v.bin"  FileName_v  - name of the file containing the v-component fluctuating wind (.bin)
"wasp\Output\basic_5w.bin"  FileName_w  - name of the file containing the w-component fluctuating wind (.bin)
  64     nx          - number of grids in the x direction (in the 3 files above) (-)
  32     ny          - number of grids in the y direction (in the 3 files above) (-)
  32     nz          - number of grids in the z direction (in the 3 files above) (-)
  16     dx          - distance (in meters) between points in the x direction (m)
   3     dy          - distance (in meters) between points in the y direction (m)
   3     dz          - distance (in meters) between points in the z direction (m)
  100     RefHt      - reference height; the height (in meters) of the vertical center of the grid (m)
----- Scaling parameters for turbulence -----
  1     ScaleMethod  - Turbulence scaling method [0 = none, 1 = direct scaling, 2 = calculate scaling factor based on a desired standard deviation]

```

```

1 SFx      - Turbulence scaling factor for the x direction (-) [ScaleMethod=1]
1 SFy      - Turbulence scaling factor for the y direction (-) [ScaleMethod=1]
1 SFz      - Turbulence scaling factor for the z direction (-) [ScaleMethod=1]
12 SigmaFx - Turbulence standard deviation to calculate scaling from in x direction (m/s) [ScaleMethod=2]
8 SigmaFy  - Turbulence standard deviation to calculate scaling from in y direction (m/s) [ScaleMethod=2]
2 SigmaFz  - Turbulence standard deviation to calculate scaling from in z direction (m/s) [ScaleMethod=2]
----- Mean wind profile parameters (added to HAWC-format files) -----
5 URef     - Mean u-component wind speed at the reference height (m/s)
2 WindProfile - Wind profile type (0=constant;1=logarithmic,2=power law)
0 PLExp    - Power law exponent (-) (used for PL wind profile type only)
0.03 Z0    - Surface roughness length (m) (used for LG wind profile type only)
===== OUTPUT =====
False      SumPrint - Print summary data to <RootName>.IfW.sum (flag)
           OutList  - The next line(s) contains a list of output parameters. See OutListParameters.xlsx for a listing of available output channels, (-)
"Wind1VelX, Wind1VelY"
"Wind2VelX, Wind2VelY"
"Wind3VelX, Wind3VelY"
"Wind4VelX, Wind4VelY"
"Wind5VelX, Wind5VelY"
"Wind6VelX, Wind6VelY"
"Wind7VelX, Wind7VelY"
"Wind8VelX, Wind8VelY"
END of input file (the word "END" must appear in the first 3 columns of this last OutList line)
-----

```

## BMODES INPUT FILE

```

===== BModes v3.00 Main Input File =====
Modes

----- General parameters -----
true  Echo      Echo input file contents to *.echo file if true.
2     beam_type 1: blade, 2: tower (-)
0.    romg:     rotor speed (rpm), automatically set to zero for tower modal analysis
1.    romg_mult: rotor speed multiplicative factor (-)

```

98 radius: rotor tip radius measured along coned blade axis OR tower height (m)  
 20. hub\_rad: hub radius measured along coned blade axis OR tower rigid-base height (m)  
 0. precone: built-in precone angle (deg), automatically set to zero for a tower  
 0. bl\_thp: blade pitch setting (deg), automatically set to zero for a tower  
 2 hub\_conn: hub-to-blade or tower-base boundary condition [1: cantilevered; 2: free-free; 3: only axial and torsion constraints] (-)  
 5 modepr: number of modes to be printed (-)  
 f TabDelim (true: tab-delimited output tables; false: space-delimited tables)  
 f mid\_node\_tw (true: output twist at mid-node of elements; false: no mid-node outputs)

----- Blade-tip or tower-top mass properties -----

350000 tip\_mass blade-tip or tower-top mass (see users' manual) (kg)  
 -0.414 cm\_loc tip-mass c.m. offset from the tower axis measured along the tower-tip x reference axis (m)  
 1.967 cm\_axial tip-mass c.m. offset tower tip measures axially along the z axis (m)  
 43700000 ixx\_tip blade lag or tower s-s mass moment of inertia about the tip-section x reference axis (kg-m<sup>2</sup>)  
 23530000 iyy\_tip blade flap or tower f-a mass moment of inertia about the tip-section y reference axis (kg-m<sup>2</sup>)  
 25420000 izz\_tip torsion mass moment of inertia about the tip-section z reference axis (kg-m<sup>2</sup>)  
 0. ixy\_tip cross product of inertia about x and y reference axes(kg-m<sup>2</sup>)  
 1169000 izx\_tip cross product of inertia about z and x reference axes(kg-m<sup>2</sup>)  
 0. iyz\_tip cross product of inertia about y and z reference axes(kg-m<sup>2</sup>)

----- Distributed-property identifiers -----

1 id\_mat: material\_type [1: isotropic; non-isotropic composites option not yet available]  
 'tower\_props\_LS.dat' sec\_props\_file name of beam section properties file (-)

Property scaling factors.....

1.0 sec\_mass\_mult: mass density multiplier (-)  
 1.0 flp\_iner\_mult: blade flap or tower f-a inertia multiplier (-)  
 1.0 lag\_iner\_mult: blade lag or tower s-s inertia multiplier (-)  
 1.0 flp\_stff\_mult: blade flap or tower f-a bending stiffness multiplier (-)  
 1.0 edge\_stff\_mult: blade lag or tower s-s bending stiffness multiplier (-)  
 1.0 tor\_stff\_mult: torsion stiffness multiplier (-)  
 1.0 axial\_stff\_mult: axial stiffness multiplier (-)  
 1.0 cg\_offst\_mult: cg offset multiplier (-)  
 1.0 sc\_offst\_mult: shear center multiplier (-)  
 1.0 tc\_offst\_mult: tension center multiplier (-)

----- Finite element discretization -----

26 nsel: no of blade or tower elements (-)

Distance of element boundary nodes from blade or flexible-tower root (normalized wrt blade or tower length), el\_loc()

0.0 0.0385 0.0769 0.1154 0.1538 0.1923 0.2308 0.2692 0.3077 0.3462 0.3846 0.4231 0.4615 0.5 0.5385 0.5769 0.6154 0.6538 0.6923 0.7308  
0.7692 0.8077 0.8462 0.8846 0.9231 0.9615 1.0

----- Properties of additional tower support subsystem (read only if beam\_type is 2) -----

2 tow\_support: : additional tower support [0: no additional support; 1: Tension guy wires for land-based tower; 2: offshore turbine support: floating platform or monopile] (-)

-20 draft : depth of tower base from the ground or the MSL (mean sea level) (m)

-20 cm\_pform : distance of platform c.m. below the MSL (m)

0 mass\_pform : platform mass (kg)

Platform mass inertia 3X3 matrix (i\_matrix\_pform):

0. 0. 0.

0. 0. 0.

0. 0. 2.48448E+06

-20 ref\_msl : distance of platform reference point below the MSL (m)

Platform-reference-point-referred hydrodynamic 6X6 matrix (hydro\_M):

0.324698E+06 0.257162E+01 -0.226679E+01 0.444600E+02 -0.444006E+07 0.267272E+02  
0.257168E+01 0.324677E+06 0.145307E+01 0.443974E+07 -0.491496E+02 -0.115271E+02  
-0.226782E+01 0.145120E+01 0.355266E+06 0.245400E+02 0.397070E+02 0.920074E+01  
0.444742E+02 0.443974E+07 0.245793E+02 0.707971E+08 -0.851351E+03 -0.171315E+03  
-0.444006E+07 -0.491525E+02 0.397482E+02 -0.851135E+03 0.708016E+08 -0.463750E+03  
0.267139E+02 -0.115054E+02 0.920427E+01 -0.170783E+03 -0.463835E+03 0.477406E+07

Platform-reference-point-referred hydrodynamic 6X6 stiffness matrix (hydro\_K):

0.493041E+08 -0.394844E+03 -0.576721E+02 -0.681254E+04 -0.848157E+09 -0.799333E+04  
-0.176808E+03 0.493102E+08 0.641474E+02 0.848193E+09 0.333782E+04 0.931174E+04  
0.987669E+03 -0.400124E+03 0.817431E+09 -0.104079E+05 -0.231345E+05 0.222656E+04  
-0.398201E+04 0.848202E+09 -0.180764E+04 0.327695E+11 0.812144E+05 0.139343E+06  
-0.848105E+09 0.780683E+04 -0.539920E+04 0.137924E+06 0.327687E+11 0.136584E+06  
-0.500876E+04 -0.174043E+04 -0.442811E+04 -0.370686E+05 0.888185E+05 0.323039E+10

Mooring-system 6X6 stiffness matrix (mooring\_K):

0. 0. 0. 0. 0. 0.

0. 0. 0. 0. 0. 0.

0. 0. 0. 0. 0. 0.  
 0. 0. 0. 0. 0. 0.  
 0. 0. 0. 0. 0. 0.  
 0. 0. 0. 0. 0. 0.

Distributed (hydrodynamic) added-mass per unit length along a flexible portion of the tower length:

0. n\_secs\_m\_distr: number of sections at which added mass per unit length is specified (-)  
 0. 0. : z\_distr\_m [row array of size n\_added\_m\_pts; section locations wrt the flexible tower base over which distributed mass is specified] (m)  
 0. 0. : distr\_m [row array of size n\_added\_m\_pts; added distributed masses per unit length] (kg/m)

Distributed elastic stiffness per unit length along a flexible portion of the tower length:

0 n\_secs\_k\_distr: number of points at which distributed stiffness per unit length is specified (-)  
 0 1 2 3 4 5 6 7 8 9 10 11 12 13 14 15 16 17 18 19 20 21 22 23 24 25 26 27 28 29 30 31 32 33 34 35 36 : z\_distr\_k [row array of size n\_added\_m\_pts; section locations wrt the flexible tower base over which distributed stiffness is specified] (m)  
 595318000.0 1165208000 1129400000 1095553000 1059931000 1024493000 989209000 953643000 918718000 883287000 847803000 812541000  
 777187000 741870000 706616000 671440000 636229000 600957000 565919000 530470000 495081000 459574000 385327000 305479000 280059000  
 254125000 227500000 200112000 171927000 143115000 114173000 80184000 52237000 35561000 20912000 9000000 1156000 : distr\_k [row array of size n\_added\_m\_pts; distributed stiffness per unit length] (N/m<sup>2</sup>)

Tension-wires data

0 n\_attachments: no of wire-attachment locations on tower, maxm allowable is 2; 0: no tension-wire support (-)  
 3 3 n\_wires: no of wires attached at each location (must be 3 or higher) (-)  
 6 9 node\_attach: node numbers of attachments location (node number must be more than 1 and less than nself+2) (-)  
 9.0e9 1.6e9 wire\_stfness: wire sifnness in each set (see users' manual) (N/m)  
 45. 30. th\_wire: angle of tension wires wrt the tower axis at each attachment point (deg)

## BMODES TOWER PROPERTIES FILE

Tower section properties

27 n\_secs: number of blade or tower sections at which properties are specified (-)

sec_loc	str_tw	tw_iner	mass_den	flp_iner	edge_iner	flp_stff	edge_stff	tor_stff	axial_stff	cg_offst	sc_offst	tc_offst				
(-)	(deg)	(deg)	(kg/m)	(kg-m)	(kg-m)	(Nm <sup>2</sup> )	(Nm <sup>2</sup> )	(Nm <sup>2</sup> )	(N)	(m)	(m)	(m)				
0.00000	0.0	0.0	4717.128858	17611.07629	17611.07629	4.711243E+11	4.711243E+11	3.63E+11	1.26E+11	0.0	0.0	0.0				

0.03850	0.0	0.0	4717.128858	17611.07629	17611.07629	4.711243E+11	4.711243E+11	3.63E+11	1.26E+11	0.0	0.0	0.0
0.07690	0.0	0.0	4609.983509	17216.06367	17216.06367	4.605571E+11	4.605571E+11	3.55E+11	1.23E+11	0.0	0.0	0.0
0.11540	0.0	0.0	4502.806593	16820.70182	16820.70182	4.499806E+11	4.499806E+11	3.47E+11	1.20E+11	0.0	0.0	0.0
0.15380	0.0	0.0	4395.598110	16424.99053	16424.99053	4.393947E+11	4.393947E+11	3.39E+11	1.18E+11	0.0	0.0	0.0
0.19230	0.0	0.0	4288.358060	16028.92960	16028.92960	4.287994E+11	4.287994E+11	3.31E+11	1.15E+11	0.0	0.0	0.0
0.23080	0.0	0.0	4181.086444	15632.51881	15632.51881	4.181948E+11	4.181948E+11	3.23E+11	1.12E+11	0.0	0.0	0.0
0.26920	0.0	0.0	4073.783261	15235.75797	15235.75797	4.075808E+11	4.075808E+11	3.14E+11	1.09E+11	0.0	0.0	0.0
0.30770	0.0	0.0	3966.448511	14838.64686	14838.64686	3.969574E+11	3.969574E+11	3.06E+11	1.06E+11	0.0	0.0	0.0
0.34620	0.0	0.0	3859.082194	14441.18528	14441.18528	3.863247E+11	3.863247E+11	2.98E+11	1.03E+11	0.0	0.0	0.0
0.38460	0.0	0.0	3751.684311	14043.37303	14043.37303	3.756826E+11	3.756826E+11	2.90E+11	1.00E+11	0.0	0.0	0.0
0.42310	0.0	0.0	3644.254861	13645.20990	13645.20990	3.650311E+11	3.650311E+11	2.82E+11	9.75E+10	0.0	0.0	0.0
0.46150	0.0	0.0	3536.793844	13246.69567	13246.69567	3.543702E+11	3.543702E+11	2.73E+11	9.46E+10	0.0	0.0	0.0
0.50000	0.0	0.0	3429.301261	12847.83016	12847.83016	3.436999E+11	3.436999E+11	2.65E+11	9.17E+10	0.0	0.0	0.0
0.53850	0.0	0.0	3321.777111	12448.61314	12448.61314	3.330202E+11	3.330202E+11	2.57E+11	8.89E+10	0.0	0.0	0.0
0.57690	0.0	0.0	3214.221394	12049.04442	12049.04442	3.223311E+11	3.223311E+11	2.49E+11	8.60E+10	0.0	0.0	0.0
0.61540	0.0	0.0	3106.634110	11649.12378	11649.12378	3.116326E+11	3.116326E+11	2.40E+11	8.31E+10	0.0	0.0	0.0
0.65380	0.0	0.0	2999.015260	11248.85102	11248.85102	3.009247E+11	3.009247E+11	2.32E+11	8.02E+10	0.0	0.0	0.0
0.69230	0.0	0.0	2891.364843	10848.22593	10848.22593	2.902073E+11	2.902073E+11	2.24E+11	7.73E+10	0.0	0.0	0.0
0.73080	0.0	0.0	2783.682859	10447.24831	10447.24831	2.794805E+11	2.794805E+11	2.16E+11	7.45E+10	0.0	0.0	0.0
0.76920	0.0	0.0	2675.969308	10045.91795	10045.91795	2.687443E+11	2.687443E+11	2.07E+11	7.16E+10	0.0	0.0	0.0
0.80770	0.0	0.0	2568.224191	9644.23465	9644.23465	2.579986E+11	2.579986E+11	1.99E+11	6.87E+10	0.0	0.0	0.0
0.84620	0.0	0.0	2460.447507	9242.19819	9242.19819	2.472435E+11	2.472435E+11	1.91E+11	6.58E+10	0.0	0.0	0.0
0.88460	0.0	0.0	2352.639257	8839.80837	8839.80837	2.364789E+11	2.364789E+11	1.82E+11	6.29E+10	0.0	0.0	0.0
0.92310	0.0	0.0	2244.799439	8437.06498	8437.06498	2.257049E+11	2.257049E+11	1.74E+11	6.01E+10	0.0	0.0	0.0
0.96150	0.0	0.0	2136.928055	8033.96781	8033.96781	2.149214E+11	2.149214E+11	1.66E+11	5.72E+10	0.0	0.0	0.0
1.00000	0.0	0.0	2029.025104	7630.51667	7630.51667	2.041285E+11	2.041285E+11	1.57E+11	5.43E+10	0.0	0.0	0.0

\*\*Note: If this file is for a TOWER. the following section properties are read but overwritten as follows:

str\_tw is set to zero  
tw\_iner is set to zero  
cg\_offst is set to zero  
sc\_offst is set to zero  
tc\_offst is set to zero  
edge\_iner is set equal to flp\_iner  
edge\_stff is set equal to flp\_stff



**ELASTODYN INPUT FILE**

```

----- ELASTODYN v1.03.* INPUT FILE -----
NREL 5.0 MW Baseline Wind Turbine for Use in Offshore Analysis. Properties from Dutch Offshore Wind Energy Converter (DOWEC) 6MW Pre-Design
(10046_009.pdf) and REpower 5M 5MW (5m_uk.pdf);
----- SIMULATION CONTROL -----
False      Echo      - Echo input data to "<RootName>.ech" (flag)
          3 Method    - Integration method: {1: RK4, 2: AB4, or 3: ABM4} (-)
"DEFAULT"  DT          - Integration time step (s)
----- ENVIRONMENTAL CONDITION -----
          9.80665 Gravity - Gravitational acceleration (m/s^2)
----- DEGREES OF FREEDOM -----
True      FlapDOF1    - First flapwise blade mode DOF (flag)
True      FlapDOF2    - Second flapwise blade mode DOF (flag)
True      EdgeDOF     - First edgewise blade mode DOF (flag)
False     TeetDOF     - Rotor-teeter DOF (flag) [unused for 3 blades]
True      DrTrDOF    - Drivetrain rotational-flexibility DOF (flag)
True      GenDOF     - Generator DOF (flag)
true      YawDOF     - Yaw DOF (flag)
True      TwFADOF1    - First fore-aft tower bending-mode DOF (flag)
True      TwFADOF2    - Second fore-aft tower bending-mode DOF (flag)
True      TwSSDOF1    - First side-to-side tower bending-mode DOF (flag)
True      TwSSDOF2    - Second side-to-side tower bending-mode DOF (flag)
True      PtfmSgDOF   - Platform horizontal surge translation DOF (flag)
True      PtfmSwDOF   - Platform horizontal sway translation DOF (flag)
True      PtfmHvDOF   - Platform vertical heave translation DOF (flag)
True      PtfmRDOF    - Platform roll tilt rotation DOF (flag)
True      PtfmPDOF    - Platform pitch tilt rotation DOF (flag)
True      PtfmYDOF    - Platform yaw rotation DOF (flag)
----- INITIAL CONDITIONS -----
0 OoPDefl  - Initial out-of-plane blade-tip displacement (meters)
0 IPDefl   - Initial in-plane blade-tip deflection (meters)
0 BIPitch(1) - Blade 1 initial pitch (degrees)
0 BIPitch(2) - Blade 2 initial pitch (degrees)
0 BIPitch(3) - Blade 3 initial pitch (degrees) [unused for 2 blades]

```

0 TeetDefl - Initial or fixed teeter angle (degrees) [unused for 3 blades]  
 0 Azimuth - Initial azimuth angle for blade 1 (degrees)  
 9 RotSpeed - Initial or fixed rotor speed (rpm)  
 0 NacYaw - Initial or fixed nacelle-yaw angle (degrees)  
 0 TTDspFA - Initial fore-aft tower-top displacement (meters)  
 0 TTDspSS - Initial side-to-side tower-top displacement (meters)  
 0 PtfmSurge - Initial or fixed horizontal surge translational displacement of platform (meters)  
 0 PtfmSway - Initial or fixed horizontal sway translational displacement of platform (meters)  
 -0.002 PtfmHeave - Initial or fixed vertical heave translational displacement of platform (meters)  
 0 PtfmRoll - Initial or fixed roll tilt rotational displacement of platform (degrees)  
 0 PtfmPitch - Initial or fixed pitch tilt rotational displacement of platform (degrees)  
 0 PtfmYaw - Initial or fixed yaw rotational displacement of platform (degrees)

----- TURBINE CONFIGURATION -----

3 NumBl - Number of blades (-)  
 63 TipRad - The distance from the rotor apex to the blade tip (meters)  
 1.5 HubRad - The distance from the rotor apex to the blade root (meters)  
 -2.5 PreCone(1) - Blade 1 cone angle (degrees)  
 -2.5 PreCone(2) - Blade 2 cone angle (degrees)  
 -2.5 PreCone(3) - Blade 3 cone angle (degrees) [unused for 2 blades]  
 0 HubCM - Distance from rotor apex to hub mass [positive downwind] (meters)  
 0 UndSling - Undersling length [distance from teeter pin to the rotor apex] (meters) [unused for 3 blades]  
 0 Delta3 - Delta-3 angle for teetering rotors (degrees) [unused for 3 blades]  
 0 AzimB1Up - Azimuth value to use for I/O when blade 1 points up (degrees)  
 -5.0191 OverHang - Distance from yaw axis to rotor apex [3 blades] or teeter pin [2 blades] (meters)  
 1.912 ShftGagL - Distance from rotor apex [3 blades] or teeter pin [2 blades] to shaft strain gages [positive for upwind rotors] (meters)  
 -5 ShftTilt - Rotor shaft tilt angle (degrees)  
 1.9 NacCMxn - Downwind distance from the tower-top to the nacelle CM (meters)  
 0 NacCMyn - Lateral distance from the tower-top to the nacelle CM (meters)  
 1.75 NacCMzn - Vertical distance from the tower-top to the nacelle CM (meters)  
 -3.09528 NcIMUxn - Downwind distance from the tower-top to the nacelle IMU (meters)  
 0 NcIMUyn - Lateral distance from the tower-top to the nacelle IMU (meters)  
 2.23336 NcIMUzn - Vertical distance from the tower-top to the nacelle IMU (meters)  
 1.96256 Twr2Shft - Vertical distance from the tower-top to the rotor shaft (meters)  
 98 TowerHt - Height of tower above ground level [onshore] or MSL [offshore] (meters)  
 20 TowerBsHt - Height of tower base above ground level [onshore] or MSL [offshore] (meters)

0 PtfmCMxt - Downwind distance from the ground level [onshore] or MSL [offshore] to the platform CM (meters)  
 0 PtfmCMyt - Lateral distance from the ground level [onshore] or MSL [offshore] to the platform CM (meters)  
 20 PtfmCMzt - Vertical distance from the ground level [onshore] or MSL [offshore] to the platform CM (meters)  
 20 PtfmRefzt - Vertical distance from the ground level [onshore] or MSL [offshore] to the platform reference point (meters)

----- MASS AND INERTIA -----

0 TipMass(1) - Tip-brake mass, blade 1 (kg)  
 0 TipMass(2) - Tip-brake mass, blade 2 (kg)  
 0 TipMass(3) - Tip-brake mass, blade 3 (kg) [unused for 2 blades]  
 56780 HubMass - Hub mass (kg)  
 115926 HubIner - Hub inertia about rotor axis [3 blades] or teeter axis [2 blades] (kg m<sup>2</sup>)  
 534.116 GenIner - Generator inertia about HSS (kg m<sup>2</sup>)  
 240000 NacMass - Nacelle mass (kg)  
 2.60789E+06 NacYIner - Nacelle inertia about yaw axis (kg m<sup>2</sup>)  
 0 YawBrMass - Yaw bearing mass (kg)  
 0 PtfmMass - Platform mass (kg)  
 0 PtfmRIner - Platform inertia for roll tilt rotation about the platform CM (kg m<sup>2</sup>)  
 0 PtfmPIner - Platform inertia for pitch tilt rotation about the platform CM (kg m<sup>2</sup>)  
 2.48448E+06 PtfmYIner - Platform inertia for yaw rotation about the platform CM (kg m<sup>2</sup>)

----- BLADE -----

17 BldNodes - Number of blade nodes (per blade) used for analysis (-)  
 "NRELOffshrBsline5MW\_Blade.dat" BldFile(1) - Name of file containing properties for blade 1 (quoted string)  
 "NRELOffshrBsline5MW\_Blade.dat" BldFile(2) - Name of file containing properties for blade 2 (quoted string)  
 "NRELOffshrBsline5MW\_Blade.dat" BldFile(3) - Name of file containing properties for blade 3 (quoted string) [unused for 2 blades]

----- ROTOR-TEETER -----

0 TeetMod - Rotor-teeter spring/damper model {0: none, 1: standard, 2: user-defined from routine UserTeet} (switch) [unused for 3 blades]  
 0 TeetDmpP - Rotor-teeter damper position (degrees) [used only for 2 blades and when TeetMod=1]  
 0 TeetDmp - Rotor-teeter damping constant (N-m/(rad/s)) [used only for 2 blades and when TeetMod=1]  
 0 TeetCDmp - Rotor-teeter rate-independent Coulomb-damping moment (N-m) [used only for 2 blades and when TeetMod=1]  
 0 TeetSStP - Rotor-teeter soft-stop position (degrees) [used only for 2 blades and when TeetMod=1]  
 0 TeetHStP - Rotor-teeter hard-stop position (degrees) [used only for 2 blades and when TeetMod=1]  
 0 TeetSSSp - Rotor-teeter soft-stop linear-spring constant (N-m/rad) [used only for 2 blades and when TeetMod=1]  
 0 TeetHSSp - Rotor-teeter hard-stop linear-spring constant (N-m/rad) [used only for 2 blades and when TeetMod=1]

----- DRIVETRAIN -----

100 GBoxEff - Gearbox efficiency (%)  
 97 GBRatio - Gearbox ratio (-)

```

8.67637E+08 DTTorSpr - Drivetrain torsional spring (N-m/rad)
6.215E+06 DTTorDmp - Drivetrain torsional damper (N-m/(rad/s))
----- FURLING -----
False Furling - Read in additional model properties for furling turbine (flag) [must currently be FALSE]
"unused" FurlFile - Name of file containing furling properties (quoted string) [unused when Furling=False]
----- TOWER -----
27 TwrNodes - Number of tower nodes used for analysis (-)
"NRELOffshrBsline5MW_OC3Tripod_ElastoDyn_Tower_try_LS_AF.dat" TwrFile - Name of file containing tower properties (quoted string)
----- OUTPUT -----
False SumPrint - Print summary data to "<RootName>.sum" (flag)
2 OutFile - Switch to determine where output will be placed: {1: in module output file only; 2: in glue code output file only; 3: both} (currently
unused)
True TabDelim - Use tab delimiters in text tabular output file? (flag) (currently unused)
"ES10.3E2" OutFmt - Format used for text tabular output (except time). Resulting field should be 10 characters. (quoted string) (currently unused)
0 TStart - Time to begin tabular output (s) (currently unused)
1 DecFact - Decimation factor for tabular output {1: output every time step} (-) (currently unused)
1 NTwGages - Number of tower nodes that have strain gages for output [0 to 9] (-)
27 TwrGagNd - List of tower nodes that have strain gages [1 to TwrNodes] (-) [unused if NTwGages=0]
3 NBIGages - Number of blade nodes that have strain gages for output [0 to 9] (-)
5, 9, 13 BldGagNd - List of blade nodes that have strain gages [1 to BldNodes] (-) [unused if NBIGages=0]
OutList - The next line(s) contains a list of output parameters. See OutListParameters.xlsx for a listing of available output channels, (-)
"YawBrFxp, YawBrFyp, YawBrFzp" - Fore-aft shear, side-to-side shear, and vertical forces at the top of the tower (not rotating with nacelle yaw)
"YawBrMxp, YawBrMyp, YawBrMzp" - Side-to-side bending, fore-aft bending, and yaw moments at the top of the tower (not rotating with nacelle yaw)
END of input file (the word "END" must appear in the first 3 columns of this last OutList line)
-----

```

## ELASTODYN TOWER INPUT FILE

```

----- ELASTODYN V1.00.* TOWER INPUT FILE -----
NREL 5.0 MW offshore baseline tripod tower with flexible Tripod SubStructure (however SS cantilevered at seabed).
----- TOWER PARAMETERS -----
27 NTwInpSt - Number of input stations to specify tower geometry
1 TwrFADmp(1) - Tower 1st fore-aft mode structural damping ratio (%)
1 TwrFADmp(2) - Tower 2nd fore-aft mode structural damping ratio (%)
1 TwrSSDmp(1) - Tower 1st side-to-side mode structural damping ratio (%)

```

1 TwrSSDmp(2) - Tower 2nd side-to-side mode structural damping ratio (%)

----- TOWER ADJUSTMUNT FACTORS -----

- 1 FASTunr(1) - Tower fore-aft modal stiffness tuner. 1st mode (-)
- 1 FASTunr(2) - Tower fore-aft modal stiffness tuner. 2nd mode (-)
- 1 SSStunr(1) - Tower side-to-side stiffness tuner. 1st mode (-)
- 1 SSStunr(2) - Tower side-to-side stiffness tuner. 2nd mode (-)
- 1 AdjTwMa - Factor to adjust tower mass density (-)
- 1 AdjFAST - Factor to adjust tower fore-aft stiffness (-)
- 1 AdjSSSt - Factor to adjust tower side-to-side stiffness (-)

----- DISTRIBUTED TOWER PROPERTIES -----

HtFract (-)	TMassDen (kg/m)	TwFASTif (Nm^2)	TwSSStif (Nm^2)	
0.000000E+00	4717.12885830082		4.71124E+11	4.71124E+11
3.846000E-02	4717.12885830082		4.71124E+11	4.71124E+11
7.692000E-02	4609.9835088148		4.60557E+11	4.60557E+11
1.154000E-01	4502.80659260587		4.49981E+11	4.49981E+11
1.538000E-01	4395.59810967394		4.39395E+11	4.39395E+11
1.923000E-01	4288.35806001905		4.28799E+11	4.28799E+11
2.308000E-01	4181.08644364114		4.18195E+11	4.18195E+11
2.692000E-01	4073.78326054027		4.07581E+11	4.07581E+11
3.077000E-01	3966.44851071637		3.96957E+11	3.96957E+11
3.462000E-01	3859.08219416955		3.863247E+11	3.863247E+11
3.846000E-01	3751.68431089971		3.75683E+11	3.75683E+11
4.231000E-01	3644.25486090691		3.65031E+11	3.65031E+11
4.615000E-01	3536.79384419112		3.5437E+11	3.5437E+11
5.000000E-01	3429.3012607523		3.437E+11	3.437E+11
5.385000E-01	3321.77711059055		3.33E+11	3.33E+11
5.769000E-01	3214.22139370582		3.22331E+11	3.22331E+11
6.154000E-01	3106.63411009809		3.116326E+11	3.116326E+11
6.538000E-01	2999.01525976738		3.00925E+11	3.00925E+11
6.923000E-01	2891.36484271364		2.90207E+11	2.90207E+11
7.308000E-01	2783.68285893697		2.794805E+11	2.794805E+11
7.692000E-01	2675.96930843731		2.68744E+11	2.68744E+11
8.077000E-01	2568.22419121469		2.5799E+11	2.5799E+11
8.462000E-01	2460.44750726906		2.4724E+11	2.4724E+11

```

8.846000E-01 2352.63925660042 2.364789E+11 2.364789E+11
9.231000E-01 2244.79943920883 2.257049E+11 2.257049E+11
9.615000E-01 2136.92805509425 2.14921E+11 2.14921E+11
1.000000E+00 2029.02510425671 2.04128E+11 2.04128E+11

```

----- TOWER FORE-AFT MODE SHAPES -----

```

1.30958 TwFAM1Sh(2) - Mode 1. coefficient of x^2 term
-0.26409 TwFAM1Sh(3) - . coefficient of x^3 term
-0.02702 TwFAM1Sh(4) - . coefficient of x^4 term
0.00744 TwFAM1Sh(5) - . coefficient of x^5 term
-0.02591 TwFAM1Sh(6) - . coefficient of x^6 term
0.73426 TwFAM2Sh(2) - Mode 2. coefficient of x^2 term
0.50314 TwFAM2Sh(3) - . coefficient of x^3 term
-0.19644 TwFAM2Sh(4) - . coefficient of x^4 term
-0.05612 TwFAM2Sh(5) - . coefficient of x^5 term
0.01517 TwFAM2Sh(6) - . coefficient of x^6 term

```

----- TOWER SIDE-TO-SIDE MODE SHAPES -----

```

1.2959 TwSSM1Sh(2) - Mode 1. coefficient of x^2 term
-0.23683 TwSSM1Sh(3) - . coefficient of x^3 term
-0.06411 TwSSM1Sh(4) - . coefficient of x^4 term
0.04162 TwSSM1Sh(5) - . coefficient of x^5 term
-0.03658 TwSSM1Sh(6) - . coefficient of x^6 term
0.65032 TwSSM2Sh(2) - Mode 2. coefficient of x^2 term
0.50061 TwSSM2Sh(3) - . coefficient of x^3 term
-0.09892 TwSSM2Sh(4) - . coefficient of x^4 term
-0.08649 TwSSM2Sh(5) - . coefficient of x^5 term
0.03448 TwSSM2Sh(6) - . coefficient of x^6 term

```

## AERODYN INPUT FILE

----- AERODYN v15.03.\* INPUT FILE -----

NREL 5.0 MW offshore baseline aerodynamic input properties.

```

===== General Options =====
true      Echo          - Echo the input to "<rootname>.AD.ech"? (flag)
"DEFAULT" DTAero        - Time interval for aerodynamic calculations {or "default"} (s)
          1 WakeMod      - Type of wake/induction model (switch) {0=none, 1=BEMT}

```

```

2  AFAeroMod  - Type of blade airfoil aerodynamics model (switch) {1=steady model, 2=Beddoes-Leishman unsteady model}
1  TwrPotent  - Type tower influence on wind based on potential flow around the tower (switch) {0=none, 1=baseline potential flow, 2=potential
flow with Bak correction}
False  TwrShadow  - Calculate tower influence on wind based on downstream tower shadow? (flag)
True   TwrAero    - Calculate tower aerodynamic loads? (flag)
False  FrozenWake - Assume frozen wake during linearization? (flag) [used only when WakeMod=1 and when linearizing]
===== Environmental Conditions =====
1.225  AirDens   - Air density (kg/m^3)
1.464E-05 KinVisc - Kinematic air viscosity (m^2/s)
335    SpdSound  - Speed of sound (m/s)
===== Blade-Element/Momentum Theory Options ===== [used only
when WakeMod=1]
2  SkewMod    - Type of skewed-wake correction model (switch) {1=uncoupled, 2=Pitt/Peters, 3=coupled} [used only when WakeMod=1]
True  TipLoss   - Use the Prandtl tip-loss model? (flag) [used only when WakeMod=1]
True  HubLoss   - Use the Prandtl hub-loss model? (flag) [used only when WakeMod=1]
true  TanInd    - Include tangential induction in BEMT calculations? (flag) [used only when WakeMod=1]
False AIDrag     - Include the drag term in the axial-induction calculation? (flag) [used only when WakeMod=1]
False TIDrag     - Include the drag term in the tangential-induction calculation? (flag) [used only when WakeMod=1 and TanInd=TRUE]
"Default" IndToler - Convergence tolerance for BEMT nonlinear solve residual equation {or "default"} (-) [used only when WakeMod=1]
100  MaxIter   - Maximum number of iteration steps (-) [used only when WakeMod=1]
===== Beddoes-Leishman Unsteady Airfoil Aerodynamics Options ===== [used only when
AFAeroMod=2]
3  UAMod      - Unsteady Aero Model Switch (switch) {1=Baseline model (Original), 2=Gonzalez's variant (changes in Cn,Cc,Cm), 3=Minemma/Pierce
variant (changes in Cc and Cm)} [used only when AFAeroMod=2]
True  FLookup   - Flag to indicate whether a lookup for f' will be calculated (TRUE) or whether best-fit exponential equations will be used (FALSE);
if FALSE S1-S4 must be provided in airfoil input files (flag) [used only when AFAeroMod=2]
===== Airfoil Information =====
1  InCol_Alfa  - The column in the airfoil tables that contains the angle of attack (-)
2  InCol_Cl    - The column in the airfoil tables that contains the lift coefficient (-)
3  InCol_Cd    - The column in the airfoil tables that contains the drag coefficient (-)
4  InCol_Cm    - The column in the airfoil tables that contains the pitching-moment coefficient; use zero if there is no Cm column (-)
0  InCol_Cpmin - The column in the airfoil tables that contains the Cpmin coefficient; use zero if there is no Cpmin column (-)
8  NumAFiles  - Number of airfoil files used (-)
"Airfoils/Cylinder1.dat" AFilesNames - Airfoil file names (NumAFiles lines) (quoted strings)
"Airfoils/Cylinder2.dat"

```

```

"Airfoils/DU40_A17.dat"
"Airfoils/DU35_A17.dat"
"Airfoils/DU30_A17.dat"
"Airfoils/DU25_A17.dat"
"Airfoils/DU21_A17.dat"
"Airfoils/NACA64_A17.dat"
===== Rotor/Blade Properties =====
True      UseBICm      - Include aerodynamic pitching moment in calculations? (flag)
"NRELOffshrBsline5MW_AeroDyn_blade.dat"  ADBIFile(1)      - Name of file containing distributed aerodynamic properties for Blade #1 (-)
"NRELOffshrBsline5MW_AeroDyn_blade.dat"  ADBIFile(2)      - Name of file containing distributed aerodynamic properties for Blade #2 (-) [unused if NumBl
< 2]
"NRELOffshrBsline5MW_AeroDyn_blade.dat"  ADBIFile(3)      - Name of file containing distributed aerodynamic properties for Blade #3 (-) [unused if NumBl
< 3]
===== Tower Influence and Aerodynamics ===== [used only
when TwrPotent/=0, TwrShadow=True, or TwrAero=True]
      27 NumTwrNds      - Number of tower nodes used in the analysis (-) [used only when TwrPotent/=0, TwrShadow=True, or TwrAero=True]
TwrElev   TwrDiam   TwrCd
(m)       (m)       (-)
2.0000000E+01 5.5000000E+00 1.0000000E+00
2.3000000E+01 5.5000000E+00 1.0000000E+00
2.6000000E+01 5.5000000E+00 1.0000000E+00
2.9000000E+01 5.5000000E+00 1.0000000E+00
3.2000000E+01 5.5000000E+00 1.0000000E+00
3.5000000E+01 5.5000000E+00 1.0000000E+00
3.8000000E+01 5.5000000E+00 1.0000000E+00
4.1000000E+01 5.5000000E+00 1.0000000E+00
4.4000000E+01 5.5000000E+00 1.0000000E+00
4.7000000E+01 5.5000000E+00 1.0000000E+00
5.0000000E+01 5.5000000E+00 1.0000000E+00
5.3000000E+01 5.5000000E+00 1.0000000E+00
5.6000000E+01 5.5000000E+00 1.0000000E+00
5.9000000E+01 5.5000000E+00 1.0000000E+00
6.2000000E+01 5.5000000E+00 1.0000000E+00
6.5000000E+01 5.5000000E+00 1.0000000E+00
6.8000000E+01 5.5000000E+00 1.0000000E+00

```



```

7.1000000E+01 5.5000000E+00 1.0000000E+00
7.4000000E+01 5.5000000E+00 1.0000000E+00
7.7000000E+01 5.5000000E+00 1.0000000E+00
8.0000000E+01 5.5000000E+00 1.0000000E+00
8.3000000E+01 5.5000000E+00 1.0000000E+00
8.6000000E+01 5.5000000E+00 1.0000000E+00
8.9000000E+01 5.5000000E+00 1.0000000E+00
9.2000000E+01 5.5000000E+00 1.0000000E+00
9.5000000E+01 5.5000000E+00 1.0000000E+00
9.8000000E+01 5.5000000E+00 1.0000000E+00

```

```

===== Outputs =====
False      SumPrint      - Generate a summary file listing input options and interpolated properties to "<rootname>.AD.sum"? (flag)
  0 NBIOuts      - Number of blade node outputs [0 - 9] (-)
  1,      8,      19 BOutNd      - Blade nodes whose values will be output (-)
  8 NTwOuts      - Number of tower node outputs [0 - 9] (-)
  1, 5, 9, 13, 17, 21, 25, 27 TwOutNd      - Tower nodes whose values will be output (-)
      OutList      - The next line(s) contains a list of output parameters. See OutListParameters.xlsx for a listing of available output channels, (-)
"TwN1Fdx, TwN1Fdy"
"TwN2Fdx, TwN2Fdy"
"TwN3Fdx, TwN3Fdy"
"TwN4Fdx, TwN4Fdy"
"TwN5Fdx, TwN5Fdy"
"TwN6Fdx, TwN6Fdy"
"TwN7Fdx, TwN7Fdy"
"TwN8Fdx, TwN8Fdy"
END of input file (the word "END" must appear in the first 3 columns of this last OutList line)
-----

```

## SERVODYN INPUT FILE

```

----- SERVODYN v1.05.* INPUT FILE -----
OC3 Tripod + NREL 5.0 MW Baseline Wind Turbine
----- SIMULATION CONTROL -----
False      Echo      - Echo input data to <RootName>.ech (flag)

```

"DEFAULT" DT - Communication interval for controllers (s) (or "default")

----- PITCH CONTROL -----

5 PCMode - Pitch control mode {0: none, 3: user-defined from routine PitchCntrl, 4: user-defined from Simulink/Labview, 5: user-defined from Bladed-style DLL} (switch)

0 TPCOn - Time to enable active pitch control (s) [unused when PCMode=0]

9999.9 TPitManS(1) - Time to start override pitch maneuver for blade 1 and end standard pitch control (s)

9999.9 TPitManS(2) - Time to start override pitch maneuver for blade 2 and end standard pitch control (s)

9999.9 TPitManS(3) - Time to start override pitch maneuver for blade 3 and end standard pitch control (s) [unused for 2 blades]

8 PitManRat(1) - Pitch rate at which override pitch maneuver heads toward final pitch angle for blade 1 (deg/s)

8 PitManRat(2) - Pitch rate at which override pitch maneuver heads toward final pitch angle for blade 2 (deg/s)

8 PitManRat(3) - Pitch rate at which override pitch maneuver heads toward final pitch angle for blade 3 (deg/s) [unused for 2 blades]

90 BIPitchF(1) - Blade 1 final pitch for pitch maneuvers (degrees)

90 BIPitchF(2) - Blade 2 final pitch for pitch maneuvers (degrees)

90 BIPitchF(3) - Blade 3 final pitch for pitch maneuvers (degrees) [unused for 2 blades]

----- GENERATOR AND TORQUE CONTROL -----

5 VSContrl - Variable-speed control mode {0: none, 1: simple VS, 3: user-defined from routine UserVSCont, 4: user-defined from Simulink/Labview, 5: user-defined from Bladed-style DLL} (switch)

2 GenModel - Generator model {1: simple, 2: Thevenin, 3: user-defined from routine UserGen} (switch) [used only when VSContrl=0]

94.4 GenEff - Generator efficiency [ignored by the Thevenin and user-defined generator models] (%)

True GenTiStr - Method to start the generator {T: timed using TimGenOn, F: generator speed using SpdGenOn} (flag)

True GenTiStp - Method to stop the generator {T: timed using TimGenOf, F: when generator power = 0} (flag)

9999.9 SpdGenOn - Generator speed to turn on the generator for a startup (HSS speed) (rpm) [used only when GenTiStr=False]

0 TimGenOn - Time to turn on the generator for a startup (s) [used only when GenTiStr=True]

9999.9 TimGenOf - Time to turn off the generator (s) [used only when GenTiStp=True]

----- SIMPLE VARIABLE-SPEED TORQUE CONTROL -----

9999.9 VS\_RtGnSp - Rated generator speed for simple variable-speed generator control (HSS side) (rpm) [used only when VSContrl=1]

9999.9 VS\_RtTq - Rated generator torque/constant generator torque in Region 3 for simple variable-speed generator control (HSS side) (N-m) [used only when VSContrl=1]

9999.9 VS\_Rgn2K - Generator torque constant in Region 2 for simple variable-speed generator control (HSS side) (N-m/rpm<sup>2</sup>) [used only when VSContrl=1]

9999.9 VS\_SIPc - Rated generator slip percentage in Region 2 1/2 for simple variable-speed generator control (%) [used only when VSContrl=1]

----- SIMPLE INDUCTION GENERATOR -----

9999.9 SIG\_SIPc - Rated generator slip percentage (%) [used only when VSContrl=0 and GenModel=1]

9999.9 SIG\_SySp - Synchronous (zero-torque) generator speed (rpm) [used only when VSContrl=0 and GenModel=1]

9999.9 SIG\_RtTq - Rated torque (N-m) [used only when VSContrl=0 and GenModel=1]

9999.9 SIG\_PORT - Pull-out ratio (Tpullout/Trated) (-) [used only when VSContrl=0 and GenModel=1]  
 ----- THEVENIN-EQUIVALENT INDUCTION GENERATOR -----  
 9999.9 TEC\_Freq - Line frequency [50 or 60] (Hz) [used only when VSContrl=0 and GenModel=2]  
 9998 TEC\_NPol - Number of poles [even integer > 0] (-) [used only when VSContrl=0 and GenModel=2]  
 9999.9 TEC\_SRes - Stator resistance (ohms) [used only when VSContrl=0 and GenModel=2]  
 9999.9 TEC\_RRes - Rotor resistance (ohms) [used only when VSContrl=0 and GenModel=2]  
 9999.9 TEC\_VLL - Line-to-line RMS voltage (volts) [used only when VSContrl=0 and GenModel=2]  
 9999.9 TEC\_SLR - Stator leakage reactance (ohms) [used only when VSContrl=0 and GenModel=2]  
 9999.9 TEC\_RLR - Rotor leakage reactance (ohms) [used only when VSContrl=0 and GenModel=2]  
 9999.9 TEC\_MR - Magnetizing reactance (ohms) [used only when VSContrl=0 and GenModel=2]  
 ----- HIGH-SPEED SHAFT BRAKE -----  
 0 HSSBrMode - HSS brake model {0: none, 1: simple, 3: user-defined from routine UserHSSBr, 4: user-defined from Simulink/Labview, 5: user-defined from Bladed-style DLL} (switch)  
 9999.9 THSSBrDp - Time to initiate deployment of the HSS brake (s)  
 0.6 HSSBrDT - Time for HSS-brake to reach full deployment once initiated (sec) [used only when HSSBrMode=1]  
 28116.2 HSSBrTqF - Fully deployed HSS-brake torque (N-m)  
 ----- NACELLE-YAW CONTROL -----  
 0 YCMode - Yaw control mode {0: none, 3: user-defined from routine UserYawCont, 4: user-defined from Simulink/Labview, 5: user-defined from Bladed-style DLL} (switch)  
 9999.9 TYCon - Time to enable active yaw control (s) [unused when YCMode=0]  
 0 YawNeut - Neutral yaw position--yaw spring force is zero at this yaw (degrees)  
 9.02832E+09 YawSpr - Nacelle-yaw spring constant (N-m/rad)  
 1.916E+07 YawDamp - Nacelle-yaw damping constant (N-m/(rad/s))  
 9999.9 TYawManS - Time to start override yaw maneuver and end standard yaw control (s)  
 0.3 YawManRat - Yaw maneuver rate (in absolute value) (deg/s)  
 0 NacYawF - Final yaw angle for override yaw maneuvers (degrees)  
 ----- TUNED MASS DAMPER -----  
 False CompNTMD - Compute nacelle tuned mass damper {true/false} (flag)  
 "unused" NTMDfile - Name of the file for nacelle tuned mass damper (quoted string) [unused when CompNTMD is false]  
 False CompTTMD - Compute tower tuned mass damper {true/false} (flag)  
 "unused" TTMDfile - Name of the file for tower tuned mass damper (quoted string) [unused when CompTTMD is false]  
 ----- BLADED INTERFACE ----- [used only with Bladed Interface]  
 "ServoData/DISCON\_win32.dll" DLL\_FileName - Name/location of the dynamic library {.dll [Windows] or .so [Linux]} in the Bladed-DLL format (-) [used only with Bladed Interface]  
 "DISCON.IN" DLL\_InFile - Name of input file sent to the DLL (-) [used only with Bladed Interface]

"DISCON" DLL\_ProcName - Name of procedure in DLL to be called (-) [case sensitive; used only with DLL Interface]  
"default" DLL\_DT - Communication interval for dynamic library (s) (or "default") [used only with Bladed Interface]  
false DLL\_Ramp - Whether a linear ramp should be used between DLL\_DT time steps [introduces time shift when true] (flag) [used only with Bladed Interface]

9999.9 BPCutoff - Cutoff frequency for low-pass filter on blade pitch from DLL (Hz) [used only with Bladed Interface]  
0 NacYaw\_North - Reference yaw angle of the nacelle when the upwind end points due North (deg) [used only with Bladed Interface]  
0 Ptch\_Cntrl - Record 28: Use individual pitch control {0: collective pitch; 1: individual pitch control} (switch) [used only with Bladed Interface]  
0 Ptch\_SetPnt - Record 5: Below-rated pitch angle set-point (deg) [used only with Bladed Interface]  
0 Ptch\_Min - Record 6: Minimum pitch angle (deg) [used only with Bladed Interface]  
0 Ptch\_Max - Record 7: Maximum pitch angle (deg) [used only with Bladed Interface]  
0 PtchRate\_Min - Record 8: Minimum pitch rate (most negative value allowed) (deg/s) [used only with Bladed Interface]  
0 PtchRate\_Max - Record 9: Maximum pitch rate (deg/s) [used only with Bladed Interface]  
0 Gain\_OM - Record 16: Optimal mode gain (Nm/(rad/s)^2) [used only with Bladed Interface]  
0 GenSpd\_MinOM - Record 17: Minimum generator speed (rpm) [used only with Bladed Interface]  
0 GenSpd\_MaxOM - Record 18: Optimal mode maximum speed (rpm) [used only with Bladed Interface]  
0 GenSpd\_Dem - Record 19: Demanded generator speed above rated (rpm) [used only with Bladed Interface]  
0 GenTrq\_Dem - Record 22: Demanded generator torque above rated (Nm) [used only with Bladed Interface]  
0 GenPwr\_Dem - Record 13: Demanded power (W) [used only with Bladed Interface]

----- BLADED INTERFACE TORQUE-SPEED LOOK-UP TABLE -----  
0 DLL\_NumTrq - Record 26: No. of points in torque-speed look-up table {0 = none and use the optimal mode parameters; nonzero = ignore the optimal mode PARAMETERS by setting Record 16 to 0.0} (-) [used only with Bladed Interface]  
GenSpd\_TLU GenTrq\_TLU  
(rpm) (Nm)

----- OUTPUT -----  
False SumPrint - Print summary data to <RootName>.sum (flag) (currently unused)  
2 OutFile - Switch to determine where output will be placed: {1: in module output file only; 2: in glue code output file only; 3: both} (currently unused)  
True TabDelim - Use tab delimiters in text tabular output file? (flag) (currently unused)  
"ES10.3E2" OutFmt - Format used for text tabular output (except time). Resulting field should be 10 characters. (quoted string) (currently unused)  
30 TStart - Time to begin tabular output (s) (currently unused)  
OutList - The next line(s) contains a list of output parameters. See OutListParameters.xlsx for a listing of available output channels, (-)  
END of input file (the word "END" must appear in the first 3 columns of this last OutList line)

-----

**HYDRODYN INPUT FILE**

----- HydroDyn v2.03.\* Input File -----

NREL 5.0 MW offshore fixed-bottom HydroDyn input properties for the OC3 Tripod.

FALSE Echo - Echo the input file data (flag)

----- ENVIRONMENTAL CONDITIONS -----

1025 WtrDens - Water density (kg/m<sup>3</sup>)

45 WtrDpth - Water depth (meters)

0 MSL2SWL - Offset between still-water level and mean sea level (meters) [positive upward; unused when WaveMod = 6; must be zero if PotMod=1 or 2]

----- WAVES -----

"0" WaveMod - Incident wave kinematics model {0: none=still water, 1: regular (periodic), 1P#: regular with user-specified phase, 2: JONSWAP/Pierson-Moskowitz spectrum (irregular), 3: White noise spectrum (irregular), 4: user-defined spectrum from routine UserWaveSpctrm (irregular), 5: Externally generated wave-elevation time series, 6: Externally generated full wave-kinematics time series [option 6 is invalid for PotMod/=0]} (switch)

0 WaveStMod - Model for stretching incident wave kinematics to instantaneous free surface {0: none=no stretching, 1: vertical stretching, 2: extrapolation stretching, 3: Wheeler stretching} (switch) [unused when WaveMod=0 or when PotMod/=0]

3630 WaveTMax - Analysis time for incident wave calculations (sec) [unused when WaveMod=0; determines WaveDOmega=2Pi/WaveTMax in the IFFT]

0.25 WaveDT - Time step for incident wave calculations (sec) [unused when WaveMod=0; 0.1<=WaveDT<=1.0 recommended; determines WaveOmegaMax=Pi/WaveDT in the IFFT]

2.69 WaveHs - Significant wave height of incident waves (meters) [used only when WaveMod=1, 2, or 3]

6.57 WaveTp - Peak-spectral period of incident waves (sec) [used only when WaveMod=1 or 2]

"DEFAULT" WavePkShp - Peak-shape parameter of incident wave spectrum (-) or DEFAULT (string) [used only when WaveMod=2; use 1.0 for Pierson-Moskowitz]

0 WvLowCOff - Low cut-off frequency or lower frequency limit of the wave spectrum beyond which the wave spectrum is zeroed (rad/s) [unused when WaveMod=0, 1, or 6]

500 WvHiCOff - High cut-off frequency or upper frequency limit of the wave spectrum beyond which the wave spectrum is zeroed (rad/s) [unused when WaveMod=0, 1, or 6]

0 WaveDir - Incident wave propagation heading direction (degrees) [unused when WaveMod=0 or 6]

0 WaveDirMod - Directional spreading function {0: none, 1: COS2S} (-) [only used when WaveMod=2,3, or 4]

1 WaveDirSpread - Wave direction spreading coefficient ( > 0 ) (-) [only used when WaveMod=2,3, or 4 and WaveDirMod=1]

1 WaveNDir - Number of wave directions (-) [only used when WaveMod=2,3, or 4 and WaveDirMod=1; odd number only]

0 WaveDirRange - Range of wave directions (full range: WaveDir +/- 1/2\*WaveDirRange) (degrees) [only used when WaveMod=2,3,or 4 and WaveDirMod=1]

123456789 WaveSeed(1) - First random seed of incident waves [-2147483648 to 2147483647] (-) [unused when WaveMod=0, 5, or 6]  
 1011121314 WaveSeed(2) - Second random seed of incident waves [-2147483648 to 2147483647] (-) [unused when WaveMod=0, 5, or 6]  
 False WaveNDamp - Flag for normally distributed amplitudes (flag) [only used when WaveMod=2, 3, or 4]  
 "" WvKinFile - Root name of externally generated wave data file(s) (quoted string) [used only when WaveMod=5 or 6]  
 0 NWaveElev - Number of points where the incident wave elevations can be computed (-) [maximum of 9 output locations]  
 0 WaveElevxi - List of xi-coordinates for points where the incident wave elevations can be output (meters) [NWaveElev points, separated by commas or white space; unused if NWaveElev = 0]  
 0 WaveElevyi - List of yi-coordinates for points where the incident wave elevations can be output (meters) [NWaveElev points, separated by commas or white space; unused if NWaveElev = 0]  
 ----- 2ND-ORDER WAVES ----- [unused with WaveMod=0 or 6]  
 False WvDiffQTF - Full difference-frequency 2nd-order wave kinematics (flag)  
 False WvSumQTF - Full summation-frequency 2nd-order wave kinematics (flag)  
 0 WvLowCOffD - Low frequency cutoff used in the difference-frequencies (rad/s) [Only used with a difference-frequency method]  
 3.5 WvHiCOffD - High frequency cutoff used in the difference-frequencies (rad/s) [Only used with a difference-frequency method]  
 0.1 WvLowCOffS - Low frequency cutoff used in the summation-frequencies (rad/s) [Only used with a summation-frequency method]  
 3.5 WvHiCOffS - High frequency cutoff used in the summation-frequencies (rad/s) [Only used with a summation-frequency method]  
 ----- CURRENT ----- [unused with WaveMod=6]  
 0 CurrMod - Current profile model {0: none=no current, 1: standard, 2: user-defined from routine UserCurrent} (switch)  
 0 CurrSSV0 - Sub-surface current velocity at still water level (m/s) [used only when CurrMod=1]  
 "DEFAULT" CurrSSDir - Sub-surface current heading direction (degrees) or DEFAULT (string) [used only when CurrMod=1]  
 20 CurrNSRef - Near-surface current reference depth (meters) [used only when CurrMod=1]  
 0 CurrNSV0 - Near-surface current velocity at still water level (m/s) [used only when CurrMod=1]  
 0 CurrNSDir - Near-surface current heading direction (degrees) [used only when CurrMod=1]  
 0 CurrDIV - Depth-independent current velocity (m/s) [used only when CurrMod=1]  
 0 CurrDIDir - Depth-independent current heading direction (degrees) [used only when CurrMod=1]  
 ----- FLOATING PLATFORM ----- [unused with WaveMod=6]  
 0 PotMod - Potential-flow model {0: none=no potential flow, 1: frequency-to-time-domain transforms based on WAMIT output, 2: fluid-impulse theory (FIT)} (switch)  
 "unused" PotFile - Root name of potential-flow model data; WAMIT output files containing the linear, nondimensionalized, hydrostatic restoring matrix (.hst), frequency-dependent hydrodynamic added mass matrix and damping matrix (.1), and frequency- and direction-dependent wave excitation force vector per unit wave amplitude (.3) (quoted string) [MAKE SURE THE FREQUENCIES INHERENT IN THESE WAMIT FILES SPAN THE PHYSICALLY-SIGNIFICANT RANGE OF FREQUENCIES FOR THE GIVEN PLATFORM; THEY MUST CONTAIN THE ZERO- AND INFINITE-FREQUENCY LIMITS!]  
 1 WAMITULEN - Characteristic body length scale used to redimensionalize WAMIT output (meters) [only used when PotMod=1]  
 0 PtfmVol0 - Displaced volume of water when the platform is in its undisplaced position (m<sup>3</sup>) [only used when PotMod=1; USE THE SAME VALUE COMPUTED BY WAMIT AS OUTPUT IN THE .OUT FILE!]

0 PtfmCOBxt - The xt offset of the center of buoyancy (COB) from the platform reference point (meters) [only used when PotMod=1]  
0 PtfmCOByt - The yt offset of the center of buoyancy (COB) from the platform reference point (meters) [only used when PotMod=1]  
1 RdtnMod - Radiation memory-effect model {0: no memory-effect calculation, 1: convolution, 2: state-space} (switch) [only used when PotMod=1; STATE-SPACE REQUIRES \*.ss INPUT FILE]  
60 RdtnTMax - Analysis time for wave radiation kernel calculations (sec) [only used when PotMod=1; determines RdtnDOmega=Pi/RdtnTMax in the cosine transform; MAKE SURE THIS IS LONG ENOUGH FOR THE RADIATION IMPULSE RESPONSE FUNCTIONS TO DECAY TO NEAR-ZERO FOR THE GIVEN PLATFORM!]  
0.025 RdtnDT - Time step for wave radiation kernel calculations (sec) [only used when PotMod=1; DT<=RdtnDT<=0.1 recommended; determines RdtnOmegaMax=Pi/RdtnDT in the cosine transform]  
----- 2ND-ORDER FLOATING PLATFORM FORCES ----- [unused with WaveMod=0 or 6, or PotMod=0 or 2]  
0 MnDrift - Mean-drift 2nd-order forces computed {0: None; [7, 8, 9, 10, 11, or 12]: WAMIT file to use} [Only one of MnDrift, NewmanApp, or DiffQTF can be non-zero]  
0 NewmanApp - Mean- and slow-drift 2nd-order forces computed with Newman's approximation {0: None; [7, 8, 9, 10, 11, or 12]: WAMIT file to use} [Only one of MnDrift, NewmanApp, or DiffQTF can be non-zero. Used only when WaveDirMod=0]  
0 DiffQTF - Full difference-frequency 2nd-order forces computed with full QTF {0: None; [10, 11, or 12]: WAMIT file to use} [Only one of MnDrift, NewmanApp, or DiffQTF can be non-zero]  
0 SumQTF - Full summation -frequency 2nd-order forces computed with full QTF {0: None; [10, 11, or 12]: WAMIT file to use}  
----- FLOATING PLATFORM FORCE FLAGS ----- [unused with WaveMod=6]  
True PtfmSgF - Platform horizontal surge translation force (flag) or DEFAULT  
True PtfmSwF - Platform horizontal sway translation force (flag) or DEFAULT  
True PtfmHvF - Platform vertical heave translation force (flag) or DEFAULT  
True PtfmRF - Platform roll tilt rotation force (flag) or DEFAULT  
True PtfmPF - Platform pitch tilt rotation force (flag) or DEFAULT  
True PtfmYF - Platform yaw rotation force (flag) or DEFAULT  
----- PLATFORM ADDITIONAL STIFFNESS AND DAMPING -----  
0 0 0 0 0 0 AddF0 - Additional preload (N, N-m)  
0 0 0 0 0 0 AddCLin - Additional linear stiffness (N/m, N/rad, N-m/m, N-m/rad)  
0 0 0 0 0 0  
0 0 0 0 0 0  
0 0 0 0 0 0  
0 0 0 0 0 0  
0 0 0 0 0 0  
0 0 0 0 0 0 AddBLin - Additional linear damping(N/(m/s), N/(rad/s), N-m/(m/s), N-m/(rad/s))  
0 0 0 0 0 0  
0 0 882607 0 0 0

0	0	0	0	0	0
0	0	0	0	0	0
0	0	0	0	0	0
0	0	0	0	0	0
0	0	0	0	0	0
0	0	0	0	0	0
0	0	0	0	0	0
0	0	0	0	0	0
0	0	0	0	0	0

AddBQuad - Additional quadratic drag(N/(m/s)^2, N/(rad/s)^2, N-m(m/s)^2, N-m/(rad/s)^2)

----- AXIAL COEFFICIENTS -----

1 NAXCoef - Number of axial coefficients (-)

AxCoefID	AxCd	AxCa	AxCp
(-)	(-)	(-)	(-)
1	1.00	1.00	1.00

----- MEMBER JOINTS -----

55 NJoints - Number of joints (-) [must be exactly 0 or at least 2]

JointID	Jointxi	Jointyi	Jointzi	JointAxID	JointOvrlp	[JointOvrlp= 0: do nothing at joint, 1: eliminate overlaps by calculating super member]
(-)	(m)	(m)	(m)	(-)	(switch)	

1	-24.80250	0.00000	-45.02000	1	0
2	12.40125	21.47960	-45.02000	1	0
3	12.40125	-21.47960	-45.02000	1	0
4	-24.80250	0.00000	-42.97930	1	0
5	12.40125	21.47960	-42.97930	1	0
6	12.40125	-21.47960	-42.97930	1	0
7	-24.80250	0.00000	-41.14260	1	0
8	12.40125	21.47960	-41.14260	1	0
9	12.40125	-21.47960	-41.14260	1	0
10	-24.80250	0.00000	-39.30610	1	0
11	12.40125	21.47960	-39.30610	1	0
12	12.40125	-21.47960	-39.30610	1	0
13	-6.20062	10.73980	-42.97930	1	0
14	12.40125	0.00000	-42.97930	1	0
15	-6.20062	-10.73980	-42.97930	1	0
16	-12.40125	0.00000	-36.66545	1	0
17	6.20062	10.73980	-36.66545	1	0



---

18	6.20062	-10.73980	-36.66545	1	0
19	-12.40172	0.00000	-19.65380	1	0
20	6.20086	10.74021	-19.65380	1	0
21	6.20086	-10.74021	-19.65380	1	0
22	-24.80250	0.00000	-34.07060	1	0
23	12.40125	21.47960	-34.07060	1	0
24	12.40125	-21.47960	-34.07060	1	0
25	0.00000	0.00000	-34.71330	1	0
26	-6.31009	0.00000	-10.00000	1	0
27	3.15504	5.46470	-10.00000	1	0
28	3.15504	-5.46470	-10.00000	1	0
29	-5.04807	0.00000	-8.00000	1	0
30	2.52404	4.37176	-8.00000	1	0
31	2.52404	-4.37176	-8.00000	1	0
32	-3.78605	0.00000	-6.00000	1	0
33	1.89303	3.27882	-6.00000	1	0
34	1.89303	-3.27882	-6.00000	1	0
35	-2.52404	0.00000	-4.00000	1	0
36	1.26202	2.18588	-4.00000	1	0
37	1.26202	-2.18588	-4.00000	1	0
38	-1.26202	0.00000	-2.00000	1	0
39	0.63101	1.09294	-2.00000	1	0
40	0.63101	-1.09294	-2.00000	1	0
41	0.00000	0.00000	-32.18830	1	0
42	0.00000	0.00000	-10.00000	1	0
43	0.00000	0.00000	-8.00000	1	0
44	0.00000	0.00000	-6.00000	1	0
45	0.00000	0.00000	-4.00000	1	0
46	0.00000	0.00000	-2.00000	1	0
47	0.00000	0.00000	0.00000	1	0
48	0.00000	0.00000	4.00000	1	0
49	0.00000	0.00000	8.00000	1	0
50	0.00000	0.00000	12.00000	1	0
51	0.00000	0.00000	16.00000	1	0
52	0.00000	0.00000	20.00000	1	0

53	-24.80250	0.00000	-50.00000	1	0
54	12.40125	21.47960	-50.00000	1	0
55	12.40125	-21.47960	-50.00000	1	0

----- MEMBER CROSS-SECTION PROPERTIES -----

8 NPropSets - Number of member property sets (-)

PropSetID	PropD	PropThck
(-)	(m)	(m)
1	3.15000	0.02500
2	3.15000	0.02500
3	1.87500	0.01500
4	2.47500	0.02000
5	1.20000	0.01500
6	3.14188	0.03000
7	3.40000	0.03000
8	5.50000	0.05000

----- SIMPLE HYDRODYNAMIC COEFFICIENTS (model 1) -----

SimplCd	SimplCdMG	SimplCa	SimplCaMG	SimplCp	SimplCpMG	SimplAxCa	SimplAxCaMG	SimplAxCp	SimplAxCpMG
(-)	(-)	(-)	(-)	(-)	(-)	(-)	(-)	(-)	(-)
1.00	0.00	1.00	0.00	1.00	0.00	1.00	0.00	1.00	0.00

----- DEPTH-BASED HYDRODYNAMIC COEFFICIENTS (model 2) -----

0 NCoefDpth - Number of depth-dependent coefficients (-)

Dpth	DpthCd	DpthCdMG	DpthCa	DpthCaMG	DpthCp	DpthCpMG	DpthAxCa	DpthAxCaMG	DpthAxCp	DpthAxCpMG
(m)	(-)	(-)	(-)	(-)	(-)	(-)	(-)	(-)	(-)	(-)

----- MEMBER-BASED HYDRODYNAMIC COEFFICIENTS (model 3) -----

0 NCoefMembers - Number of member-based coefficients (-)

MemberID	MemberCd1	MemberCd2	MemberCdMG1	MemberCdMG2	MemberCa1	MemberCa2	MemberCaMG1	MemberCaMG2	MemberCp1	MemberCp2	MemberCpMG1	MemberCpMG2	MemberAxCa1	MemberAxCa2	MemberAxCaMG1	MemberAxCaMG2	MemberAxCp1	MemberAxCp2	MemberAxCpMG1	MemberAxCpMG2	
(-)	(-)	(-)	(-)	(-)	(-)	(-)	(-)	(-)	(-)	(-)	(-)	(-)	(-)	(-)	(-)	(-)	(-)	(-)	(-)	(-)	(-)

----- MEMBERS -----

60 NMembers - Number of members (-)

MemberID	MJointID1	MJointID2	MPropSetID1	MPropSetID2	MDivSize	MCoefMod	PropPot	[MCoefMod=1: use simple coeff table, 2: use depth-based coeff table, 3: use member-based coeff table]	[ PropPot/=0 if member is modeled with potential-flow theory]
(-)	(-)	(-)	(-)	(-)	(m)	(switch)	(flag)		

1	1	4	1	1	1.0000	1	FALSE
2	2	5	1	1	1.0000	1	FALSE
3	3	6	1	1	1.0000	1	FALSE
4	4	7	2	2	1.0000	1	FALSE
5	5	8	2	2	1.0000	1	FALSE
6	6	9	2	2	1.0000	1	FALSE
7	7	10	2	2	1.0000	1	FALSE
8	8	11	2	2	1.0000	1	FALSE
9	9	12	2	2	1.0000	1	FALSE
10	10	22	2	2	1.0000	1	FALSE
11	11	23	2	2	1.0000	1	FALSE
12	12	24	2	2	1.0000	1	FALSE
13	7	16	3	3	1.0000	1	FALSE
14	16	41	3	3	1.0000	1	FALSE
15	8	17	3	3	1.0000	1	FALSE
16	17	41	3	3	1.0000	1	FALSE
17	9	18	3	3	1.0000	1	FALSE
18	18	41	3	3	1.0000	1	FALSE
19	10	19	4	4	1.0000	1	FALSE
20	19	26	4	4	1.0000	1	FALSE
21	11	20	4	4	1.0000	1	FALSE
22	20	27	4	4	1.0000	1	FALSE
23	12	21	4	4	1.0000	1	FALSE
24	21	28	4	4	1.0000	1	FALSE
25	26	29	4	4	1.0000	1	FALSE
26	29	32	4	4	1.0000	1	FALSE
27	32	35	4	4	1.0000	1	FALSE
28	35	38	4	4	1.0000	1	FALSE
29	38	47	4	4	1.0000	1	FALSE
30	27	30	4	4	1.0000	1	FALSE
31	30	33	4	4	1.0000	1	FALSE
32	33	36	4	4	1.0000	1	FALSE
33	36	39	4	4	1.0000	1	FALSE
34	39	47	4	4	1.0000	1	FALSE
35	28	31	4	4	1.0000	1	FALSE

36	31	34	4	4	1.0000	1	FALSE
37	34	37	4	4	1.0000	1	FALSE
38	37	40	4	4	1.0000	1	FALSE
39	40	47	4	4	1.0000	1	FALSE
40	4	13	5	5	1.0000	1	FALSE
41	13	5	5	5	1.0000	1	FALSE
42	5	14	5	5	1.0000	1	FALSE
43	14	6	5	5	1.0000	1	FALSE
44	6	15	5	5	1.0000	1	FALSE
45	15	4	5	5	1.0000	1	FALSE
46	25	41	6	7	1.0000	1	FALSE
47	41	42	7	8	1.0000	1	FALSE
48	42	43	8	8	1.0000	1	FALSE
49	43	44	8	8	1.0000	1	FALSE
50	44	45	8	8	1.0000	1	FALSE
51	45	46	8	8	1.0000	1	FALSE
52	46	47	8	8	1.0000	1	FALSE
53	47	48	8	8	1.0000	1	FALSE
54	48	49	8	8	1.0000	1	FALSE
55	49	50	8	8	1.0000	1	FALSE
56	50	51	8	8	1.0000	1	FALSE
57	51	52	8	8	1.0000	1	FALSE
58	53	1	1	1	1.0000	1	FALSE
59	54	2	1	1	1.0000	1	FALSE
60	55	3	1	1	1.0000	1	FALSE

## ----- FILLED MEMBERS -----

0 NFillGroups - Number of filled member groups (-) [If FillDens = DEFAULT, then FillDens = WtrDens; FillFSLoc is related to MSL2SWL]

FillNumM FillMList FillFSLoc FillDens  
 (-) (-) (m) (kg/m<sup>3</sup>)

## ----- MARINE GROWTH -----

0 NMGDepths - Number of marine-growth depths specified (-)

MGDpth MGThck MGDens  
 (m) (m) (kg/m<sup>3</sup>)

## ----- MEMBER OUTPUT LIST -----

0 NMOutputs - Number of member outputs (-) [must be < 10]

MemberID NOutLoc NodeLocs [NOutLoc < 10; node locations are normalized distance from the start of the member, and must be >=0 and <= 1] [unused if NMOutputs=0]

----- JOINT OUTPUT LIST -----

0 NJOutputs - Number of joint outputs [Must be < 10]

0 JOutLst - List of JointIDs which are to be output (-)[unused if NJOutputs=0] plus 22, 23, 24, 25, 41, 47 4, 5, 6, 7, 8, 9, 10, 11, 12

----- OUTPUT -----

False HDSum - Output a summary file [flag]

False OutAll - Output all user-specified member and joint loads (only at each member end, not interior locations) [flag]

2 OutSwch - Output requested channels to: [1=Hydrodyn.out, 2=GlueCode.out, 3=both files]

"ES11.4e2" OutFmt - Output format for numerical results (quoted string) [not checked for validity!]

"A11" OutSFmt - Output format for header strings (quoted string) [not checked for validity!]

----- OUTPUT CHANNELS -----

END of output channels and end of file. (the word "END" must appear in the first 3 columns of this line)

## SUBDYN INPUT FILE

----- SubDyn v1.01.x MultiMember Support Structure Input File -----

FAST Certification Test #20: NREL 5.0 MW Baseline Wind Turbine with OC3 Tripod Configuration, for use in offshore analysis

----- SIMULATION CONTROL -----

False Echo - Echo input data to "<rootname>.SD.ech" (flag)

"DEFAULT" SDDeltaT - Local Integration Step. If "default", the glue-code integration step will be used.

3 IntMethod - Integration Method [1/2/3/4 = RK4/AB4/ABM4/AM2].

True SttcSolve - Solve dynamics about static equilibrium point

----- FEA and CRAIG-BAMPTON PARAMETERS-----

3 FEMMod - FEM switch: element model in the FEM. [1= Euler-Bernoulli(E-B); 2=Tapered E-B (unavailable); 3= 2-node Timoshenko; 4= 2-node tapered Timoshenko (unavailable)]

1 NDiv - Number of sub-elements per member

True CBMod - [T/F] If True perform C-B reduction, else full FEM dofs will be retained. If True, select Nmodes to retain in C-B reduced system.

12 Nmodes - Number of internal modes to retain (ignored if CBMod=False). If Nmodes=0 --> Guyan Reduction.

1 JDampings - Damping Ratios for each retained mode (% of critical) If Nmodes>0, list Nmodes structural damping ratios for each retained mode (% of critical), or a single damping ratio to be applied to all retained modes. (last entered value will be used for all remaining modes).

---- STRUCTURE JOINTS: joints connect structure members (~Hydrodyn Input File)---

161 NJoints - Number of joints (-)

JointID JointXss JointYss JointZss [Coordinates of Member joints in SS-Coordinate System]

---

(-)	(m)	(m)	(m)
1	-24.80250	0.00000	-45.00000
2	12.40125	21.47960	-45.00000
3	12.40125	-21.47960	-45.00000
4	-24.80250	0.00000	-42.97930
5	12.40125	21.47960	-42.97930
6	12.40125	-21.47960	-42.97930
7	-24.80250	0.00000	-41.14260
8	12.40125	21.47960	-41.14260
9	12.40125	-21.47960	-41.14260
10	-24.80250	0.00000	-39.30610
11	12.40125	21.47960	-39.30610
12	12.40125	-21.47960	-39.30610
13	-6.20062	10.73980	-42.97930
14	12.40125	0.00000	-42.97930
15	-6.20062	-10.73980	-42.97930
16	-12.40125	0.00000	-36.66545
17	6.20062	10.73980	-36.66545
18	6.20062	-10.73980	-36.66545
19	-12.40172	0.00000	-19.65380
20	6.20086	10.74021	-19.65380
21	6.20086	-10.74021	-19.65380
22	-24.80250	0.00000	-34.07060
23	12.40125	21.47960	-34.07060
24	12.40125	-21.47960	-34.07060
25	0.00000	0.00000	-34.71330
26	-6.31009	0.00000	-10.00000
27	3.15504	5.46470	-10.00000
28	3.15504	-5.46470	-10.00000
29	-5.04807	0.00000	-8.00000
30	2.52404	4.37176	-8.00000
31	2.52404	-4.37176	-8.00000
32	-3.78605	0.00000	-6.00000
33	1.89303	3.27882	-6.00000
34	1.89303	-3.27882	-6.00000

---

---

35	-2.52404	0.00000	-4.00000
36	1.26202	2.18588	-4.00000
37	1.26202	-2.18588	-4.00000
38	-1.26202	0.00000	-2.00000
39	0.63101	1.09294	-2.00000
40	0.63101	-1.09294	-2.00000
41	0.00000	0.00000	-32.18830
42	0.00000	0.00000	-10.00000
43	0.00000	0.00000	-8.00000
44	0.00000	0.00000	-6.00000
45	0.00000	0.00000	-4.00000
46	0.00000	0.00000	-2.00000
47	0.00000	0.00000	0.00000
48	0.00000	0.00000	4.00000
49	0.00000	0.00000	8.00000
50	0.00000	0.00000	12.00000
51	0.00000	0.00000	16.00000
52	0.00000	0.00000	20.00000
53	-24.80250	0.00000	-36.68835
54	12.40125	21.47960	-36.68835
55	12.40125	-21.47960	-36.68835
56	-22.32225	0.00000	-40.24717
57	-19.84200	0.00000	-39.35174
58	-17.36175	0.00000	-38.45631
59	-14.88150	0.00000	-37.56088
60	-9.92100	0.00000	-35.77002
61	-7.44075	0.00000	-34.87459
62	-4.96050	0.00000	-33.97916
63	-2.48025	0.00000	-33.08373
64	11.16112	19.33164	-40.24717
65	9.92100	17.18368	-39.35174
66	8.68087	15.03572	-38.45631
67	7.44075	12.88776	-37.56088
68	4.96050	8.59184	-35.77002
69	3.72037	6.44388	-34.87459

---

70	2.48025	4.29592	-33.97916
71	1.24012	2.14796	-33.08373
72	11.16112	-19.33164	-40.24717
73	9.92100	-17.18368	-39.35174
74	8.68087	-15.03572	-38.45631
75	7.44075	-12.88776	-37.56088
76	4.96050	-8.59184	-35.77002
77	3.72037	-6.44388	-34.87459
78	2.48025	-4.29592	-33.97916
79	1.24012	-2.14796	-33.08373
80	-23.25240	0.00000	-36.84956
81	-21.70230	0.00000	-34.39303
82	-20.15221	0.00000	-31.93649
83	-18.60211	0.00000	-29.47995
84	-17.05201	0.00000	-27.02341
85	-15.50192	0.00000	-24.56688
86	-13.95182	0.00000	-22.11034
87	-10.87881	0.00000	-17.24035
88	-9.35590	0.00000	-14.82690
89	-7.83300	0.00000	-12.41345
90	11.62620	20.13718	-36.84956
91	10.85115	18.79475	-34.39303
92	10.07610	17.45233	-31.93649
93	9.30105	16.10991	-29.47995
94	8.52601	14.76748	-27.02341
95	7.75096	13.42506	-24.56688
96	6.97591	12.08263	-22.11034
97	5.43940	9.42133	-17.24035
98	4.67795	8.10245	-14.82690
99	3.91650	6.78358	-12.41345
100	11.62620	-20.13718	-36.84956
101	10.85115	-18.79475	-34.39303
102	10.07610	-17.45233	-31.93649
103	9.30105	-16.10991	-29.47995
104	8.52601	-14.76748	-27.02341

---



---

105	7.75096	-13.42506	-24.56688
106	6.97591	-12.08263	-22.11034
107	5.43940	-9.42133	-17.24035
108	4.67795	-8.10245	-14.82690
109	3.91650	-6.78358	-12.41345
110	-22.47726	1.34248	-42.97930
111	-20.15203	2.68495	-42.97930
112	-17.82679	4.02743	-42.97930
113	-15.50156	5.36990	-42.97930
114	-13.17633	6.71238	-42.97930
115	-10.85109	8.05485	-42.97930
116	-8.52586	9.39733	-42.97930
117	-3.87539	12.08228	-42.97930
118	-1.55015	13.42475	-42.97930
119	0.77508	14.76723	-42.97930
120	3.10031	16.10970	-42.97930
121	5.42555	17.45218	-42.97930
122	7.75078	18.79465	-42.97930
123	10.07602	20.13713	-42.97930
124	12.40125	18.79465	-42.97930
125	12.40125	16.10970	-42.97930
126	12.40125	13.42475	-42.97930
127	12.40125	10.73980	-42.97930
128	12.40125	8.05485	-42.97930
129	12.40125	5.36990	-42.97930
130	12.40125	2.68495	-42.97930
131	12.40125	-2.68495	-42.97930
132	12.40125	-5.36990	-42.97930
133	12.40125	-8.05485	-42.97930
134	12.40125	-10.73980	-42.97930
135	12.40125	-13.42475	-42.97930
136	12.40125	-16.10970	-42.97930
137	12.40125	-18.79465	-42.97930
138	10.07602	-20.13713	-42.97930
139	7.75078	-18.79465	-42.97930

140	5.42555	-17.45218	-42.97930
141	3.10031	-16.10970	-42.97930
142	0.77508	-14.76723	-42.97930
143	-1.55015	-13.42475	-42.97930
144	-3.87539	-12.08228	-42.97930
145	-8.52586	-9.39733	-42.97930
146	-10.85109	-8.05485	-42.97930
147	-13.17633	-6.71238	-42.97930
148	-15.50156	-5.36990	-42.97930
149	-17.82679	-4.02743	-42.97930
150	-20.15203	-2.68495	-42.97930
151	-22.47726	-1.34248	-42.97930
152	0.00000	0.00000	-29.41476
153	0.00000	0.00000	-26.64122
154	0.00000	0.00000	-23.86769
155	0.00000	0.00000	-21.09415
156	0.00000	0.00000	-18.32061
157	0.00000	0.00000	-15.54708
158	0.00000	0.00000	-12.77354
159	-24.80250	0.00000	-60.60000
160	12.40125	21.47960	-60.60000
161	12.40125	-21.47960	-60.60000

----- BASE REACTION JOINTS: 1/0 for Locked/Free DOF @ each Reaction Node -----

3 NReact - Number of Joints with reaction forces; be sure to remove all rigid motion DOFs of the structure (else  $\det([K])=[0]$ )

RJointID	RctTDXss	RctTDYss	RctTDZss	RctRDXss	RctRDYss	RctRDZss	[Global Coordinate System]
(-)	(flag)	(flag)	(flag)	(flag)	(flag)	(flag)	
159	1	1	1	1	1	1	
160	1	1	1	1	1	1	
161	1	1	1	1	1	1	

----- INTERFACE JOINTS: 1/0 for Locked (to the TP)/Free DOF @each Interface Joint (only Locked-to-TP implemented thus far (=rigid TP)) -----

1 NInterf - Number of interface joints locked to the Transition Piece (TP): be sure to remove all rigid motion dofs

IJointID	ItfTDXss	ItfTDYss	ItfTDZss	ItfRDXss	ItfRDYss	ItfRDZss	[Global Coordinate System]
(-)	(flag)	(flag)	(flag)	(flag)	(flag)	(flag)	
52	1	1	1	1	1	1	

----- MEMBERS -----

166 NMembers - Number of frame members					
MemberID	MJointID1	MJointID2	MPropSetID1	MPropSetID2	COSMID
(-)	(-)	(-)	(-)	(-)	(-)
1	1	4	1	1	
2	2	5	1	1	
3	3	6	1	1	
4	4	7	2	2	
5	5	8	2	2	
6	6	9	2	2	
7	7	10	2	2	
8	8	11	2	2	
9	9	12	2	2	
10	10	53	2	2	
11	11	54	2	2	
12	12	55	2	2	
13	7	56	3	3	
14	16	60	3	3	
15	8	64	3	3	
16	17	68	3	3	
17	9	72	3	3	
18	18	76	3	3	
19	10	80	4	4	
20	19	87	4	4	
21	11	90	4	4	
22	20	97	4	4	
23	12	100	4	4	
24	21	107	4	4	
25	26	29	4	4	
26	29	32	4	4	
27	32	35	4	4	
28	35	38	4	4	
29	38	47	4	4	
30	27	30	4	4	
31	30	33	4	4	
32	33	36	4	4	

---

33	36	39	4	4
34	39	47	4	4
35	28	31	4	4
36	31	34	4	4
37	34	37	4	4
38	37	40	4	4
39	40	47	4	4
40	4	110	5	5
41	13	117	5	5
42	124	5	5	5
43	131	14	5	5
44	138	6	5	5
45	145	15	5	5
46	25	41	6	7
47	41	152	7	9
48	42	43	8	8
49	43	44	8	8
50	44	45	8	8
51	45	46	8	8
52	46	47	8	8
53	47	48	8	8
54	48	49	8	8
55	49	50	8	8
56	50	51	8	8
57	51	52	8	8
58	53	22	2	2
59	54	23	2	2
60	55	24	2	2
61	56	57	3	3
62	57	58	3	3
63	58	59	3	3
64	59	16	3	3
65	60	61	3	3
66	61	62	3	3
67	62	63	3	3

---

---

68	63	41	3	3
69	64	65	3	3
70	65	66	3	3
71	66	67	3	3
72	67	17	3	3
73	68	69	3	3
74	69	70	3	3
75	70	71	3	3
76	71	41	3	3
77	72	73	3	3
78	73	74	3	3
79	74	75	3	3
80	75	18	3	3
81	76	77	3	3
82	77	78	3	3
83	78	79	3	3
84	79	41	3	3
85	80	81	4	4
86	81	82	4	4
87	82	83	4	4
88	83	84	4	4
89	84	85	4	4
90	85	86	4	4
91	86	19	4	4
92	87	88	4	4
93	88	89	4	4
94	89	26	4	4
95	90	91	4	4
96	91	92	4	4
97	92	93	4	4
98	93	94	4	4
99	94	95	4	4
100	95	96	4	4
101	96	20	4	4
102	97	98	4	4

---

103	98	99	4	4
104	99	27	4	4
105	100	101	4	4
106	101	102	4	4
107	102	103	4	4
108	103	104	4	4
109	104	105	4	4
110	105	106	4	4
111	106	21	4	4
112	107	108	4	4
113	108	109	4	4
114	109	28	4	4
115	110	111	5	5
116	111	112	5	5
117	112	113	5	5
118	113	114	5	5
119	114	115	5	5
120	115	116	5	5
121	116	13	5	5
122	117	118	5	5
123	118	119	5	5
124	119	120	5	5
125	120	121	5	5
126	121	122	5	5
127	122	123	5	5
128	123	5	5	5
129	125	124	5	5
130	126	125	5	5
131	127	126	5	5
132	128	127	5	5
133	129	128	5	5
134	130	129	5	5
135	14	130	5	5
136	132	131	5	5
137	133	132	5	5

---

138	134	133	5	5
139	135	134	5	5
140	136	135	5	5
141	137	136	5	5
142	6	137	5	5
143	139	138	5	5
144	140	139	5	5
145	141	140	5	5
146	142	141	5	5
147	143	142	5	5
148	144	143	5	5
149	15	144	5	5
150	146	145	5	5
151	147	146	5	5
152	148	147	5	5
153	149	148	5	5
154	150	149	5	5
155	151	150	5	5
156	4	151	5	5
157	152	153	9	10
158	153	154	10	11
159	154	155	11	12
160	155	156	12	13
161	156	157	13	14
162	157	158	14	15
163	158	42	15	8
164	159	1	16	16
165	160	2	16	16
166	161	3	16	16

----- MEMBER X-SECTION PROPERTY data 1/2 [isotropic material for now: use this table for circular-tubular elements] -----

PropSetID	YoungE	ShearG	MatDens	XsecD	XsecT
(-)	(N/m <sup>2</sup> )	(N/m <sup>2</sup> )	(kg/m <sup>3</sup> )	(m)	(m)
1	2.10000e+11	8.10000e+10	7850.00	3.150000	0.025000
2	2.10000e+11	8.10000e+10	7850.00	3.150000	0.025000

3	2.10000e+11	8.10000e+10	7850.00	1.875000	0.015000
4	2.10000e+11	8.10000e+10	7850.00	2.475000	0.020000
5	2.10000e+11	8.10000e+10	7850.00	1.200000	0.015000
6	2.10000e+11	8.10000e+10	7850.00	3.141880	0.030000
7	2.10000e+11	8.10000e+10	7850.00	3.400000	0.030000
8	2.10000e+11	8.10000e+10	7850.00	5.500000	0.050000
9	2.10000e+11	8.10000e+10	7850.00	3.687500	0.030000
10	2.10000e+11	8.10000e+10	7850.00	3.975000	0.030000
11	2.10000e+11	8.10000e+10	7850.00	4.262500	0.030000
12	2.10000e+11	8.10000e+10	7850.00	4.550000	0.030000
13	2.10000e+11	8.10000e+10	7850.00	4.837500	0.030000
14	2.10000e+11	8.10000e+10	7850.00	5.125000	0.030000
15	2.10000e+11	8.10000e+10	7850.00	5.412500	0.030000
16	2.10000e+11	8.10000e+10	7850.00	3.150000	0.028000

----- MEMBER X-SECTION PROPERTY data 2/2 [isotropic material for now: use this table if any section other than circular, however provide COSM(i,j) below] -----

0 NXPropSets - Number of structurally unique non-circular x-sections (if 0 the following table is ignored)

PropSetID	YoungE	ShearG	MatDens	XsecA	XsecAsx	XsecAsy	XsecJxx	XsecJyy	XsecJ0
(-)	(N/m <sup>2</sup> )	(N/m <sup>2</sup> )	(kg/m <sup>3</sup> )	(m <sup>2</sup> )	(m <sup>2</sup> )	(m <sup>2</sup> )	(m <sup>4</sup> )	(m <sup>4</sup> )	(m <sup>4</sup> )

----- MEMBER COSINE MATRICES COSM(i,j) -----

0 NCOSMs - Number of unique cosine matrices (i.e., of unique member alignments including principal axis rotations); ignored if NXPropSets=0 or 9999 in any element below

COSMID	COSM11	COSM12	COSM13	COSM21	COSM22	COSM23	COSM31	COSM32	COSM33
(-)	(-)	(-)	(-)	(-)	(-)	(-)	(-)	(-)	(-)

----- JOINT ADDITIONAL CONCENTRATED MASSES -----

0 NCmass - Number of joints with concentrated masses; Global Coordinate System

CMJointID	JMass	JMXX	JMYX	JMZZ
(-)	(kg)	(kg*m <sup>2</sup> )	(kg*m <sup>2</sup> )	(kg*m <sup>2</sup> )

----- OUTPUT: SUMMARY & OUTFILE -----

True SSSum - Output a Summary File (flag).It contains: matrices K,M and C-B reduced M\_BB, M-BM, K\_BB, K\_MM(OMG<sup>2</sup>), PHI\_R, PHI\_L. It can also contain COSMs if requested.

False OutCOSM - Output cosine matrices with the selected output member forces (flag)

False OutAll - [T/F] Output all members' end forces

2 OutSwch - [1/2/3] Output requested channels to: 1=<rootname>.SD.out; 2=<rootname>.out (generated by FAST); 3=both files.

True TabDelim - Generate a tab-delimited output in the <rootname>.SD.out file



1 OutDec - Decimation of output in the <rootname>.SD.out file  
"ES11.4e2" OutFmt - Output format for numerical results in the <rootname>.SD.out file  
"A11" OutSFmt - Output format for header strings in the <rootname>.SD.out file  
----- MEMBER OUTPUT LIST -----  
0 NMOutputs - Number of members whose forces/displacements/velocities/accelerations will be output (-) [Must be <= 9].  
MemberID NOutCnt NodeCnt [NOutCnt=how many nodes to get output for [< 10]; NodeCnt are local ordinal numbers from the start of the member, and  
must be >=1 and <= NDiv+1] If NMOutputs=0 leave blank as well.  
(-) (-) (-)  
----- SSOuList: The next line(s) contains a list of output parameters that will be output in <rootname>.SD.out or <rootname>.out. -----  
END of output channels and end of file. (the word "END" must appear in the first 3 columns of this line)